UNIVERSITY OF OKLAHOMA

GRADUATE COLLEGE

ENZYMES INVOLVED IN ENERGY CONSERVATION VIA SUBSTRATE-LEVEL PHOSPHORYLATION IN THE SYNTROPHIC BENZOATE DEGRADER, *SYNTROPHUS ACIDITROPHICUS*

A DISSERTATION

SUBMITTED TO THE GRADUATE FACULTY

in partial fulfillment of the requirements for the

Degree of

DOCTOR OF PHILOSOPHY

By

KIMBERLY LASHUN THOMAS
Norman, Oklahoma
2014

ENZYMES INVOLVED IN ENERGY CONSERVATION VIA SUBSTRATE-LEVEL PHOSPHORYLATION IN THE SYNTROPHIC BENZOATE DEGRADER, *SYNTROPHUS ACIDITROPHICUS*

A DISSERTATION APPROVED FOR THE
DEPARTMENT OF MICROBIOLOGY AND PLANT BIOLOGY

BY

_____
Dr. Michael J. McInerney, Chair

_____
Dr. Ann H. West

_____
Dr. Ben F. Holt

_____
Dr. Anne K. Dunn

_____
Dr. Joseph M. Suflita

I dedicate this work to my children, Naya Zahara James, Natheniel Alec-Jahaziel James, and Jacobe Zachi-Jahaziel James. Naya thank you for your charisma, you are a wonderfully talented individual, you have always inspired me to press forward. Natheniel thank you for your quick-wit, you have challenged me to move outside my comfort zone. Jacobe your determination is awesome. To my children always know that through hard work, strong work ethic, and faith in God all things are possible. I also dedicate this work to my husband, Kevin James. Thank you for your support and encouragement this academic accomplishment has been a journey for all of us and I look forward to our future.

Acknowledgments

First, I need to acknowledge the support and encouragement of my committee chair, Dr. Michael McInerney. I thank Dr. McInerney for the opportunity to work in his laboratory, not only has he shown me how to be a good scientist, he has shown me how to be a better person. Thank you Dr. McInerney for your leadership both in the laboratory and in life. I also need to acknowledge, my outstanding colleague, Neil Wofford, he has shown me how to work effectively and efficiently in the laboratory. I thank Neil for his patience and willingness to guide me during long gruelling hours of assaying for activities. I would also like to acknowledge my colleagues, Huynh Le, Dr. Jessica Sieber, and Dr. Bryan Crable. My colleagues have all helped me immensely with my research, and I thank them for their support and encouragement. To my outstanding committee members, Dr. Suflita, Dr. West, Dr. Dunn, and Dr. Holt thank you for your critical evaluations of my work. Lastly, I would like to acknowledge my family. Michelle Worthy, my twin sister, thank you for your continued support, she has always been an invaluable source of strength and direction. Thanks Chelle! My Mom and Dad thank you. To my siblings, Renee, Orlando, Kendra, and Aisha thank you all for your support. And although my sister, Kia, has gone on to a better place, I would like to acknowledge her life, she would be so proud of my accomplishments.

Table of Contents

List of Tables

List of Figures

Abstract

Syntrophus aciditrophicus (SB) degrades benzoate, cyclohexane-1-carboxylate and certain fatty acids in syntrophic association with hydrogen/formate-using microorganisms and ferments crotonate in pure culture. ATP formation coupled to acetate production is the main mechanism of energy conservation by *S. aciditrophicus.* However, the method by which *S. aciditrophicus* synthesizes ATP from acetyl-CoA is unclear. The genome of *S. aciditrophicus* does not contain an annotated acetate kinase gene, but has two genes for butyrate kinase; several genes for AMP-forming, acetyl-CoA synthetases; and nine genes for archaeal ADP-forming, acetyl-CoA synthetases all of which could be used to synthesize ATP from acetyl-CoA. Two-dimensional gel electrophoresis and quantitative-real time-polymerase chain reaction detected peptides and transcripts, respectively, from AMP-forming, acetyl-CoA synthetase; ADP-forming, acetyl-CoA synthetases; and butyrate kinase genes. Acetyl-CoA synthetase activity was high (0.5 ± 0.01 to 7.4 ± 0.3 μmol min^{-1} mg^{-1} of protein) in cell-free extracts of *S. aciditrophicus* grown in pure culture on crotonate or in coculture with *Methanospirillum hungatei* on crotonate, benzoate and cyclohexane-1-carboxylate. Acetate kinase, butyrate kinase and phosphotransacetylase activities were low (< 0.2 ± 0.03 μmol min^{-1} mg^{-1} of protein) and only detected in cell-free extracts of crotonate-grown pure and coculture cells. Only the acetyl-CoA synthetase activity was high enough to account for the acetate production rate (1.2 ± 0.2 μmol min^{-1} mg^{-1} of protein) during crotonate growth. Competitive inhibition of the native adenylate kinase

showed that the dominant acetyl-CoA synthetase activity was an AMP-forming, acetyl-CoA synthetase; ADP-forming, acetyl-CoA synthetase activity was not detected. The acetyl-CoA synthetase activity was purified to homogeneity with an 80% recovery. The purified protein was an AMP-forming, acetyl-CoA synthetase encoded by gene SYN_02635 (*acs1*), which had a V_{max} of 7.5 ± 1.2 μmol min^{-1} mg^{-1} of protein in the acetate-forming direction, sufficient to account for the acetate production rates under all growth conditions. A recombinant Acs1 had similar kinetic properties. Transcripts of *acs1* represented 0.58 to 0.76% of the total transcriptome compared to 0 to 0.1% for the other possible candidates. Polypeptides of the Acs1 represented 1.3 to 4.4% of the total peptides detected compared to 0 to 0.1% for other possible candidates. The above analyses show that *S. aciditrophicus* uses Acs1 for ATP formation from acetyl-CoA.

S. aciditrophicus has two candidate genes that could encode for acetate kinase, SYN_03090 and SYN_01210, which share 99% identity with each other at the nucleotide level, and both of which annotate as butyrate kinases. The nucleotide sequence of SYN_03090 was cloned heterologously expressed in *Escherichia coli* Bl21. The purified recombinant protein had acetate kinase activity but not propionate or butyrate kinase activity. ATP was the preferred nucleotide triphosphate with acetate as the substrate. The purified recombinant protein synthesized ATP from acetyl-phosphate. Phylogenetic analyses showed butyrate kinases clustered together and acetate kinases clustered together on a neighbor joining phylogenetic tree. The amino acid sequences of both

SYN_03090 and SYN_01210 grouped with those of the butyrate kinases. These data support the conclusion that SYN_03090/SYN_01210 gene product is an acetate kinase.

Previous studies indicated that *S. aciditrophicus* uses AMP-forming, acyl-CoA synthetases (substrate:CoA ligase) rather than CoA transferases for substrate activation. Here, two crotonate/benzoate:CoA ligases were purified and characterized from cell-free extracts of *S. aciditrophicus*. Peptide analysis showed that these proteins were gene products of SYN_02896 and SYN_02898. The gene for SYN_03128, annotated as a long-chain fatty acid-CoA ligase, was cloned and heterologously expressed in *Escherichia coli*. The purified SYN_03128 gene product had high activity and affinity for cyclohexane-1-carboxylate (V_{max} and K_m of 15 ± 0.5 μmol $min^{-1}mg^{-1}$ and 0.04 ± 0.007 mM, respectively), showing that it is a cyclohexane-1-carboxylate:CoA ligase. *S. aciditrophicus* uses benzoate:CoA ligase for activation of both benzoate and crotonate, and uses a separate ligase for activation of cyclohexane-1-carboxylate. By coupling the activation of benzoate, crotonate, and cyclohexane-1-carboxylate to the AMP-forming, acetyl-CoA synthetase reaction for ATP synthesis the net reaction is functionally equivalent to a CoA transferase reaction.

Preface

The main objective of this research is to investigate mechanisms for energy conservation in the syntrophic benzoate degrader *Syntrophus aciditrophicus.* In 2007, the genome of *S. aciditrophicus* was sequenced and revealed multiple strategies that could potentially be used by the cell to synthesize ATP. In this work, I identify the AMP-forming, acetyl-CoA synthetase as the main mechanism for ATP synthesis by substrate-level phosphorylation in *S. aciditrophicus*. I also identify and characterize the enzymes used for activation of benzoate, cyclohexane-1-carboxylate, and crotonate by *S. aciditrophicus*.

Chapter 2 is an investigation into the candidate gene systems for ATP synthesis that were dominant in *S. aciditrophicus*. Dr. Housna Mouttaki grew the cultures for the 2-D gel proteome. Dr. Jessica Sieber coordinated the high-throughput proteome project, and Huynh Le and I grew the cultures. Both 2-D gel and high-throughput proteomes were sequenced and analyzed by our collaborators at University of California-Los Angeles, Dr. Rachel Loo laboratory. The proteome data sets were used to determine the presence of polypeptides from candidate genes for ATP production via substrate-level phosphorylation. Also in Chapter 2, RNA sequencing data was analyzed to determine gene expression of potential gene candidates for ATP synthesis via substrate-level phosphorylation. The transcriptome data was a collaborative effort in Dr. McInerney's laboratory. Dr. Sieber grew the crotonate pure cultures and

crotonate cocultures, and I grew the cyclohexane-1-carboxylate and benzoate cultures. Transcriptome processing and annotation of RAW data files were done in collaboration with Dr. Cody Sheik. In addition, in Chapter 2 annotated ADP-forming, acetyl-CoA synthetases were cloned and expressed with both N-terminus and C-terminus his-tags supplied by Dr. Elizabeth Karr.

In Chapter 4, I purified and characterized gene product SYN_02896 and partial purified and characterized gene products SYN_02896 and SYN_02898. To confirm the activities of SYN_02896 and SYN_02898, Dr. Johannes Kung cloned and expressed the gene products in *Escherichia coli*, and determined kinetic constants for the expressed gene products.

Chapter 1: Overview

Carbon dioxide, methane, nitrous oxide, and chlorofluorocarbon are known to play a significant role in increasing atmospheric temperatures (Forster, 2007). In recent years, attention has been focused on methane gas production and its role as a greenhouse gas (Forster, 2007). Methane gas has 25 times the global warming potential of carbon dioxide (Forster, 2007; Yvon-Durocher, 2014), and recent data suggests atmospheric methane has contributed to 20% of the Earth's warming since pre-industrial times (Kirschke, 2013; Yvon-Durocher, 2014). Methane emissions into the atmosphere are primarily from three sources: biogenic due to recent microbial degradation; thermogenic due to geological or ancient biotic processes millions of years ago; and pyrogenic due to the incomplete combustion of biomass (Kirschke, 2013). As energy demands of industrialized nations increase, so does the demand for more efficient energy sources. Methane can be harvested from naturally occurring and anthropogenic sources and used to meet increasing energy demands. Conversion of naturally occurring methane to carbon dioxide would be carbon-neutral, and help slow global warming due to increased use of fossil fuels.

The majority of methane released in the atmosphere is from biogenic sources. Biogenic methane production occurs in natural systems such as wet lands (tundra), ruminants (digestion in domestic animals), animal wastes, oceans, and lakes, and in engineered systems such as landfills, anaerobic digesters, and rice paddy fields (Breas, Guillou, Reniero, & Wada, 2001). In these environments, biomass conversion to methane is an important process in

global carbon cycling (Breas et al., 2001). Thus, understanding the biological processes involved in methane production is important to understand global carbon cycling and the role that biotic methane plays in global warming.

Naturally occurring methane is primarily made during anaerobic degradation of organic matter by microorganisms in a process known as methanogenesis (Lowe, Jain, & Zeikus, 1993). In methanogenic environments, the degradation of complex organic matter such as hydrocarbons, polysaccharides, proteins, lipids, and nucleic acids to methane and carbon dioxide involves a diverse community of interacting microorganisms and proceeds in discrete metabolic steps (McInerney et al., 2008; Sieber, McInerney, & Gunsalus, 2012). In the first step, primary fermenters hydrolyze complex polymers into monomeric units that are further fermented to acetate, longer chain fatty acids, aromatic compounds, alcohols, formate, and hydrogen. In the next step, a second group of fermenting microorganisms, syntrophic metabolizers, degrade propionate, longer chain fatty acids, aromatic compounds, and alcohols to methanogenic substrates, formate, acetate, hydrogen, and carbon dioxide (McInerney et al., 2008). In the last step, methanogens convert the acetate, formate, hydrogen, and carbon dioxide made by the fermentative microoganisms to methane and carbon dioxide. Syntrophic metabolizers reoxidize their reduced cofactors by reducing protons or carbon dioxide to produce hydrogen or formate, respectively (McInerney et al., 2008). The syntrophic degradation of fatty acids, aromatic compounds, and alcohols is only thermodynamically favorable when the hydrogen and/or formate

concentrations are kept very low by the methanogen. (McInerney et al., 2008; Sieber et al., 2012).

The anaerobic degradation of many aromatic compounds, such as toluene, phenol, xylenes, cresols, and phenylacetic acid converges to either benzoate and/or its CoA derivative, benzoyl-CoA, prior to ring reduction and cleavage (Fuchs, 2008; Peters, Shinoda, McInerney, & Boll, 2007). After glucose, the six-carbon benzene ring is the second most abundant carbon structure and is found in lignin, flavenoids, amino acids, and crude oil making this compound an important carbon source for microorganisms (Peters et al., 2007). Due to the resonance stability of the benzene ring, benzoate degradation poses a challenge for biodegradation in anaerobic environments. Facultative anaerobic organisms such as the phototrophic *Rhodopseudomonas palustris* (Dutton & Evans, 1969; Harwood & Gibson, 1988), and the denitrifying *Thauera aromatica* (Schuhle et al., 2003) are both capable of anaerobic degradation of aromatic compounds. In addition, many strict anaerobes such as iron- and sulfate-reducing microorganisms have also been shown to degrade benzoate (Harwood, Burchhardt, Herrmann, & Fuchs, 1999). A well-studied iron-reducing microorganisms that degrades benzoate is *Geobacter metallireducins* (Peters et al., 2007). In methanogenic environments, fermentative syntrophic metabolizers are responsible for benzoate degradation in association with a hydrogen/formate-using methanogens (McInerney et al., 2008). *Sporotomaculum syntrophicum* (Qiu et al., 2003), *Syntrophorhabdus aromaticivorans* (Qiu et al., 2008), *Pelotomaculum isothalicicus* (Qiu et al., 2006),

Pelotomaculum terethalicicum (Qiu et al., 2006), and members of the *Syntrophus* genus, *Syntrophus aciditrophicus* (Jackson, Bhupathiraju, Tanner, Woese, & McInerney, 1999), *Syntrophus buswellii* (Mountfort, Brulla, Krumholz, & Bryant, 1984), *Syntrophus gentianae* (Schocke & Schink, 1997) all catalyze the syntrophic degradation of benzoate in methanogenic environments.

R. palustris, a photoheterotrophic, α-Proteobacterium, degrades benzoate, 4-hydroxybenzoate, and cyclohexane-1-carboxylate (Dutton & Evans, 1969; Harwood et al., 1999). Under anaerobic conditions, *R. palustris* grows photosynthetically degrading aromatic compounds and is a model organism for anaerobic benzoate degradation (Harwood et al., 1999) (Figure 1.1). The first step in the degradation of benzoate, 4-hydroxybenzoate, and cyclohexane-1-carboxylate is the activation of these compounds to their respective CoA thioester (Kuver, Xu, & Gibson, 1995). The activation of substrates in *R. palustris* is catalyzed by an AMP-forming, acyl-CoA ligase that hydrolyzes ATP to AMP and pyrophosphate in the process (Egland, Gibson, & Harwood, 1995). 4-Hydroxybenzoyl-CoA and cyclohexane-1-carboxyl-CoA are converted benzoyl-CoA before ring cleavage (Fuchs, 2008). In *R. palustris*, benzoyl-CoA is reduced to cyclohex-1-ene-1-carboxyl-CoA by a benzoyl-CoA reductase, hydrolyzing two ATP molecules to transfer the first pair of electrons (Boll and Fuchs, 1995; Boll *et al*., 2000). It is unclear whether the conversion of benzoyl-CoA to cyclohex-1-ene-1-carboxyl-CoA is accomplished by a four-electron reduction reaction or whether the enzyme adds two electrons at a time (Fuchs, 2008). Cyclohex-1-ene-1-carboxyl-CoA is converted to pimelyl-CoA by hydroxylation, oxidation of

the hydroxyl group, and hydrolytic cleavage to pimelyl-CoA (Fuchs, 2008; Perrotta & Harwood, 1994) (Figure 1.1). Pimelyl-CoA is subsequently converted to 2-heptenedioyl-CoA and hydroxylated to 3-hydroxypimelyl-CoA (Figure 1.1). 3-Hydroxylpimelyl-CoA is metabolized by the β-oxidation to acetyl-CoA and carbon dioxide (Figure 1.1) (Perrotta & Harwood, 1994). The acetyl-CoA generated by the oxidation of benzoate is used by *R. palustris* as either a carbon source for biosynthesis, or metabolized to carbon dioxide. In the activation and reduction of benzoate, four ATP equivalents are consumed (two ATP during activation when ATP is hydrolyzed to two phosphates and two ATP during ring reduction) (Fuchs, 2008). *R. palustris* is able to provide the ATP needed for benzoate metabolism through photosynthesis (Fuchs, 2008).

Figure 1.1: Anaerobic benzoate metabolism in *R. palustris*, *T. aromatica*, *S. aciditrophicus*, and *G. metallireducens*.

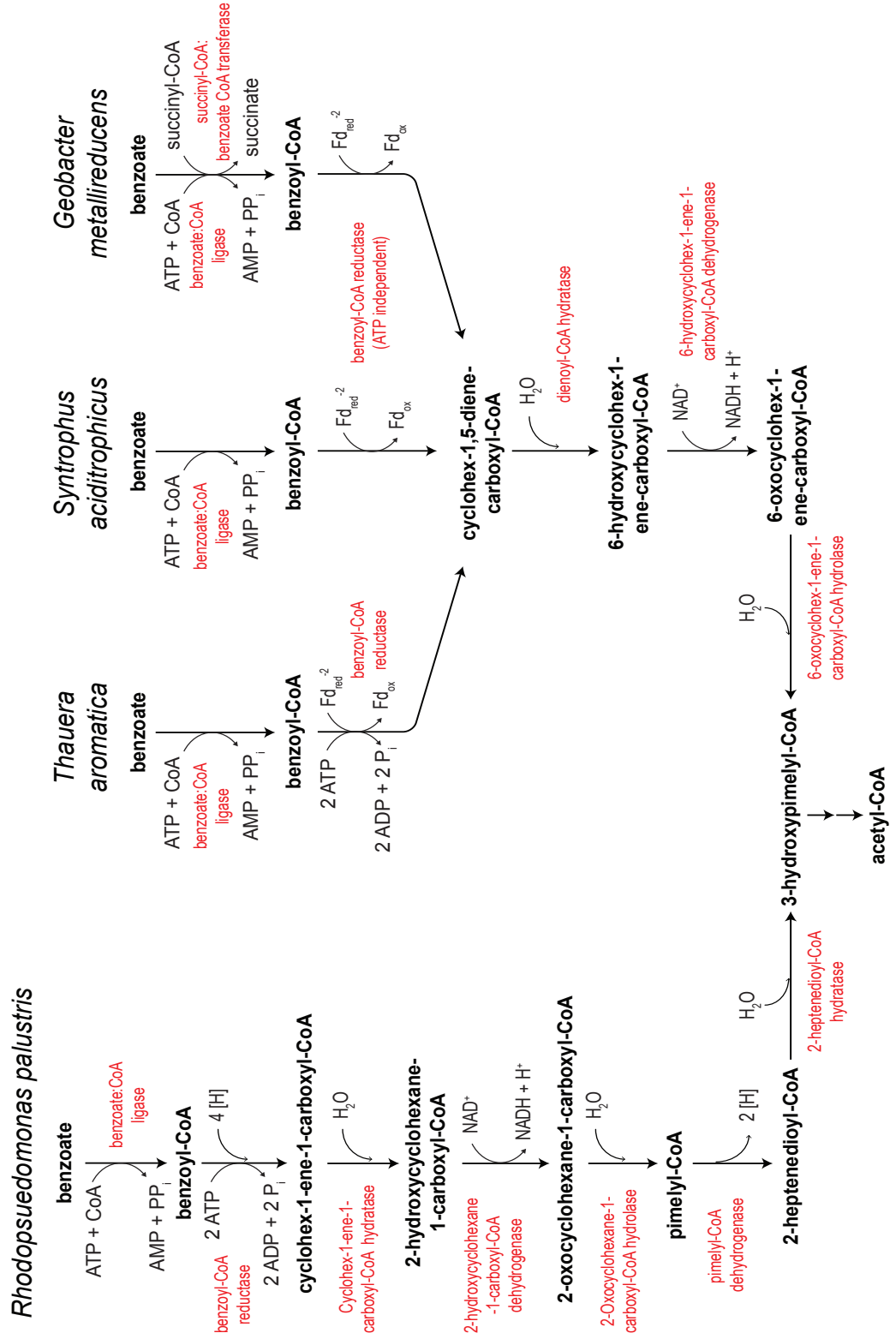

The iron-reducer, *G. metallireducins*, and the denitryifing, *T. aromatica*, use a different set of enzymes to degrade benzoate than does *R. palustris* (Figure 1.1). The activation of benzoate to benzoyl-CoA is catalyzed by an AMP-forming, acyl-CoA ligase similar to *R. palustris,* which hydrolyzes ATP to AMP and pyrophosphate and subsequently hydrolyzes pyrophosphate, consuming 2 ATP equivalents (Egland et al., 1995). However, in *G. metallireducins,* the reductive dearomatization of benzoyl-CoA to cyclohex-1,5-diene-1-carboxyl-CoA is a two-electron reduction step that is ATP independent (Fuchs, 2008). The energy needed to drive ring reduction in *G. metallireducins* is not known at this time. In *T. aromatica* the reduction of benzoyl-CoA to cyclohex-1,5-diene carboxyl-CoA requires the hydrolysis of two ATP to ADP and reduced ferredoxin. For both *T. aromatica*, and *G. metallireducins*, cyclohex-1,5-diene-1-carboxyl-CoA is metabolized to 3-hydroxypimelyl-CoA by a different set of enzymes than those used by *R. palustris*, cyclohex-1,5-diene carboxyl-CoA hydratase, 6-hydroxycyclohex-1-ene-carboxyl-CoA dehydrogenase, and 6-oxocyclohex-1-ene-1-carboxyl-CoA hydrolase (Figure 1.1) (Fuchs, 2008). 3-Hydroxypimelyl-CoA is then converted to acetyl-CoA by β-oxidation. Three molecules of acetyl-CoA formed from benzoate are oxidized to carbon dioxide by the tricarboxylic acid cycle. The energy needed for benzoate activation and reduction comes from electron transport-linked phosphorylation during iron respiration in *G. metallireducins* and nitrate respiration for *T. aromatica* (Fuchs, 2008).

S. aciditrophicus is a member of the Deltaproteobacteria, and syntrophically degrades benzoate, alicyclic compounds such as cyclohexane-1-carboxylate, and some fatty acids when grown in coculture with hydrogen and/or formate-using microorganisms (Jackson et al., 1999). *S. aciditrophicus* is a model benzoate degrader and can grow in pure culture by fermenting crotonate. (Elshahed, Bhupathiraju, Wofford, Nanny, & McInerney, 2001; Hopkins, McInerney, & Warikoo, 1995; Jackson et al., 1999; Mouttaki, Nanny, & McInerney, 2008). The genome of *S. aciditrophicus* has been sequenced, allowing for further insight into the syntrophic lifestyle (McInerney et al., 2007). *S. aciditrophicus* has genes homologous to those for benzoyl-CoA metabolism in *G. metallireducins* (Fuchs, 2008; Peters et al., 2007). Benzoate is first activated by a benzoyl-CoA ligase, which is an ATP-dependent reaction as in *G. metallireducins, T. aromatica*, and *R. palustris* (Figure 1.1). In the next step, the reduction of benzoyl-CoA to cyclohex-1,5-diene carboxyl CoA is catalyzed by an ATP-independent benzoyl-CoA reductase homologous to that found in *G. metallireducins* (Figure 1.1). The energy needed to reduce the ring is most likely obtained by electron bifurcation (Sieber, 2011). Cyclohexane-1-carboxylate and cyclohex-1-ene-1-carboxylate are metabolized to cyclohex-1,5-diene-1-carboxyl-CoA (Figure 1.2) (Kung, Seifert, von Bergen, & Boll, 2013). *S. aciditrophicus* metabolizes cyclohex-1,5-diene-1-carboxyl-CoA to 3-hydroxypimelyl-CoA by the same enzymes as found in *G. metallireducins* and *T. aromatica*: cyclohex-1,5-diene-1-carboxyl-CoA hydratase, 6-hydroxycyclohex-1-ene-1-carboxyl-CoA dehydrogenase, and 6-oxocyclohex-1-ene-1-carboxyl-CoA

hydrolase (Kuntze et al., 2008; Peters, Shinoda, McInerney, & Boll, 2007). 3-Hydroxypimelyl-CoA is then metabolized to acetyl-CoA by the β-oxidation pathway (Figure 1.2). The syntrophic metabolism of benzoate, alicyclic acids and fatty acids by *S. aciditrophicus* leads to the production acetyl-CoA, which is then metabolized to acetate (Figure 1.2). *S. aciditrophicus* does not oxidize acetyl-CoA to carbon dioxide by respiration as does *G. metallireducins* and *T. aromatica,* nor does *S. aciditrophicus* have a photosynthetic system to acquire energy as does *R. palustris*. Rather, *S. aciditrophicus* uses acetyl-CoA to synthesize ATP via substrate-level phosphorylation, and gets one mole of ATP per mole of acetyl-CoA (Elshahed et al., 2001). Thus, *S. aciditrophicus* gets three ATP per benzoate, and two ATP per crotonate. However, the enzymes used by *S. aciditrophicus* for ATP formation from acetyl-CoA are unclear.

Figure 1.2: Metabolism of benzoate, cyclohexane-1-carboxylate, and crotonate by *S. aciditrophicus*.

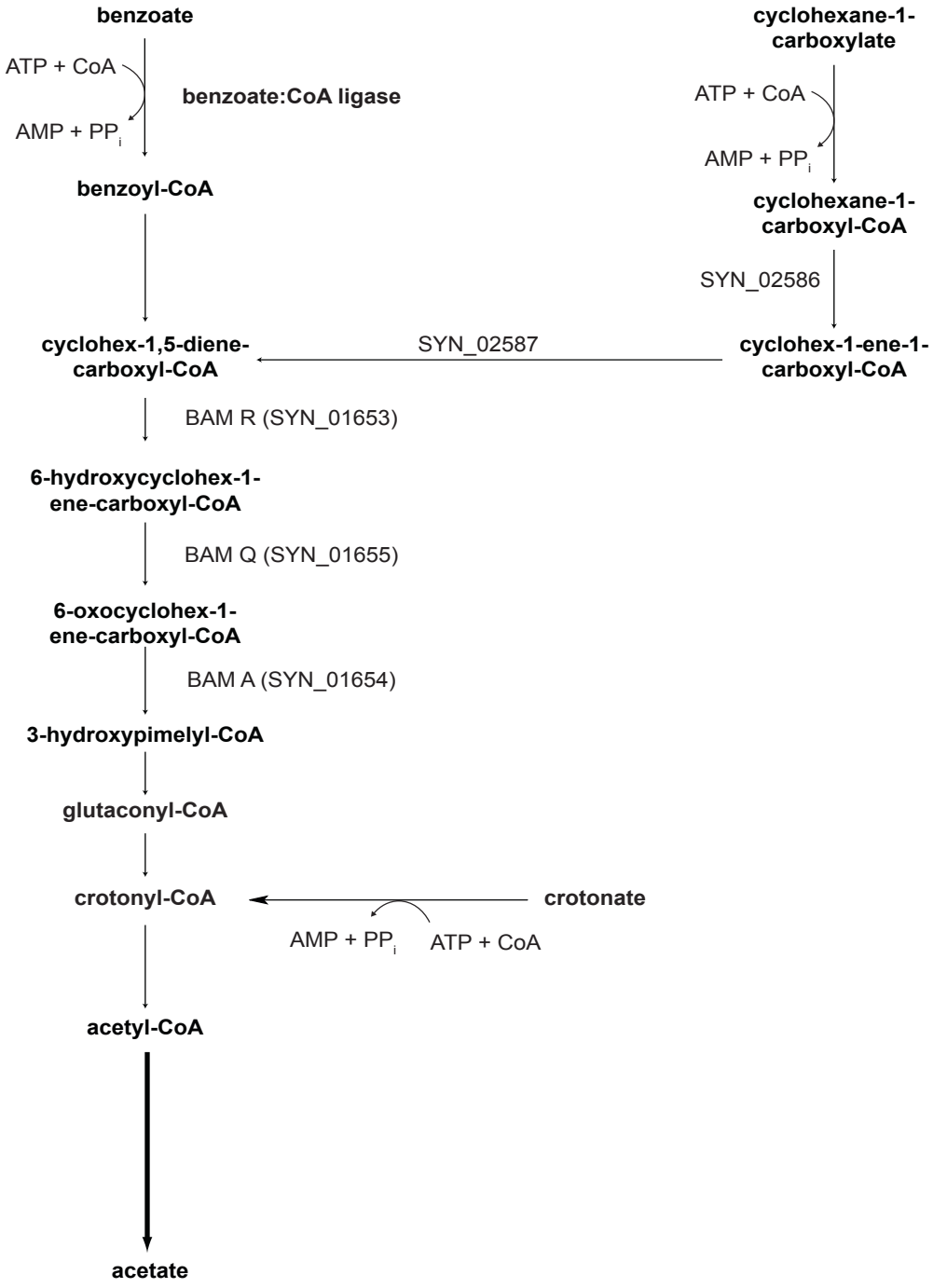

There are three known methods that convert acetyl-CoA to ATP and acetate, each catalyzed by different enzymes (Figure 1.3). The most common approach, which is used by almost all fermentative bacteria, is catalyzed by two enzymes, phosphotransacetylase and acetate kinase (Ingram-Smith, Martin, & Smith, 2006). Phosphotransacetylase first converts acetyl-CoA to acetyl-phosphate, which is then used by acetate kinase to phosphorylate ADP to ATP (Figure 1.3) (Wanner & Wilmes-Riesenberg, 1992). Another method for making ATP and acetate from acetyl-CoA is catalyzed by one enzyme, an ADP-forming, acetyl-CoA synthetase. ADP-forming, acetyl-CoA synthetases are primarly used by acetate-producing archaea and some eukaryotic microorganisms (Figure 1.3). ADP-forming, acetyl-CoA synthetases convert acetyl-CoA to acetate and in the process phosphorylate ADP to ATP (Glasemacher, Bock, Schmid, & Schonheit, 1997). Lastly, an AMP-forming, acetyl-CoA synthetase has been shown to synthesize ATP from AMP in *Aspergillus nidulans,* a fungus capable of nitrate reduction (Figure 1.3) (Takasaki et al., 2004). This is the only published instance where an AMP-forming, acetyl-CoA synthetase is used to make ATP. AMP-forming, acetyl-CoA synthetases are found in all domains of life, most often, to make acetyl-CoA when organisms grow with acetate as the carbon and/or energy source (Takasaki et al., 2004).

Figure 1.3: Known enzymes that make ATP from acetyl-CoA by substrate-level phosphorylation.

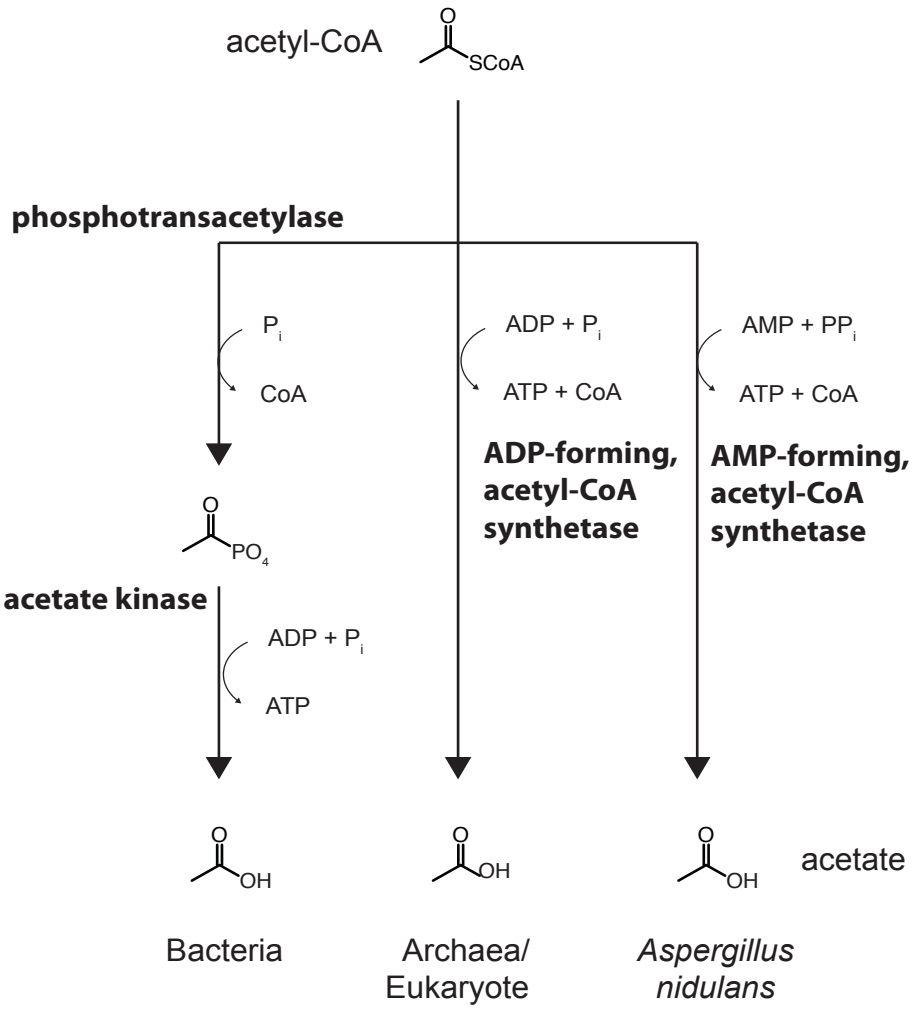

Genomic analysis of *S. aciditrophicus* revealed three possible strategies for ATP formation from acetyl-CoA. As previously stated, most fermentative microorganisms use acetate kinase and phosphotransacetylase to make ATP from acetyl-CoA. The genome of *S. aciditrophicus* lacks homologs for both acetate kinase and phosphotransacetylase (McInerney et al., 2007), and cell-free extracts have very low activities for acetate kinase and phosphotransacetylase (Elshahed et al., 2001). However, *S. aciditrophicus* has two genes annotated as butyrate kinases each of which is associated with acetyl/butyryl transferase genes that could be used for ATP formation from acetyl-CoA. In addition, *S. aciditrophicus* has nine ADP-forming, acetyl-CoA synthetase genes, and two AMP-forming, acetyl-CoA synthetase genes (McInerney et al., 2007).

The predicted UniProtKB proteomes of other Deltaproteobacteria were analyzed to determine whether acetate kinases and phosphotransacetylase genes were absent in other fermenting organisms. BLAST searches using HAMAP (http://hamap.expasy.org/proteomes.html) were performed with the following deduced amino acid sequences: acetate kinase from *Escherichia coli*, ACKA_ECOLI, the annotated butyrate kinase from *S. aciditrophicus*, SYN_03090, the phosphotransacetylase from *E. coli*, PTA_ECOLI, and the annotated phosphate/butyryl transferase gene from *S. aciditrophicus*, SYN_00654. Of the 51 proteomes listed in the Deltaproteobacteria on HAMAP, five anaerobic microorganisms were identified that did not have either acetate kinase, butyrate kinase, phosphotransactylase, or phosphobutylryltransferases annotated in the genomes: *Desulfobacterium autotrophicum* (strain ATCC

43914/DSM 3382/HRM2), *Desulfovibrio magneticus* (strain ATCC 700980 / DSM 13731 /RS-1), *Desulfococcus oleovorans* (strain DSM 6200 / Hxd3), *Desulfobacula toluolica* (strain DSM 7467 / Tol2), and *Hippea maritima* (strain ATCC 700847 / DSM 10411 / MH2). All of these Deltaproteobacteria are sulfate reducers capable of metabolizing a variety of growth substrates to acetyl-CoA which is then oxidized to carbon dioxide (Matsunaga, Nemoto, Arakaki, & Tanaka, 2009; Miroshnichenko, Rainey, Rhode, & Bonch-Osmolovskaya, 1999; Wohlbrand et al., 2013). Organisms capable of oxidizing acetyl-CoA to carbon dioxide would not need acetate kinases or phosphotransacetylases to make acetate.

After identifying members of the Deltaproteobacteria that did not have acetate kinases or phosphotransacetylase, I performed BLAST analysis within the Clostridia, a class within the Firmicutes phylum. Of the 108 genomes on HAMAP for Clostridia, six were identified that did not have genes annotated as acetate kinase, butyrate kinase, phosphotransactylase, or phosphobutylryltransferases: *Ammonifex degensii* (strain DSM 10501 / KC4), *Desulforudis audaxviator* (strain MP104C), *Desulfotomaculum kuznetsovii* (strain DSM 6115 / VKM B-1805 / 17), *Pelotomaculum thermopropionicum* (strain DSM 13744 / JCM 10971 / SI), *Sulfobacillus acidophilus* (strain ATCC 700253 / DSM 10332 / NAL), *Sulfobacillus acidophilus* (strain TPY). In addition, there were members of the Clostridia that had an annotated acetate kinase but no phosphotransacetylase: *Desulfitobacterium dichloroeliminans* (strain LMG P-21439 / DCA1), *Heliobacterium modesticaldum* (strain ATCC 51547 / Ice1),

Moorella thermoacetica (strain ATCC 39073), and *Syntrophobotulus glycolicus* (strain DSM 8271/FlGlyR). Of the members of the Firmicutes that do not have both acetate kinases or phosphotransacetylases*, A. degensii*, *H. modesticaldum*, and *M. thermoaceticum* are known to make acetate during growth. *A. degensii* is generally an autotropic organism, but can ferment pyruvate to acetate, carbon dioxide and hydrogen (Huber et al., 1996). *H. modesticaldum* produces acetate during both phototrophic and chemotrophic growth on substrates (Sattley et al., 2008). *M. thermoacetica* also produces acetate and grows on a variety of substrates including sugars such as glucose, alcohols, organic acids, and methoyxlated aromatic compounds (Drake & Daniel, 2004). *M. thermoacetica* does have an annotated acetate kinase (MOTH_0940), but it does not have a phosphotranscacetylase, and the genes upstream and downstream of the acetate kinase (MOTH_0939 and MOTH_0941) are proteins of unknown function. The absence of gene homologues for both acetate kinase and phosphotransacetylase for organisms that are known to produce acetate suggests there are other enzyme systems within these organisms that are used to make acetate and ATP from acetyl-CoA. To determine whether or not *A. degensii, H. modesticaldum*, and *M. thermoacetica*, had ADP-forming, acetyl-CoA synthetases and/or AMP-forming, acetyl-CoA synthetases, I used HAMAP to blast the predicted proteomes against annotated AMP-forming, acetyl-CoA synthetase, SYN_02635, and the ADP-forming, acetyl-CoA synthetase, SYN_02609, both from *S. aciditrophicus*. The BLAST results indicated that *A. degensii, H. modesticaldum*, and *M. thermoacetica*all had possible AMP-forming,

acetyl-CoA synthetases. *A. degensii* had two possible AMP-forming, acetyl-CoA synthetases, one was annotated as an acetyl-CoA synthetase (ADEG_1852) and the other annotated as an acetate/CoA ligase (ADEG_1846). *H. modesticaldum* had two possible AMP-forming acetyl-CoA synthetases, and both of them annotated as acetyl-CoA synthetases (HELMI_09900 and HELMI_10420). *M. thermoacetica* had one possible AMP-forming, acetyl-CoA synthetase annotated as an AMP-dependent synthetase and ligase (MOTH_0503).

Here, I use proteomics, transcriptomic and enzymatic analyses to determine the mechanism of ATP formation from acetyl-CoA by *S. aciditrophicus*. The analyses lead to the conclusion that *S. aciditrophicus* uses an AMP-forming, acetyl-CoA synthetase to synthesize ATP from acetyl-CoA. In additon, I heterologously expressed the gene product for SYN_03090 and showed that it functions as an acetate kinase and could also be used by *S. aciditrophicus* to make ATP from acetyl-CoA. Lastly, I used protein purification and recombinant DNA approaches to identify the gene products involved in the activation of crotonate, benzoate, and cyclohexane-1-carboxylate in *S. aciditrophicus*. Two crotonate/benzoate:CoA ligases were purified and characterized from cell-free extracts of *S. aciditrophicus*. In addition, heterologous expression of SYN_03128 showed that its gene product is likely involved in the activation of cyclohexane-1-carboxylate and cyclohex-1-ene-1-carboxylate. The identification of the above three ligase enzymes confirms that *S. aciditrophicus* uses ligases rather than coenzyme A transferase reactions for substrate activation.

Chapter 2: *Syntrophus aciditrophicus* uses an AMP-forming, acetyl-CoA synthetase to make acetate and ATP via substrate-level phosphorylation

Abstract

Syntrophus aciditrophicus (SB) degrades benzoate, cyclohexane-1-carboxylate and certain fatty acids in syntrophic association with hydrogen/formate-using microorganisms and ferments crotonate in pure culture. ATP formation coupled to acetate production is the main source for energy conservation by *S. aciditrophicus.* However, the method by which *S. aciditrophicus* synthesizes ATP from acetyl-CoA is unclear. The genome of *S. aciditrophicus* does not contain an acetate kinase gene, but has two genes for butyrate kinase, several genes for AMP-forming, acetyl-CoA synthetases, and nine genes for archaeal ADP-forming, acetyl-CoA synthetases, all of which could be used to synthesize ATP from acetyl-CoA. Two-dimensional gel electrophoresis and quantitative-real time-polymerase chain reaction detected peptides and transcripts, respectively, from AMP-forming, acetyl-CoA synthetase, ADP-forming, acetyl-CoA synthetases, and butyrate kinase genes. Acetyl-CoA synthetase activity was high (0.5 ± 0.01 to 7.4 ± 0.3 μmol min^{-1} mg^{-1} of protein) in cell-free extracts of *S. aciditrophicus* grown in pure culture on crotonate or in coculture with *Methanospirillum hungatei* on crotonate, benzoate and cyclohexane-1-carboxylate. Acetate kinase, butyrate kinase and phosphotransacetylase activities were low (< 0.2 ± 0.03 μmol min^{-1} mg^{-1} of protein) and only detected in cell-free extracts of crotonate-grown pure and coculture cells. Only the acetyl-CoA synthetase activity was high enough to account for the acetate production rate (1.2 ± 0.2 μmol min^{-1} mg^{-1} of protein) during crotonate growth. Inhibition of the native adenylate kinase showed that

the dominant acetyl-CoA synthetase activity was AMP-forming, acetyl-CoA synthetase; ADP-forming, acetyl-CoA synthetase activity was not detected. The acetyl-CoA synthetase activity was purified to homogeneity with an 80% recovery. The purified protein was an AMP-forming, acetyl-CoA synthetase encoded by gene SYN_02635 (*acs1*), which had a V_{max} of 7.5 ± 1.2 μmol min^{-1} mg^{-1} of protein and K_m of 0.41 mM acetyl-CoA in the acetate-forming direction, sufficient to account for the acetate production rates under all growth conditions. The recombinant Acs1 had similar kinetic properties. Transcripts of *acs1* represented 0.58 to 0.76% of the total transcriptome compared to 0 to 0.1% for the other possible candidates. Polypeptides of the Acs1 represented 1.3 to 4.4% of the total peptides detected compared to 0 to 0.1% for other possible candidates. The above analyses show that *S. aciditrophicus* uses Acs1 as the main enzyme for ATP formation from acetyl-CoA as opposed to the phosphotransacetylase and acetate kinase or ADP-forming, acetyl-CoA synthetase used by acetate-forming *Bacteria* and *Archaea*, respectively.

Introduction

In anaerobic environments the degradation of natural polymers such as polysaccharides, proteins, lipids and nucleic acids to methane and carbon dioxide involves a diverse community of interacting microorganisms and proceeds in discrete metabolic steps. In the first step, fermentative microorganisms hydrolyze complex polymers into monomeric units that are fermented to acetate and longer chain fatty acids, aromatic compounds like benzoate, alcohols, formate, hydrogen, and carbon dioxide (McInerney, Sieber, & Gunsalus, 2009; McInerney et al., 2008). In the next step, a second group of fermenting microorganisms, syntrophic metabolizers, degrade propionate, longer chain fatty acids, aromatic compounds, and alcohols to methanogenic substrates, formate, acetate, hydrogen and carbon dioxide. Methanogens convert the acetate, formate, hydrogen, and carbon dioxide made by other microorganisms to methane and carbon dioxide. Syntrophic metabolizers reoxidize their reduced cofactors by reducing protons or carbon dioxide to produce hydrogen or formate, respectively. However, hydrogen or formate production from these electron carriers is thermodynamically unfavorable unless the concentrations of hydrogen and formate are very low (Sieber et al., 2012). Hydrogen and formate-using microorganisms such as methanogens maintain low levels of hydrogen and formate, which allows the catabolic reactions of syntrophic metabolizers to be thermodynamically favorable.

The anaerobic catabolism of many aromatic compounds, such as monomers derived from lignin, halogenated aromatic compounds, and aromatic

hydrocarbons, converges to benzoate and its CoA derivative, benzoyl-CoA, prior to ring reduction and cleavage (Harwood et al. 2001). In methanogenic environments, syntrophic metabolizers catalyze the reduction and cleavage of benzoyl-CoA (McInerney et al., 2008). Microorganisms capable of syntrophically degrading aromatic compounds include *Sporotomaculum syntrophicum* (Qiu et al., 2003), *Pelotomaculum terephthalicicum* and *Pelotomaculum isophthalicicum* (Qiu et al., 2006), and three species in the genus *Syntrophus, S. buswellii* (Mountfort et al., 1984), *S. gentianae* (Schocke & Schink, 1997) and *S. aciditrophicus* (Jackson et al., 1999). *Syntrophus aciditrophicus* syntrophically degrades benzoate, alicyclic compounds such as cyclohexane-1-carboxylate, and some fatty acids when grown in coculture with hydrogen and/or formate-using microorganisms (Elshahed et al., 2001; Jackson et al., 1999). It can grow in pure culture on crotonate and crotonate plus benzoate (Hopkins et al., 1995; Mouttaki et al., 2008). *S. aciditrophicus* has served as the model organism to study the pathway involved in syntrophic benzoyl-CoA metabolism (Elshahed & McInerney, 2001; Mouttaki, Nanny, & McInerney, 2007; Peters et al., 2007) and its genome has been sequenced (McInerney et al., 2007). *S. aciditrophicus* has genes homologous to those for benzyl-CoA metabolism in *Geobacter metallireducens* (Peters et al., 2007), where benzoyl-CoA is reduced to cyclohex-1,5-diene-1-carboxyl-CoA in an ATP-independent reaction. Cyclohexane-1-carboxylate and 1-cyclohexene-1-carboxylate are metabolized to cyclohex-1,5-diene-1-carboxyl-CoA (Kung et al., 2013). Cyclohex-1,5-diene-1-carboxyl-CoA is metabolized to 3-hydroxypimelyl-CoA

(Kuntze et al., 2008; Peters et al., 2007), which is then metabolized to acetyl-CoA by β-oxidation. Thus, the syntrophic metabolism of benzoate, alicyclic acids and fatty acids by *S. aciditrophicus* leads to the production of acetyl-CoA, which is then metabolized to acetate. ATP formation coupled to acetate formation is the main mechanism of energy conservation by *S. aciditrophicus*. However, the method used by *S. aciditrophicus* for ATP formation from acetyl-CoA is unclear.

Almost all fermentative bacteria use two enzymes, phosphotransacetylase and acetate kinase, to synthesize ATP and acetate from acetyl-CoA. However, the genome of *S. aciditrophicus* lacks a homolog for acetate kinase and cell-free extracts have very low acetate kinase and phosphotransacetylase activities (Balch, Fox, Magrum, Woese, & Wolfe, 1979; McInerney et al., 2007). *S. gentianae* and *S. buswellii* also have low acetate kinase activities and phosphotransacetylase activity was not detected in *S. buswellii* grown either in pure culture or in coculture (Auburger & Winter, 1996; Schocke & Schink, 1997). *S. aciditrophicus* has two gene clusters, each with a butyrate kinase gene and two phosphate acetyl/butyryl transferase genes, which could function to make ATP (Figure 2.1) (McInerney et al., 2007). In addition, *S. aciditrophicus* contains nine genes predicted to encode archaeal ADP-forming, acetyl-CoA synthatases (McInerney et al., 2007), which acetate-forming archaea use to make ATP from acetyl-CoA (Glasemacher et al., 1997). Lastly, there are two AMP-forming, acetyl-CoA synthetases, which could be used to make ATP from acetyl-CoA, AMP and pyrophosphate (Figure 2.1). However,

only *Aspergillus nidulans* is known to use an AMP-forming, acetyl-CoA synthetase for ATP synthesis (Takasaki et al., 2004).

Here, I use proteomics, transcriptomic and enzymatic analyses to determine the mechanism of ATP formation from acetyl-CoA by *S. aciditrophicus*. The analyses lead to the conclusion that *S. aciditrophicus* uses an AMP-forming, acetyl-CoA synthetase to synthesize ATP from acetyl-CoA.

Figure 2.1: Mechanisms for ATP synthesis by substrate-level phosphorylation in S*. aciditrophicus* with annotated locus ID tags for candidate genes.

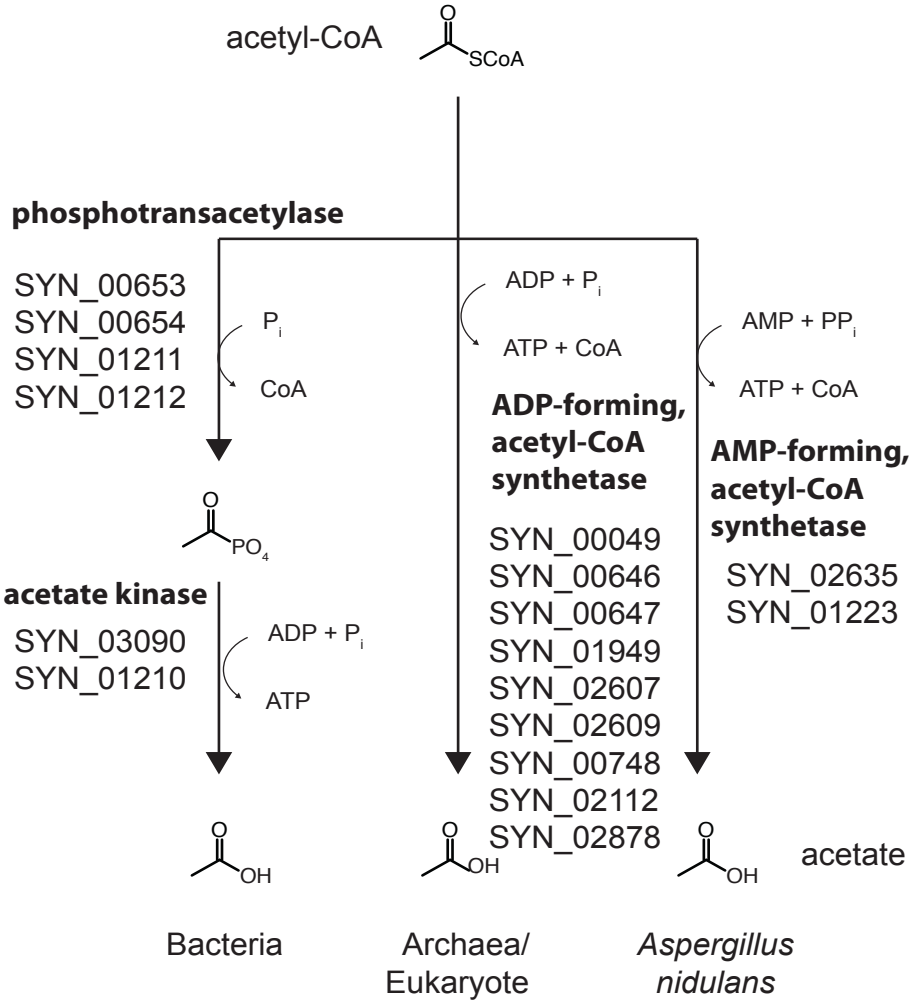

Materials and Methods

Media and conditions for cultivation. *Syntrophus aciditrophicus* strain SB (DSM 26646) was grown anaerobically in a minimal medium without rumen fluid amended with 2.5% cysteine sulfide, 3.75 g/L of sodium bicarbonate, and 0.1% resazurin (McInerney and Bryant, 1979). The Wolin's metal solution was modified to include $Na_2MoO_4{\cdot}2H_2O$ (0.01g/L) Na_2SeO_4 (0.01g/L) and $Na_2WO_4{\cdot}2H_2O$ (0.01g/L) (Sieber, Le, & McInerney, 2014). Stock solutions of the modified Wolin's trace metals and Balch vitamins were added at a volume of 5 ml/L and 10 ml/L (Balch et al., 1979; Sieber et al., 2014). The headspace was pressurized to 27.5 kPa with a mixture of N_2/CO_2 (80% : 20%, vol/vol). *S. aciditrophicus* was grown in pure culture on 20 mM crotonate or 20 mM crotonate plus 5 mM benzoate. *S. aciditrophicus* was also grown in coculture with *Methanospirillum hungatei* JF1 (ATCC 27890) on 20 mM crotonate, 10 mM benzoate, and 10 mM cyclohexane-1-carboxylate. *M. hungatei* was grown in pure culture on hydrogen in 160 ml serum bottles on Pfennig's medium amended with 5 mM acetate. Cultures of *M. hungatei* were pressurized daily with H_2/CO_2 (80% : 20%, vol/vol) pressurized to 137 kPa (Crable, 2013). All cultures were checked for contamination using thioglycollate medium, which does not support the growth of *S. aciditrophicus* and by microscopic analysis.

Cell harvesting. For two-dimensional (2-D) gel electrophoresis proteome analysis, enzyme activity determination, and enzyme purification, cultures were grown in 1.5-L volumes in 2-L Schott bottles with the substrates indicated above, and harvested at mid-log phase by centrifugation (14,300 x g,

20min, 4°C). Cells were resuspended in 50 mM anoxic phosphate buffer (pH 8.5). Pellets were stored at -80°C until use. For cell-free extract preparation, pellets were broken by French press (82.7 MPa), and the lysate was ultracentrifuged (120,000 x g, 1 hour, 4°C), and designated the cell-free extract. For coculture pellets, *S. aciditrophicus* cells were separated from *M. hungatei* cells using Percoll density gradient centrifugation as described previously (Beaty, Wofford, & McInerney, 1987; Sieber et al., 2014).

For quantitative reverse transcriptase polymerase chain reactions (qRT-PCR) analysis and RNA sequencing. Cells were grown in triplicate cultures as described above in 500-ml Schott bottles and 250-ml serum bottles. Cultures were monitored daily for substrate loss and methane production. A one-milliliter sample was taken daily to measure the optical density at 600 nm and determine substrate concentrations. Cultures were grown to 50% substrate loss and then transferred to new medium using 30% inoculum. After the third consecutive transfer, cells were harvested at 50% substrate loss. Cell activity was terminated by cooling at 4°C using dry ice and ethanol (Sieber et al., 2014). Cultures were then centrifuged (14,300 x g, 20 min, 4°C), and the cell pellets were resuspended in 1 ml of RNA later. RNA was extracted using Qiagen RNA extraction kit.

2-D gel electrophoresis proteome of *S. aciditrophicus*. The proteome of *S. aciditrophicus* grown as described above in pure culture with crotonate and with crotonate plus benzoate was analyzed by the combination of 2D-gel and nanoelectrospray liquid chromotography tandem mass spectrometry (LC-

MS/MS) (Mouttaki, 2007). Proteins were separated by 2-D gels electrophoresis, excised, and digested with trypsin, and analyzed by nanoelectrospray LC-MS/MS (Mouttaki, 2007). Protein identification was accomplished by utilizing the Mascot database search engine (Matrix Science, London, UK) and was based on standard Mascot criteria for statistical analysis of the LC-MS/MS data (Mouttaki, 2007).

qRT-PCR preparation. For quantitative reverse transcriptase polymerase chain reactions (qRT-PCR) analysis, methods for cultivation, RNA preparation, and qRT-PCR amplification were described previously (Bustin et al., 2009; Sieber et al., 2014). RNA was checked for DNA contamination by PCR amplification without reverse transcriptase using gene SYN_0646 primers, annotated as an ADP-forming, acetyl-CoA synthetase. Primers were designed using primer-BLAST on NCBI. Potential primer sequences were further analyzed for tertiary structures and primer dimers using Net Primer-Premier Biosoft International. Primers were synthesized by Life Technologies (Carlsbad, CA) and are listed in Table 2.1. All primers were tested against *S. aciditrophicus* DNA and *M. hungatei* DNA as template for PCR amplification. One PCR product band was observed on 8% agarose for each primer set using DNA from *S. aciditrophicus*, and no PCR products were observed using DNA from *M. hungatei*.

Table 2.1: Primers used for quantitative reverse transcriptase polymerase chain reaction analysis substrate-level phosphorylation gene candidates.

Predicted function	Locus Tag	Gene ID	Sequence (5'--> 3')
Acetyl-CoA synthetase (ADP-forming)	SYN_00049	637860402	GTTGACCTGGCGATCATTTT GCTTTATTGCCGATGGAACA
	SYN_00646	637860401	GTGCTCGCAAAAGATGAGAA AATGAAACGTCATTGAGGGC
	SYN_00748	637860516	TGATCAAAGCCAGGAGTCTT TGCGAGCAGCGACCGCAGGT
	SYN_01949	637859111	ACATTCTCGAGTATCTGGGC AGGTAGAGCGTATCCGTAGA
	SYN_02112	637859378	CGTAAGATCCTGCTTGGAGA CAAGTTTGAGACCAACGAGG
	SYN_02607	637858761	AAGAGACAAGGATTTCGGCT AGTCTTCGCTGGATTGGATT
	SYN_02609	637858763	TCGATTACCGGATCTATGGC CGGAAGGACAAAGGAAAAGG
	SYN_02878	637860278	GAAAGCATGGAACGGCTAAA TCAGGGGTTTCATAGTTCGG
Acetyl-CoA synthetase (AMP-forming)	SYN_01223	637860804	AACGATGTCTACCGACGAAT TAGATGGTTACGCGATCTCC
	SYN_02635	637860993	GAGCTGAAGAACATGGAAGC TGTAGGCATAGATGGACTGC
Butyrate kinase	SYN_01210/ SYN_03090[a]	637860790 / 637860410	AGGAAAACGATTTCGGATGC CTCCCGCTGATACTTCTTCA

[a]Genes SYN_01210 and SYN_03090 share over 99% nucleotide identity. The primer set designed would amplify transcripts for both SYN_01210 and SYN_03090.

Quantitative reverse transcriptase polymerase chain reactions (qRT-PCR) amplification was performed using biological triplicates for all growth conditions. In addition, technical duplicates for each biological replicate were analyzed. qRT-PCR was performed using BioRad's Reverse Transcriptase for One-Step RT-PCR. The amplification parameters for the BioRad MyIQ Single Color Real Time PCR Detection System were as follow: 50°C for ten minutes, 95°C for five minutes, 95°C for ten seconds, and 56°C for 30 seconds. To calculate the fold expression of each transcript relative to DNA gyrase, the average of the triplicate threshold cycle number (Ct) was used in the following equation:

Fold Expression Relative to DNA Gyrase = Efficiency Test $^{Ct\ test}$/ Efficiency Reference $^{Ct\ Reference}$ (Pfaffl, 2001).

Enzyme assays. All enzyme assays were performed anaerobically and aerobically to determine if the activities were affected by oxygen. All activities were linear with time and proportional with the protein concentration. Controls for all assays included the deletion of each substrate and the cell-free extract, and the use of heat-treated extracts. All assays were performed at 37°C. Assay buffers were aliquoted in 1 cm cuvettes and warmed to 37°C in water bath prior to addition of reagents.

Acetate kinase and butyrate kinase activities were determined by following the formation of the hydroxymate (Bowman, Valdez, & Nishimura, 1976). The assay mixture contained 50 mM tris(hydroxymethyl)aminomethane (Tris) (pH 8.3), 10 mM ATP, 10 mM magnesium chloride, 0.5 M hydroxylamine,

and 20 mM potassium acetate or sodium butyrate. The reaction was stopped after 20 minutes at 37°C by the addition of ferric reagent (10% iron chloride, 3% trichloroacetic acid, in 0.7 N hydrochloric acid) and the reaction mixture was centrifuged for 5 minutes at 13,000 x g. The molar extinction coefficient for acetyl hydroxamate was 594 $M^{-1}cm^{-1}$ at 535 nm.

Phosphotransacetylase activities were measured using arsenolysis combined with the hydroxymate assay as described previously (Bergmeyer, Holz, Klotzsch, & Lang, 1963; Stadtman, 1952). The reaction mixture contained 10 mM Tris-HCl buffer (pH 8.6), 6 mM acetyl phosphate, 100 mM cysteine, 100 mM potassium chloride, and 500 µM CoA. The reaction was started with the addition of 50 mM sodium arsenate and incubated for 45 minutes at 37°C. The reaction mixture was then diluted 1:1 with 2 M hydroxylamine and neutralized with potassium hydroxide. After 5 minutes, the reaction was stopped by the addition of trichloroacetic acid to a final concentration of 5%. The reaction mixture was brought to a final volume of 1.5 ml with 2.5% iron chloride in 2 M hydrochloric acid and incubated for 15 minutes at room temperature. The mixture was then centrifuged for 5 minutes at 13,000 x g and the absorbance at 540 nm was determined. Acetyl-phosphate standard curve was generated, and used to determine the remaining acetyl-phosphate in assay mixture.

AMP- and ADP-forming ligase activities were measured by coupling the AMP or ADP formation with pyruvate kinase (PK) and lactate dehydrogenase (LDH) to measure the oxidation of reduced nicotinamide adenine dinucleotide (NADH) spectrophotometrically at 340 nm (Schuhle et al., 2003). The assay

mixture contained 50 mM Tris-HCl buffer (pH 8.5), 10 mM magnesium chloride, 5 mM ATP, 1 mM phosphoenolpyruvate (PEP), 375 μM NADH, 2.8 U myokinase, 2.2 U pyruvate kinase, 2.2 U lactate dehydrogenase, and 480 μM coenzyme A (CoA). The reaction was started with the addition of the fatty acid. ADP-forming, acetyl-CoA synthetases was measured as above with the deletion of myokinase from the reaction mixture. The oxidation of NADH was measured at 340 nm and the extinction coefficient was 6220 M^{-1} cm^{-1} (McComb, Bond, Burnett, Keech, & Bowers, 1976).

Inhibition of native adenylate kinase. To determine the nucleotide specificity (ADP-forming versus AMP-forming) of acetyl-CoA synthetase activity purified from *S. aciditrophicus* cell-free extracts, adenylate kinase activity was inhibited with the addition of P1, P5-Di(Adenosine-5')Pentaphosphate (Ap5A) (Kurebayashi, Kodama, & Ogawa, 1980; Nageswara Rao & Cohn, 1977). Cell-free extracts were desalted on G20 column and adenylate kinase activity was measured by coupling ATP formation from ADP with the reduction of $NADP^+$ using glucose-6-phosphate dehydrogenase and hexokinase (Szasz, Gruber, & Bernt, 1976). Ap5A was added in a range of 0 to 1.5 mM. Once adenylate kinase activity was inhibited, ADP, phosphate, and acetyl-CoA were sequentially added to measure ADP-forming, acetyl-CoA synthetase activity. The absorbance at 340 nm was measured after each addition of substrate to determine which components were needed for $NADP^+$ reduction. As a control, AMP and pyrophosphate were also sequentially added to the reaction mixture, and

activity was measured after each addition to determine if an AMP-forming, acetyl-CoA synthetase activity was present.

Acetate production rates. Acetate production rates of *S. aciditrophicus* grown in pure culture and coculture with crotonate were calculated by measuring the growth rate (μ) and molar growth yields (Y) of triplicate 250-ml cultures. Substrate loss, protein concentration, and optical density were monitored with time (Mouttaki et al., 2007). The specific rate of crotonate use (q_s; μmol/min/mg) was calculated using the following expression: $q_c = u/Y$ (Stouthamer, 1973). The specific rate of acetate production was calculated by multiplying the specific rate of crotonate use by the stoichiometry of acetate production from crotonate (1.5 mol of acetate per mol of crotonate) (Mouttaki et al., 2007).

To measure acetate production rates in resting cell suspensions, 1.5-L cultures of *S. aciditrophicus* were grown on crotonate. The cells were harvested anaerobically in late log phase by centrifugation (18,000 rpm for 20 minutes at 24°C). Cell pellets were washed three times by resuspending in 50 mM anoxic phosphate buffer reduced with 2.5% cysteine sulfide (pH 7.5) and centrifugation. The final pellet was resuspended in 375 ml of resting medium. Resting medium was Pfennig's medium without ammonium chloride and vitamins, which was prepared anaerobically, and reduced with cysteine sulfide and amended with 1 mM crotonate. To deplete nutrients and prevent growth, the cells were repeatedly incubated overnight with 1 mM crotonate, and the optical density and protein concentrations were monitored. After no increase in

protein concentration was observed, the cells were washed as described above and pelleted anaerobically by centrifugation. The cell pellet was resuspended in 10 ml of 50 mM anoxic phosphate buffer, and the suspension was transferred to serum bottles with 75 ml of resting medium. Three cell volumes (2.5 ml, 0.5 ml, 0.025 ml) were used, each of which was done in triplicates to ensure the acetate production rate was proportional to cell concentration. To ensure that the cells were metabolically active, each bottle was amended with 1 mM crotonate and incubated overnight at 37°C. Bottles were then amended with 10 mM crotonate and incubated at 37°C. Samples were taken before addition of crotonate and every 30 minutes to measure absorbance, protein concentrations, and crotonate and acetate concentrations. Incubations with cells and without crotonate, with crotonate and no cells, and without cells and without crotonate served, as controls. All solutions and materials used to prepare and incubate washed cell suspensions were sterile.

Purification of acetate-producing activity. For purification of the dominant acetate-producing activity, approximately 2 grams of crotonate-grown, pure culture cells of *S. aciditrophicus* were broken by French pressure cell as described previously. The cell-free extracts were treated with 45% ammonium sulfate and centrifuged (21,000 x g, 10 minutes, 4°C). The soluble portion was desalted on a G20 column equilibrated with diethylaminoethyl (DEAE) binding buffer (20 mM triethanolamine (TEA) and 5 mM magnesium chloride, pH 7.8). Three milliliters of the desalted ammonium sulfate fraction were loaded onto a DEAE column at a flow rate of 3 ml per minute. Proteins

were eluted with DEAE elution buffer (DEAE binding buffer with 500 mM sodium chloride, pH 7.8) with a linear gradient of 0 to 200 mM sodium chloride and 1.5 ml fractions were collected. The active acetyl-CoA synthetase fractions were pooled, concentrated, and desalted using an Amicon filtration device with a 30-kDA molecular weight membrane filter. The concentrated activity was then loaded onto a hydroxyapatite column equilibrated with hydroxyapatite buffer (20 mM TEA, 5 mM magnesium chloride, and 5 mM potassium phosphate, pH 7.8) and the activity was eluted by using a step gradient with hydroxyapatite buffer with potassium phosphate at 5 mM, 20 mM, 40 mM, 60 mM, 100 mM, and 200 mM. The active acetyl-CoA synthetase fraction eluted at 40 mM potassium phosphate. Active fractions were pooled and concentrated with a 30 kDA molecular weight cut off membrane and with DEAE binding buffer. Two milliliters of concentrated active fraction were added to an affinity reactive green column equilibrated with DEAE binding buffer. Proteins were eluted with DEAE elution buffer. Acetyl-CoA synthetase activity was eluted in 500 mM sodium chloride. The reactive green fraction was analyzed on sodium dodecyl sulfate gel electrophoresis (SDS-gel) and a single band was observed. The band was excised and sent to the laboratory for Molecular Biology and Cytometry Research (Oklahoma City, USA) for in gel trypsin digestion and sequencing by high performance liquid chromatography and tandem mass spectrometry (HPLC/MS/MS) (University of Oklahoma Health Sciences Center Proteomics Core Facility, Oklahoma City, OK 73104).

Kinetic constants were determined for the homogenous reactive green fraction by non-linear regression data analysis fit to the Michaelis-Menten equation on Kaleidagraph (Synergy Software, Reading, PA). The K_m for purified acetyl-CoA synthetase fraction from *S. aciditrophicus* was determined with the following range of substrates: acetate (0.05 - 6 mM) and CoA (0.03 - 0.6 mM CoA) with the respective coenzyme A substrates kept at saturation. The K_m for acetyl-CoA was determined using a concentration range from 0.2 - 2 mM.

Expression of SYN_02635. Gene SYN_02635, annotated as an AMP-forming, acetyl-CoA synthetase, was amplified from *S. aciditrophicus* DNA using primers SYN_02635F and SYN_02635R (Table 2.2). Amplification was done using Phusion DNA polymerase (Fermentas) with the following PCR parameters: initial denaturation of five minutes at 95°C; 30 cycles of one minute denaturation at 95°C, one minute of annealing at 60 °C, and one minute of elongation at 72°C; followed by a final extension of five minutes at 72°C. The PCR product was ligated into Invitrogen PET_101 vector and transformed into *E. coli* Top 10 cells. After transformation, colonies were selected and screened using colony PCR and T7 forward and SYN_02635R primers. Plasmids with the correct PCR fragment size were extracted and sequenced by Oklahoma Memorial Research Foundation DNA Sequencing Facility to insure the correct gene sequence. Plasmid 1074c had the complete nucleotide sequence and was selected to transform into *E. coli* BL21 for expression. Protein expression was induced when the culture reached an optical density between 0.4-0.6 by the addition of 1mM IPTG (isopropyl-β-d-thiogalactopyranoside) followed by

overnight incubation at 18°C. The recombinant protein was purified by Ni-affinity chromatography and was eluted from the column with 500 mM imidazole. The K_m was determined for SYN_02635 gene product with the acetate range 0.4-10mM, and CoA range 0.004 - 5 mM. SYN_00049, SYN_01949, SYN_02112, and SYN_02878 also were cloned and expressed in *E. coli* Bl21 with methods described above using PET_101 expression system. Primers are listed in Table 2.2.

Table 2.2: Primers for heterologous expression in *E. coli* Bl21 for the annotated AMP-forming, acetyl-CoA synthetase and ADP-forming, acetyl-CoA synthetases via the PET_101 expression system from Invitrogen.

Predicted function	Locus Tag	Sequence (5'→3')
Acetyl-CoA synthetase (AMP-forming)	SYN_02635	CACCATGGGAGAAGAGTCGATAT CAGTCTGTTCTTTACCAGATCGTCC
	SYN_01223	CACCATGTCGGATTTATTGTTTC TTCCCATGCTGCCGCCGCCAA
Acetyl-CoA synthetase (ADP-forming)	SYN_00049	CACCATGCATTCATTTTTCAA CTGTCAGCAAAATTCGTTAGGA
	SYN_00646	CACCATGGAAAGCCAATCTATTG ACCGATTTTTATGCGGGCG
	SYN_02112	CACCATGAAATATTTTTTGGAGC CCAGACAATCCGTGCATCGACA
	SYN_01949	CACCATGAGTTCTCGGGCTGT GGGTTGTGCTTGTCGATCTTTTTTC
	SYN_02607	CACCATGGCGATTCTTTCCA AGCAGTCGGACGCAAACTTT
	SYN_02609	CACCATGAAAACTTTTTTTTTATCCG TCCCGGCACGTTCTCGCT
	SYN_02878	CACCGTGCCGATCCGTC CAGCTGCCTCAACTTCAAGGC

RNA-sequencing. For RNA sequencing *S. aciditrophicus* was grown in 250 ml serum bottles with 100 ml of media with crotonate, benzoate, and cyclohexane-1-carboxylate as described above. RNA was sent to University of California-Los Angeles Genotyping and Sequencing Core Facility (Illumina, Inc. 9885 Towne Centre Drive, San Diego, CA 92121 USA) for sample preparation, ribosomal removal, cDNA synthesis, and Illumina sequencing. Raw data files were received in FASTA format. Paired ends were aligned against the indexed *S. aciditrophicus* genome using BOWTIE. Output files were in SAM format. Transcripts originated from homologous genes were assigned once by randomly sorting between the genes. Using SAMtools, SAM text files were converted to compressed BAM files, sorted, and indexed to generate sorted BAM indexed files that could be used as input for Integrated Genomic Viewer (IGV). Normalized number of reads were determined for each gene. BAM files were converted to WIG file format and uploaded to DeSeq for normalization and gene annotations.

High-throughput proteome analysis. For high-throughput proteomic analysis, *S. aciditrophicus* was grown in pure culture on crotonate, benzoate, and cyclohexane-1-carboxylate as described above in 500-ml Schott bottles with 250 ml of medium. For proteomic analysis, cells were rapidly cooled using dry ice ethanol baths, and pelleted by centrifugation (14,300 x g, 20min, 4°C). Cell pellets were sent to University of California-Los Angeles for peptide analysis as described in Appendix 1 of this dissertation. Peptides were digested with trypsin in SDS gels. Peptides from the gel were sequenced using nanoflow

high performance liquid chromatography system with a nanoelectrospray (nano-ESI) interface and an Applied Biosystems/Sciex QSTAR XL (QqTOF) mass spectrometer (Appendix 1).

Analytical procedures. Growth was determined by optical density at 600 nm. Crotonate, benzoate and cyclohexane-1-carboxylate were measured by high performance liquid chromatography with a Prevail Organic acid column (250 by 4.6 mm; particle size 5 µm; Alltech Inc., Deerfield, IL, USA) as previously described by Mouttaki et. al. (Mouttaki et al., 2007; Mouttaki et al., 2008). Acetate concentrations were measured by gas chromatography (Struchtemeyer, Elshahed, Duncan, & McInerney, 2005). Protein concentrations were determined using the Bradford assay with Coomassie Plus Protein Reagent from Thermo Scientific. A standard curve was generated with bovine serum albumin from Thermo Scientific (Bradford, 1976).

Results

Two-dimensional (2-D) gel electrophoresis and qRT-PCR were used to survey the transcriptome and proteome for potential candidates for substrate-level phosphorylation in *S. aciditrophicus* grown under different growth conditions. Transcripts were detected for seven of the nine ADP-forming, acetyl-CoA synthetase genes; two AMP-forming, acetyl-CoA synthetase genes; and the butyrate kinase genes (Table 2.3) (Figure 2.1). The nucleic acid sequences of the two butyrate kinase genes are 99% identical. Thus, it was not possible to determine from which gene (SYN_01210 and SYN_03090) the transcripts were derived. The presence of transcripts for the phosphobutyryltransferase genes, SYN_00653, SYN_00654, SYN_01211, and SYN_01212, was not determined because these genes are adjacent to butyrate kinase genes and are expected to be present if the butyrate kinase transcripts are detected. Polypeptides were detected for two ADP-forming, acetyl-CoA synthetase (SYN_00646 and SYN_01949 gene products), one AMP-forming, acetyl-CoA synthetase (SYN_02635 gene product), butyrate kinase (SYN_01210 and/or SYN_03090 gene products) and phosphate butyryltransferase (SYN_01211 and SYN_01212 gene products) (Table 2.3). Substrate level-phosphorylation enzymes should be predominant in the proteome, so candidates detected by qRT-PCR but not detected in the proteome are unlikely to be the main substrate-level phosphorylation enzyme. While the above analyses reduced the number of possibilities, the analyses did not eliminate any

of the three possible mechanisms for substrate level-phosphorylation in *S. aciditrophicus*.

Table 2.3: Detection of peptides from two-dimensional gel electrophoresis and transcripts from qRT-PCR from potential candidates for substrate-level phosphorylation in *S. aciditrophicus*.

Predicted function	Gene Locus Tag Number	Gene ID	Peptide presence in				Transcript presence in			
			Crotonate pure culture	Crotonate plus benzoate pure culture	Crotonate pure culture	Crotonate plus benzoate pure culture	Crotonate coculture	Benzoate coculture	Cyclohexane carboxylate coculture	Crotonate stationary phase pure culture
Acetyl-CoA synthetase (ADP-forming)	SYN_00049	637860402	-[c]	-[d]	+	+	+	+	+	+
	SYN_00646	637860401	+	+	+	+	+	+	+	+
	SYN_00647	637860402	-	-	ND[b]	ND	ND	ND	ND	ND
	SYN_00748	637860516	-	-	-	-	-	-	-	-
	SYN_01949	637859111	+	+	+	+	+	+	+	+
	SYN_02112	637859378	-	-	+	+	+	+	+	+
	SYN_02607	637858761	-	-	+	+	+	+	+	+
	SYN_02609	637858763	-	-	+	+	+	+	+	+
	SYN_02878	637860278	-	-	+	+	+	+	+	+
Acetyl-CoA synthetase (AMP-forming)	SYN_01223	637860804	-	-	+	+	+	+	+	+
	SYN_02635	637860993	+	+	+	+	+	+	+	+
Butyrate kinase	[a]SYN_01210/ SYN_03090	637860790/ 637860410	+	+	+	+	+	+	+	+
Phosphate butyryl-transferase	SYN_00653	637860408	-	-	ND	ND	ND	ND	ND	ND
	SYN_00654	637860409	-	-	ND	ND	ND	ND	ND	ND
	SYN_01211	637860791	+	+	ND	ND	ND	ND	ND	ND
	SYN_01212	637860792	+	+	ND	ND	ND	ND	ND	ND

[a] SYN_01210 or SYN_03090 share 99% identity in the nucleic acid sequence and therefore cannot be distinguished

[b] ND is not determined

[c] (+) is detected (-) is not detected

[d] (-) is not detected

To deduce which mechanism *S. aciditrophicus* uses for substrate level-phosphorylation, enzyme activities were measured in cell-free extracts of *S. aciditrophicus* grown under various conditions. Acetyl-CoA synthetase activity was higher than the kinase-phosphotransferase activities under all growth conditions tested (Table 2.4). The specific acetyl-CoA synthetase activity ranged from 0.53 ± 0.01 to 7.4 ± 0.3 μmol min^{-1} mg^{-1} of protein (Table 2.4) dependent on how the culture was cultivated. Acetate kinase activities of 0.25 ± 0.05 and 0.067 ± 0.002 μmol min^{-1} mg^{-1} of protein were found in cell-free extracts of *S. aciditrophicus* grown on crotonate in pure and coculture, respectively, but little acetate kinase activity was observed for the other growth conditions (Table 2.4). Butyrate kinase and phosphotransacetylase activities were detected only in crotonate-grown cells. Acetyl-CoA synthetase, butyrate kinase, and phosphotransacetylase were not detected and acetate kinase activity was very low in cell-free extracts of pure culture-grown *M. hungatei* (Table 2.4). Thus, the activities detected in coculture-grown *S. aciditrophicus* cells were not affected by the small amount of *M. hungatei* contamination present after Percoll separation. As a positive control, high levels of phosphotransacetylase activities were detected in cell-free extracts of the butyrate-degrading syntrophic bacterium, *Syntrophomonas wolfei*, which is known to use this system for substrate-level phosphorylation (Wofford, Beaty, & McInerney, 1986).

Table 2.4: Enzyme activities in cell-free extracts of *S. aciditrophicus*, *M. hungatei* and *S. wolfei*.

Culture	Growth Substrate	Acetyl-CoA Synthetase [a]	Acetate Kinase	Butyrate Kinase	Phospho-trans-acetylase
S. aciditrophicus	Crotonate	4.86[b] ± 0.35	0.25 ±0.05[e]	0.19 ± 0.03	0.021 ± 0.007
S. aciditrophicus Percoll-separated	Crotonate	0.92 ± 0.34	0.067 ± 0.03	0.09 ± 0.005	0.183 ± 0.03
S. aciditrophicus Percoll-separated	Benzoate	0.53 ± 0.01	0.01 ±0.001	BDL	BDL
S. aciditrophicus Percoll-separated	Cyclohexane -1-carboxylate	7.4 ± 0.3	0.01 ± 0.001	BDL	BDL
M. hungatei	H_2 and CO_2	BDL[c]	0.004 ±0.002	BDL	BDL
Syntroph-omonas wolfei	Crotonate	ND[d]	0.37	0.06	1.11

[a] It is not possible to distinguish ADP-forming and AMP-forming, acetyl-CoA sythetase activity in extracts due to the adenylate kinase activity in *S. aciditrophicus* cell-free extracts.
[b] All activities are in μmol of substrate $min^{-1}mg^{-1}$ of protein.
[c] BDL, Below detection limit of the assay.
[d] ND, Not determined.
[e] Mean ± standard deviation of three determinations.

The AMP-forming and ADP-forming acetyl-CoA synthetase activities could not be distinguished from each other in cell-free extracts due to presence of a native adenylate kinase, which interconverts AMP and ADP in the presence of ATP (Kurebayashi et al., 1980; Nageswara Rao & Cohn, 1977). P1,P5-Di (adenosine-5') pentaphosphate (Ap5A) was used to inhibit the native adenylate kinase activity (Kurebayashi et al., 1980; Nageswara Rao & Cohn, 1977) in order to determine if cell-free extracts of *S. aciditrophicus* contained AMP-forming, acetyl-CoA synthetase and ADP-forming, acetyl-CoA synthetase activities or both (Table 2.5). The addition of 1.5 mM Ap5A to the reaction mix inhibited 99% of the native adenylate kinase activity. No ADP-forming, acetyl-CoA synthetase activity was detected when 1.5 mM Ap5A was present. However, activity was detected when AMP and pyrophosphate were added to reactions that contained the inhibitor, phosphate, ADP and cell-free extracts (Table 2.5). Thus, the acetyl-CoA synthetase activity detected in cell-free extracts was due to an AMP-forming, acetyl-CoA synthetase. The high levels of AMP-forming, acetyl-CoA synthetase activity under all tested growth conditions argue that this enzyme is important for ATP production.

Table 2.5: Inhibition of the native adenylate kinase in *S. aciditrophicus* to measure ADP-forming, acetyl-CoA ligase activity.

Activity measured	Substrates Added	Ap5A addition (mM)	Activity (μmol $min^{-1}mg^{-1}$)
Adenylate Kinase	ADP	0	3.38 ± 0.16[a]
Adenylate Kinase	ADP	0.75	0.63
Adenylate Kinase	ADP	1.5	0.02
ADP-forming acetyl-CoA synthetase	Acetyl-CoA, KPi, ADP	1.5	0.02 ± 0.003
AMP-forming acetyl-CoA synthetase	Added to reaction above AMP, PPi	1.5	1.3 ± 0.2

[a] Mean ± standard deviation of three determinations.

Two approaches were used to correlate cell-free extract activities of the possible candidates for substrate-level phosphorylation to specific acetate production rates. First, the specific growth rate and molar growth yield were determined and used to calculate the specific substrate utilization rate of *S. aciditrophicus* grown in pure and coculture on crotonate (Table 2.6). The specific rates of crotonate use were 4.7 ± 0.35 and 5.2 ± 0.1 μmol of crotonate used min^{-1} mg^{-1} of protein for *S. aciditrophicus* pure culture and cocultures, respectively. The specific substrate utilization rate was multiplied by the molar ratio for acetate produced per crotonate used (Elshahed & McInerney, 2001) to give the specific acetate production rates of 7.1 ± 0.001 and 7.8 ± 7.8 μmol of acetate produced min^{-1} mg^{-1} of protein for *S. aciditrophicus* pure cultures and cocultures, respectively (Table 2.6). The cell-free extract, acetyl-CoA synthetase specific activities accounted for 69% and 12% of the specific acetate production rate by *S. aciditrophicus* grown in pure culture and coculture on crotonate, respectively (Table 2.7). Specific activities of acetate kinase, butyrate kinase and phosphotransacetylase accounted for less than 3.5% of the specific acetate production rate under these growth conditions. The second approach was to measure the acetate production rates in resting cells of *S. aciditrophicus*. The cell-free extract, acetyl-CoA synthetase specific activity (4.86 ± 0.35 μmol min^{-1} mg^{-1} of protein; Table 2.4) was much higher than the acetate production rate by washed cell suspensions of *S. aciditrophicus* grown in pure culture on crotonate (1.18 ± 0.2 μmol of acetate produced min^{-1} mg^{-1} of protein). The acetyl-CoA synthetase activity accounted for 69% and 12% of the acetate production rates

from resting cells of *S. aciditrophicus*. Acetate kinase activity accounted for 4% and 1% of the acetate production rates from resting cells

Table 2.6: Growth yields, specific growth rates, acetate production, and substrate utilization for *S. aciditrophicus* cultures.

Culture	Growth Substrate	Specific Growth Rate (hr^{-1})	Molar Growth Yield (mg μmol^{-1})	Specific Substrate Utilization ($\mu mol\ min^{-1}\ mg^{-1}$)	Specific Acetate Production Rate[a] ($\mu mol\ min^{-1}\ mg^{-1}$)
S. aciditrophicus	Crotonate	0.014 ± 0.001	0.003 ± 0.0006	4.7 ± 0.4[b]	7.1 ± 0.001
S. aciditrophicus M. hungatei	Crotonate	0.015 ± 0.001	0.003 ± 0.0003	5.2 ± 0.1	7.8 ± 0.0005

[a] The mole ratio of acetate to crotonate is 1.5:1.
[b] mean ± standard deviation of three determinations.

Table 2.7: Percentage of acetate kinase, butyrate kinase, and phosphotransacetylase activities that account for the total acetate production rates measured from cell-free extracts of *S. aciditrophicus.*

Culture	Growth Substrate	ACS activity from extracts/ acetate production rates	Acetate kinase activity/ acetate production rates	Butyrate kinase activity/ acetate production rates	Phospho transacetylase activity/ acetate production rates
S. aciditrophicus	Crotonate	69 %	4 %	3 %	0.3 %
S. aciditrophicus + M. hungatei	Crotonate	12 %	1 %	1 %	2 %

Inhibition of the native adenylate kinase in *S. aciditrophicus* cell-free extracts indicated that dominant acetate-producing activity in cell-free extracts of *S. aciditrophicus* was an AMP-forming, acetyl-CoA synthetase. The acetyl-CoA synthetase activity was purified from cell-free extracts of *S. aciditrophicus* grown in pure culture on crotonate to verify nucleotide specificity and the identity of the gene product. Ammonium sulfate fractionation and three chromatographic steps resulted in a homogenous protein (Table 2.8). No acetyl-CoA synthetase activity was detected in the final purified fraction in absence of adenylate kinase as expected for an AMP-forming, acetyl-CoA synthetase. Acetate kinase activity was not detected during purification. The total percentage yield was 75% recovery with a 94.8-fold purification (Table 2.8). Thus, almost all of the acetyl-CoA synthetase activity present in cell-free extracts was recovered as an AMP-forming, acetyl-CoA synthetase activity. The purification resulted in a homogenous protein that migrated as a single band on denaturing gel electrophoresis. Peptide analysis identified five unique peptides with average intensities of 1903 from SYN_02635, annotated as an AMP-forming, acetyl-CoA synthetase (McInerney et al., 2007). No other peptides were identified. The average mass of the protein was 73,823 Da consistent with the predicted mass for the SYN_02635 gene product.

Table 2.8: Purification of the dominant acetyl-CoA synthetase activity from *S. aciditrophicus* cell-free extracts.

Purification Step	Volume (ml)	Total Protein (mg ml)	Specific Activity (μmol min^{-1} mg^{-1})	Total activity (μmol min^{-1} ml)	Yield %	Purification fold
Cell-free extract	3	10.1	0.6	6.1	100	1.0
45% Ammonium sulfate soluble	3	10.4	0.4	4.2	69	0.7
DEAE Pooled	3	1.1	2.3	2.5	41	3.8
Hydroxyapatite Pooled	3	0.4	11.0	4.4	72	18.3
Reactive Green	1	0.08	56.9	4.6	75	94.8

The dominant acetyl-CoA synthetase activity was purified from extracts of *S. aciditrophicus* and identified as AMP-forming, acetyl-CoA synthetase (Acs1), the gene product of SYN_02635 (*acs1*). The V_{max} and K_m were measured in each direction, acetate activation to acetyl-CoA (acetyl-CoA forming) and acetyl-CoA conversion to acetate (acetate forming) (Table 2.9), to determine whether the purified protein had activity in the acetate-forming direction sufficient to account for measured acetate production rates. In the acetyl-CoA-forming direction, Acs1 had a V_{max} of 74 ± 7 and 73 ± 16 with ATP and CoA, respectively. In the acetate-forming direction, Acs1 had the highest specific activity of 4.6 μmol min^{-1} mg^{-1} of protein exceeding that by washed cell suspensions (1.18 ± 0.2 μmol of acetate produced min^{-1} mg^{-1} of protein). The V_{max} was 7.5 ± 1.2, and the K_m for acetate and CoA was 0.59 ± 0.2 and 0.26 ± 0.1 mM, respectively (acetyl-CoA forming direction) (Table 2.9). The K_m for acetyl-CoA (acetate-forming direction) was 0.41 mM acetyl-CoA (Table 2.9).

Table 2.9: Enzyme kinetic constants for the purified Acs1 from cell-free extracts of S. *aciditrophicus* and for the purified recombinant Acs1 (SYN_02635 gene product).

Enzyme	Reaction direction	Substrate	K_m (mM)	V_{max} (µmol $min^{-1}mg^{-1}$)
Purified Acs1	Acetate→Acetyl-CoA	Acetate	0.59 ± 0.2[a]	74 ± 7
		CoA	0.26 ± 0.1	73 ± 16
	Acetyl-CoA→Acetate	Acetyl-CoA	0.41 ± 0.1	7.5 ± 1.2
Recombinant Acs1	Acetate→Acetyl-CoA	Acetate	0.96 ± 0.02	89 ± 5.7
		CoA	0.21 ± 0.05	91 ± 7
	Acetyl-CoA→Acetate	Acetyl-CoA	1.34 ± 0.5	1.2

[a] Standard error.

To ensure that SYN_02635 encodes an AMP-forming acetyl-CoA synthetase, it was cloned and expressed *Escherichia coli* Bl21 and its gene product purified and characterized (Table 2.9). The heterologously expressed Acs1 was active and the K_m and V_{max} were determined in both the acetyl-CoA- and acetate-forming directions (Table 2.9). In the acetyl-CoA-forming direction, the recombinant protein had a V_{max} of 89 μmol min^{-1} mg^{-1} of protein and K_m values of 0.96 ± 0.02 and 0.21 ± 0.05 mM for acetate and CoA, respectively. In the acetate-forming direction, the recombinant protein had a V_{max} of 1.2 μmol min^{-1} mg^{-1} of protein and a K_m of 1.34 ± 0.5 mM. The K_m and V_{max} values for both directions were consistent with those for the protein purified from extracts of *S. aciditrophicus* (Table 2.9). Both the purified protein and the recombinant had high activity with acetate as the substrate and little activity with other organic acids (<0.6 % of the acetate rate) (Table 2.10). These analyses confirmed that the SYN_02635 gene product was an AMP-forming, acetyl-CoA synthetase.

Table 2.10: Substrate specificity of the Acs1 purified from cell-free extracts of *S. aciditrophicus* and for the purified recombinant Acs1 (SYN_02635 gene product).

Fatty Acid	Purified Acs1		Recombinant Acs1	
	Concentration (mM)	Specific activity (μmol min^{-1} mg^{-1})	Concentration (mM)	Specific activity (μmol min^{-1} mg^{-1})
Acetate	2	68	2	70
Crotonate	3	0.10	2	0.28
Benzoate	3	0.26	2	0.29
Cyclohexane-1-carboxylate	3	0.03	2	0.32
Butyrate	1	0.02	2	0.35
Succinate	3	0.42	2	ND[a]
Glutarate	3	0.29	2	ND
1-cyclo-hexene carboxylate	3	0.22	2	0.38

[a] ND, not determined.

RNAseq Illumina sequencing was used to access the expression level of all candidate genes potentially involved in substrate-level phosphorylation genes when *S. aciditrophicus* was grown in coculture on crotonate, benzoate, and cyclohexane-1-carboxylate (Figure 2.2). Transcripts of SYN_02635 represented 0.68% of the crotonate transcriptome, 0.58% of the benzoate transcriptome, and 0.76% of the cyclohexane-1-carboxylate transcriptome (Figure 2.2). Transcripts of SYN_01223 (*acs2*) represented 0.05-0.06% of the total trancriptomes (Figure 2.2). Transcripts for ADP-forming, acetyl-CoA synthetase genes from 0.1-0.01% and those for butyrate kinase genes (SYN_03090 and SYN_01210) represented 0.01-0.04% of the total transcriptomes for crotonate, benzoate, and cyclohexane-1-carboxylate coculture grown cells (Figure 2.2). Transcripts from *acs1* were 80% higher than transcripts from all other potential candidate genes. In addition, Acs1 was in high abundance ranging from 1.5 to 4.5% of the total peptides detected in *S. aciditrophicus* cells grown in coculture on crotonate, benzoate and cyclohexane-1-carboxylate (Figure 2.3). Polypeptides for the butyrate kinase (SYN_03090 and SYN_01210 gene products) and the ADP-forming, acetyl-CoA synthetases were equal to or less than 0.1% of the total peptides detected (Figure 2.3). The transcriptomic and proteomic data show Acs1 is highly expressed and its gene product is in high abundance when *S. aciditrophicus* grows in coculture as would be expected for an important catabolic gene and protein, respectively.

Figure 2.2: Transcript abundance in percent of total detected RNA sequences of potential candidates for ATP synthesis by substrate-level phosphorylation.

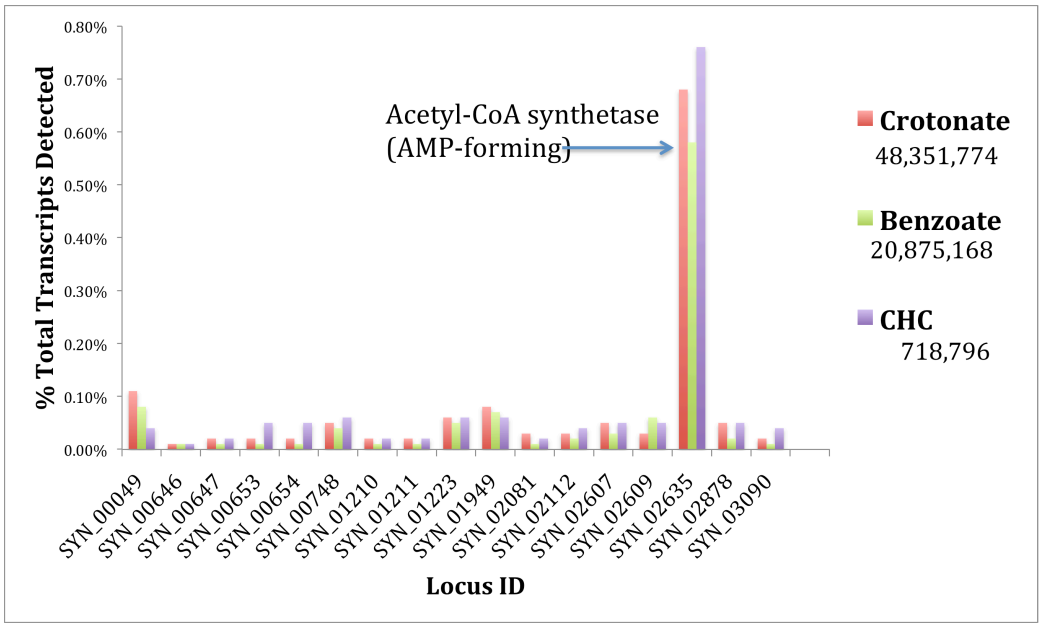

Figure 2.3: Peptide abundance in percent of total detected peptide sequences from high-throughput proteome analysis for potential candidates for ATP synthesis by substrate-level phosphorylation.

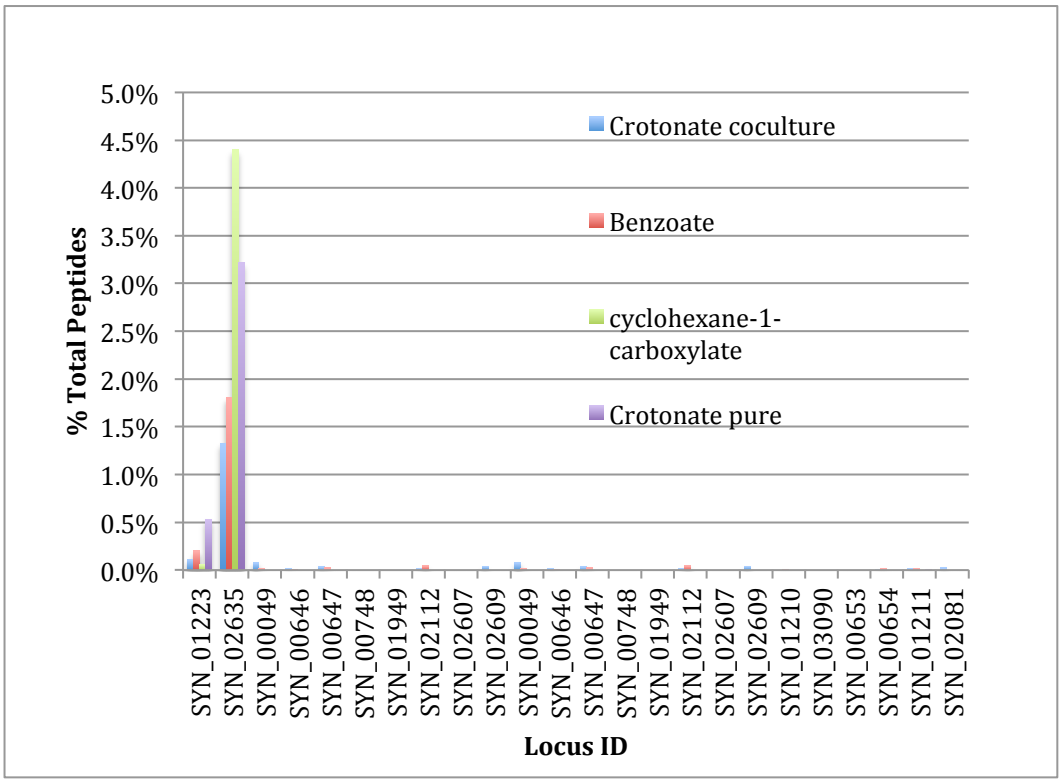

Discussion

While genomic analysis showed that *S. aciditrophicus* has multiple possibilities for ATP production from acetyl-CoA, enzymatic analyses argue that *S. aciditrophicus* uses AMP-forming, acetyl-CoA synthetase (Acs1) to synthesize ATP from acetyl-CoA. Acetyl-CoA synthetase activity was high in cell-free extracts of *S. aciditrophicus* under all growth conditions tested (Table 2.4). The acetyl-CoA synthetase activity was the only activity measured in cell-free extracts that accounted for the rate of acetate production from crotonate by washed cell suspensions. The acetate kinase activity and phosphotransacteylase activity were low and did not account for the acetate production rates in washed cell suspensions. Due to the adenylate kinase activity in cell-free extracts of *S. aciditrophicus*, it was not possible to determine the nucleotide specificity (AMP-forming versus ADP-forming) of the acetyl-CoA synthetase activity in cell-free extracts with the coupled assay. However, the use of an adenylate kinase inhibitor (Ap5A) showed that the acetyl-CoA synthetase activity present in cell-free extracts of S. *aciditrophicus* was specific for AMP (Table 2.5). The nucleotide specificity of the dominant acetyl-CoA synthetase activity was confirmed by purifying the activity to homogeneity from cell-free extracts of *S. aciditrophicus* and by characterizing the purified recombinant protein, the SYN_02635 gene product (Table 2.10). The purified Acs1 and the recombinant Acs1 had sufficient activity in the acetate-forming direction to account for the measured acetate production (Table 2.9). Acetate kinase, phosphotransacetylase, and butyrate kinase activities were detected

only when crotonate was the growth substrate (Table 2.4). However, each of these three activities was considerably less than the acetyl-CoA synthetase activity and the measured rates of acetate production (Table 2.4, Table 2.6). Thus, there is evidence for a phosphotransacetylase-kinase mechanism for acetate and ATP synthesis when *S. aciditrophicus* grows with crotonate, but this mechanism does not appear to be the dominant one when *S. aciditrophicus* grows with crotonate. Benzoate and cyclohexane-1-carboxylate, not crotonate, are most likely the ecologically important substrate for *S. aciditrophicus* (Jackson et al., 1999). We found no evidence for the operation of a phosphotransacetylase-kinase mechanism for acetate and ATP synthesis when *S. aciditrophicus* grows syntrophically on benzoate or cyclohexane-1-carboxylate (Table 2.4). The only activity detected during syntrophic growth on benzoate or cyclohexane-1-carboxylate was AMP-forming, acetyl-CoA synthetase activity (Table 2.4). High-throughput transcriptomic and proteomic analyses support the conclusion that the Acs1, encoded by SYN_02635, is the enzyme responsible for ATP formation by *S. aciditrophicus*. Transcripts for SYN_02635 were 80% higher than transcripts from all other potential candidate genes and the SYN_02635 gene product was in high abundance ranging from 1.5 to 4.5% of the total peptides when *S. aciditrophicus* was grown syntrophically (Figure 2.2 and 2.3).

AMP-forming, acetyl-CoA synthetases are found in all domains of life (Bastiaansen et al., 2013; Berger, Welte, & Deppenmeier, 2012; Brown, Jones-Mortimer, & Kornberg, 1977; Lee et al., 2011; Lin & Oliver, 2008; Mayer et al.,

2012). The primary role for AMP-forming, acetyl-CoA synthetase is the activation of acetate to acetyl-CoA, a central metabolic intermediate (Bastiaansen et al., 2013; Starai & Escalante-Semerena, 2004). AMP-forming, acetyl-CoA synthetases have not been shown to operate in the acetate-forming direction in fermentative microorganisms. The only known instance where an AMP-forming, acetyl-CoA synthetase is used for ATP synthesis and acetate is by the fungus, *A. nidulans* (Takasaki et al., 2004). *A. nidulans* is capable of growing on acetate as a sole carbon source. During anaerobic stress *A. nidulans* uses an AMP-forming, acetyl-CoA synthetase to decrease intracellular acetyl-CoA concentrations, thus, providing the cells with ATP (Takasaki et al., 2004). The specific activities for the AMP-forming, acetyl-CoA synthetase in *A. nidulans* were much higher in the acetate and ATP forming direction when *A. nidulans* was grown anaerobically (Takasaki et al., 2004). The K_m and V_{max} of the enzyme differed when *A. nidulans* was grown aerobically versus anaerobically such that the directionality of the reaction favored acetate and ATP formation during anaerobic growth (Takasaki et al., 2004). Posttranslational acetylation most likely was the reason for the change in kinetic parameters of the enzyme with different growth conditions. *A. nidulans* has two open reading frames predicted to encode acetyl-CoA synthetase (locus identification numbers AN5626.2 and AN5833.2) (David, Ozcelik, Hofmann, & Nielsen, 2008) with the activity of the AN5626.2 gene product confirmed as an AMP-forming acetyl-CoA synthetase (Connerton, Fincham, Sandeman, & Hynes, 1990). pBLAST analysis showed that the SYN_02635 and AN5626.2 gene products share 49% identity over 96% of

the protein sequence. The conserved domains for the AMP binding site (~320, 380, 420, 500-540), the CoA binding site (270, 200, 310-320, 340, 370, 530), the acetate binding site (320, 390, 420), and the acyl-activating enzyme consensus motif site (260-280) are present in the amino acid sequence of the SYN_02635.

Although cell-free extracts of crotonate-grown *S. aciditrophicus* had phosphotransacetylase and acetate kinase activities, the specific activities were much less than that detected in organisms known to use phosphotransacetylase and acetate kinase for acetate and ATP synthesis (Table 2.11) (Brown et al., 1977; Wofford et al., 1986). *S. wolfei* is a syntrophic fatty acid-degrading bacterium (McInerney, Bryant, Hespell, & Costerton, 1981). Genes for acetate kinase and phosphotransacetylase, but not for AMP-forming, acetyl-CoA synthetase, are present in the genome of *S. wolfei* (Sieber et al., 2010). The specific activities for phosphotransacetylase and acetate kianse were 9.75 μmol min^{-1} mg^{-1} of protein and 1.09 μmol min^{-1} mg^{-1} of protein, respectively, whereas AMP-forming, acetyl-CoA synthetase activity was very low, <0.01 nmol min^{-1} mg^{-1} (Wofford et al., 1986). The *S. wolfei* activities are much higher than the highest detected phosphotransacetylase activity (0.183 ± 0.03 μmol min^{-1} mg^{-1} of protein) and acetate kinase activity (0.25 μmol min^{-1} mg^{-1} of protein) in *S. aciditrophicus*. In addition, acetate kinase and phosphotransacetylase constituted from 0.6%-1.4% of the total peptides detected in *S. wolfei* cells grown on crotonate and butyrate (Figure 2.4) (Sieber, 2011). In comparison, phosphate acetyl/butyryl transferases were not detected in the proteome of *S. aciditrophicus*, while the SYN_02635 gene product represented 1.5 to 4.5% of

the total *S. aciditrophicus* proteome (Figure 2.4). Anaerobically grown *E. coli* K12 also uses acetate kinase and phosphotransacetylase for acetate and ATP synthesis. Acetate kinase and phosphotransacetylase activities from anaerobically grown, *E. coli* K12 cell-free extracts were 3.9 μmol min^{-1} mg^{-1} of protein and 3.3 μmol min^{-1} mg^{-1} of protein respectively, while AMP-forming, acetyl-CoA synthetase activity was only 0.1 μmol min^{-1} mg^{-1} of protein (Table 2.11) (Brown et al., 1977). Acetate kinase and phosphotransacetylase may play a role in acetate and ATP synthesis when *S. aciditrophicus* is grown on crotonate, but the activities of these two enzymes are much lower than that observed in organisms that rely on acetate kinase and phosphotransacetylase as the sole or dominant mechanism of acetate and ATP synthesis.

Table 2.11: Acetate kinase, phosphotransacetylase, and AMP-forming, acetyl-CoA synthetase activities from cell-free extracts of *Syntrophus* species, *S. wolfei,* and *E. coli*.

Organism	Acetyl-CoA synthetase activity (μmol min^{-1} mg^{-1})	Acetate kinase (μmol min^{-1} mg^{-1})	Phospho-transacetylase (μmol min^{-1} mg^{-1})	Reference
S. aciditrophicus	4.86	0.25	0.021	(present study)
Syntrophus gentianae	0.210	0.020	0.057	(L. Schocke & Schink, 1999)
Syntrophus buswelli GA	0.900	0.080	0	(Auburger & Winter, 1996)
Syntrophus buswelli 2612A	0.400	0.150	0	(Auburger & Winter, 1996)
S. wolfei	<0.00001 0.003	1.09	9.75	(Wofford et al., 1986)
E. coli K12				
aerobic	0.1	3.9	3.3	(Brown et al., 1977)
anearobic	ND[a]	4.2	5.4	

[a] ND, not detected.

Figure 2.4: Peptides detected from high-throughput proteome analysis of annotated phosphotransacetylase and acetate kinase gene products in *S. wolfei* grown on crotonate and butyrate.

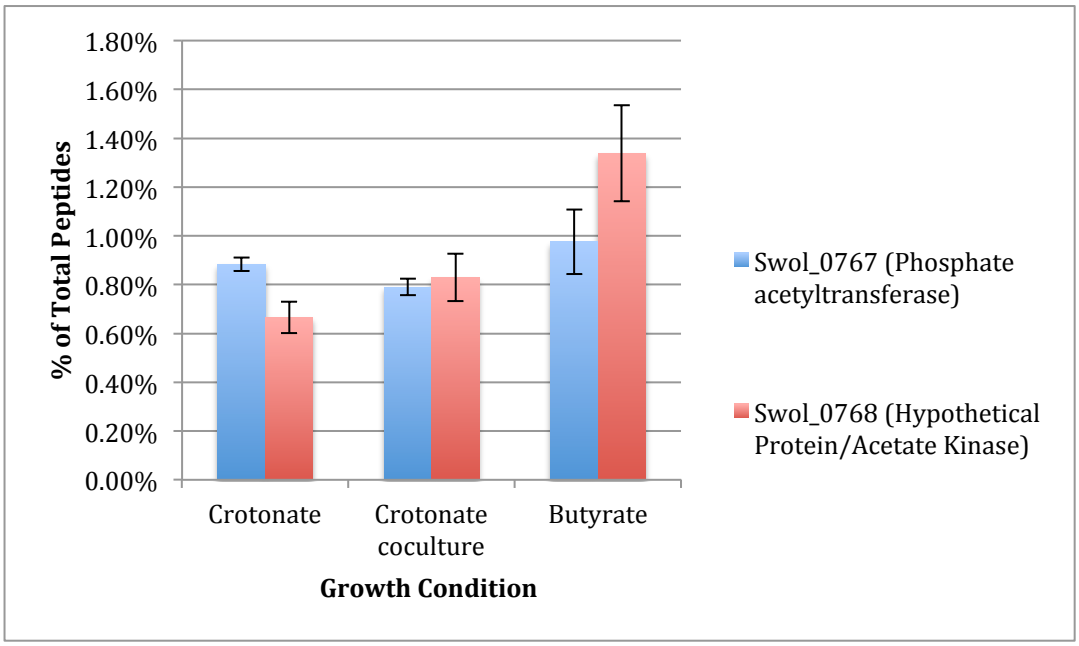

The use of an AMP-forming, acetyl-CoA synthetase for acetate and ATP formation makes physiological sense for *S. aciditrophicus*. We know that *S. aciditrophicus* uses AMP-forming ligases for activation of benzoate, cyclohexane-1-carboxylate and crotonate to their respective CoA intermediates (Elshahed et al., 2001) (Chapter 3), which results in the conversion of ATP into AMP and PP_i (Equation 1 for benzoate). Subsequent hydrolysis of PP_i (equation 2) results in the loss of two high-energy bonds during substrate activation, making this process very energy intensive for a syntrophic metabolizer that has limited ability to synthesize ATP. Part of the energy in the hydrolysis of PP_i can be conserved by a proton-translocating, membrane-bound pyrophosphatase (L. Schocke & Schink, 1998). However, it would be more energy efficient to use an acetyl-CoA: CoA transferase reaction for substrate activation in *S. aciditrophicus* because ATP is not hydrolyzed, as *S. wolfei* uses for butyrate activation (Equation 4) (Wofford et al., 1986).

Equation 1: Benzoate + CoA + ATP --> Benzoyl-CoA + AMP + PPi

Equation 2: PPi → 2 phosphates

Equation 3: Acetyl-CoA + AMP + PPi --> Acetate + CoA + ATP

Equation 4: Benzoate + acetyl-CoA → benzoyl-CoA + acetate

However, coupling the substrate activation reaction (Equation 1) with AMP-forming acetyl-CoA synthetase reaction (Equation 3) gives a net reaction (Equation 4) that is functionally equivalent to a CoA transferase reaction.

The potential use of an AMP-forming, acetyl-CoA synthetase to make ATP may be widespread among bacteria. AMP-forming, acetyl-CoA synthetase is most likely used by *S. buswellii* (Auburger & Winter, 1996), *S. gentianae* (Schocke & Schink, 1997) for ATP synthesis as both organisms have very low phosphotransacetylase and acetate kinase activities. A survey of genomes of acetate-forming anaerobes in the Clostridia revealed other fermentative microorganisms that lack genes for phosphoacetyltransacetylase, phosphobutyryltransferase, acetate kinase or butyrate kinase, but have genes for AMP-forming, acetyl-CoA synthetase*: Ammonifex degensii, Heliobacterium modesticaldum, Moorella thermoacetica* (Table 2.12). Further research will be needed to confirm whether or not these organisms use the AMP-forming, acetyl-CoA synthetase to make acetate and ATP.

Table 2.12. Members of the Clostridia that have potential AMP-forming, acetyl-CoA synthetase (ACS), either one or no acetatate kinase (AK) and no phosphotransacetylase (PTA), and no butyrate kinase (BK) and phosphobutyryltransferase (PTB). All BLAST searches were performed on HAMAP (http://hamap.expasy.org/) on 01/16/2014.

Organism	GI#	ACS	AK	PTA	BK	PTB
Ammonifex degensii (strain DSM 10501 / KC4)	260891930	2[a]	0	0	0	0
Heliobacterium modesticaldum (strain ATCC 51547 / Ice1)	255961476	2	1	0	0	0
Moorella thermoacetica (strain ATCC 39073) orginally isolated as *Clostridium thermoaceticum*	83588874	1	1	0	0	0

[a] Number of annotated genes in the predicted proteome.

Chapter 3: Purification and characterization of acetate kinase in *Syntrophus aciditrophicus*

Abstract

The syntrophic metabolism of benzoate, alicyclic acids and fatty acids by *S. aciditrophicus* leads to the production acetyl-CoA, which is then metabolized to acetate. ATP formation coupled to acetate formation is the main method for energy conservation by *S. aciditrophicus*. *S. aciditrophicus* has two candidate genes that could encode for acetate kinase, SYN_03090 and SYN_01210, which share 99% identity with each other at the nucleotide level, and both of which annotate as butyrate kinases. The nucleotide sequence of SYN_03090/ SYN_01210 was cloned and heterologously expressed in *Escherichia coli* Bl21. The purified recombinant protein had acetate kinase activity but not propionate or butyrate kinase activity. Adenosine triphosphate was the preferred nucleotide triphosphate with acetate as the substrate. The purified recombinant protein synthesized ATP from acetyl-phosphate (0.82 ± 0.21 μmol of $min^{-1}mg^{-1}$ of protein) and had a V_{max} of 0.91 and 1.03 μmol $min^{-1}mg^{-1}$ of protein and a K_m value of 0.22 ± 0.04 and 0.52 ± 0.09 mM for acetyl-phosphate and ADP, respectively. Phylogenetic analyses showed butyrate kinases clustered together and acetate kinases clustered together. The deduced amino acid sequences of both SYN_03090 and SYN_01210 grouped with those of the butyrate kinases. These data support the conclusion that the SYN_03090/SYN_01210 gene product is an acetate kinase.

Introduction

The anaerobic catabolism of many aromatic compounds, such as, monomers derived from lignin, halogenated aromatic compounds, and aromatic hydrocarbons, converges to benzoate and its CoA derivative, benzoyl-CoA, prior to ring reduction and cleavage (Harwood et al., 1999). In methanogenic environments, syntrophic metabolizers catalyze the reduction and cleavage of benzoyl-CoA (McInerney et al., 2008). *Syntrophus aciditrophicus*, serves as the model organism for syntrophic benzoate and cyclohexane-1-carboxylate metabolism (Jackon et al., 1999; Elshahed et al., 2001; McInerney 2007). The syntrophic metabolism of benzoate, alicyclic acids and fatty acids by *S. aciditrophicus* leads to the production of acetyl-CoA, which is then metabolized to acetate (McInerney et al., 2007). ATP formation coupled to acetate formation is the main mechanism of energy conservation by *S. aciditrophicus*. Almost all fermentative bacteria use two enzymes, phosphotransacetylase and acetate kinase, to synthesize ATP and acetate from acetyl-CoA (Ingram-Smith et al., 2006). However, the genome of *S. aciditrophicus* lacks a homolog for acetate kinase and cell-free extracts have very low acetate kinase and phosphotransacetylase activities (McInerney et al., 2007). *Syntrophus gentianae* and *Syntrophus buswellii* also have low acetate kinase activities and phosphotransacetylase activity was not detected in *S. buswellii* grown either in pure culture or in coculture (Auburger & Winter, 1996; Schocke & Schink, 1997). Genomic analysis showed that *S. aciditrophicus* has two gene clusters, each with a butyrate kinase and phosphate acetyl/butyryl transferase genes,

which could function to make ATP from acetyl-CoA (McInerney et al., 2007) in conjunction with the AMP-forming, acetyl-CoA synthetase (SYN_02635 gene product) discussed in Chapter 2. The nucleic acid sequences of the two butyrate kinase genes, SYN_03090 and SYN_01210 share 99% identity, and it is not possible to distinguish between the two genes. Thus, SYN_03090 will be used to describe SYN_03090 and SYN_01210. The transcripts for SYN_03090 were present in crotonate-, benzoate-, and cyclohexane-1-carboxylate-grown cultures of *S. aciditrophicus*. In addition, two-dimensional denaturing gel electrophoresis revealed the presence of peptides for SYN_03090 when *S. aciditrophicus* was grown in pure culture on crotonate and crotonate plus benzoate. Subsequent high-throughput proteomic analysis also showed the presence of peptides for SYN_03090 gene product when *S. aciditrophicus* was grown on crotonate, benzoate, and cyclohexane-1-carboxylate.

Here, I heterologously expressed the gene product for SYN_03090 and measured its activity to determine if it could function as an acetate kinase.

Materials and Methods

Media and conditions of cultivation. Anaerobic media and solutions were prepared using a modified Balch technique (McInerney and Bryant, 1979). Pure cultures and cocultures of *Syntrophus aciditrophicus* strain SB (DSM 26646) were grown anaerobically in a minimal medium without rumen fluid (McInerney and Bryant, 1979). Wolin's metal solution (McInerney and Bryant, 1979) was modified to include $Na_2MoO_4{\cdot}2H_2O$ (0.01g/L) Na_2SeO_4 (0.01g/L) and $Na_2WO_4{\cdot}2H_2O$ (0.01g/L) (Sieber et al., 2014). The headspace was pressurized to 27.5 kPa with 80% N_2: 20% CO_2 (vol/vol) gas phase. All media and solutions were sterilized by autoclaving (121^{o}C; 15 min; 103 kPa). *S. aciditrophicus* pure cultures were grown in the above medium with 20 mM sodium crotonate. Cocultures of *S. aciditrophicus* with *Methanospirillum hungatei* strain JF-1(ATCC 27890) were grown in the above medium amended with 20 mM crotonate, 10 mM benzoate, or 10 mM cyclohexane-1-carboxylate. Pure cultures of *M. hungatei* were grown in the above medium with a 80% H_2: 20% CO_2 gas phase. For DNA extraction, cultures were grown in serum bottles with 50 ml of the minimal medium. To obtain sufficient amounts of cells for enzyme analyses, cultures were grown in two liter Schott bottles with 1.5 liters of mineral medium were used.

Cell harvesting and cell-free extract preparation. Cells were harvested at mid-log phase of growth by centrifugation (14,300 x g, 20min, 4°C) in sealed centrifuge tubes or bottles and washed in anoxic 50 mM potassium phosphate buffer (pH 8.5). Transfers to and from centrifuge tubes and bottles

were performed in an anaerobic chamber (Coy, Ann Arbor, Michigan, USA). The cells were washed twice by resuspension of the pellet in 50 mM anoxic potassium phosphate buffer (pH 8.5) and centrifuging as above. The final cell pellet was stored at -80°C until use. For cell-free extract preparation, cells in 50 mM anoxic potassium phosphate buffer (pH 8.5) were broken by French press (82.7 MPa) and the lysate was centrifuged (120,000 x g, 1 hour, 4°C). DNA was extracted from *S. aciditrophicus* cells harvested as above using a DNA extraction kit by Invitrogen Life Technologies (Grand Island, NY). DNA was eluted from the mini-column with 50 µl of elution buffer (Invitrogen) and stored at -20°C until use.

Cloning of SYN_03090 and purification of recombinant SYN_03090 gene product. Gene SYN_03090, annotated as a butyrate kinase, was amplified from *S. aciditrophicus* DNA using primers SYN_03090F $^{5'}$CACCATGAATAAGGCTTGTTCC$^{3'}$ and SYN_03090R $^{5'}$CGATCCGCTCTCTCCCGCT$^{3'}$. Primers were designed according to the specifications outlined for cloning into PET_101 plasmid vector (Invitrogen 2001). Due to the close homology between SYN_03090 and SYN_01210, primers would also anneal to SYN_01210. Amplification was done using Phusion DNA polymerase (Fermentas) with the following PCR parameters: initial denaturation of five minutes at 95°C; 30 cycles of one minute denaturation at 95°C, one minute of annealing at 60 °C, and one minute of elongation at 72°C; followed by a final extension of five minutes at 72°C. The PCR product was ligated into Invitrogen PET_101 plasmid vector and transformed into *E. coli* Top 10 cells. After transformation, colonies were

selected and screened by colony PCR using T7 forward and SYN_03090R primers. Plasmids with the correct PCR fragment size were extracted and sequenced by Oklahoma Memorial Research Foundation DNA Sequencing Facility to insure the correct gene sequence. Plasmid 3090a had the complete nucleotide sequence for SYN_03090 and was selected to transform into *E. coli* BL21 for expression. Expression of the inserted gene was induced when the culture reached an optical density between 0.4-0.6 by the addition of 1 mM isopropyl β-D-1-thiogalactopyranoside (IPTG) followed by incubation at 23°C for 3 hours. The recombinant protein was purified by Ni-affinity chromatography on a 5-mL, Ni-chelating, Sepharose affinity column (HisTrap HP, GE Healthcare, Piscataway, NJ) equilibrated with Tris buffer (10 mM tris(hydroxymethyl)aminomethane (Tris), 250 mM potassium chloride, 5 mM magnesium chloride, and 20 mM imidazole, pH 7.8). The recombinant protein eluted with the above buffer with 0.5 M imidazole at a flow rate of 3 ml min^{-1}.

The activity studies used the Ni-affinity purified recombinant protein in the elution buffer with 0.5 M imidazole, and the purified recombinant protein after removal of imidazole by passage through a PD-10 desalting column (GE Healthcare, Piscataway, NJ), equilibrated with the above Tris buffer without imidazole. In addition, recombinant protein preparations with and without imidazole were incubated with *S. aciditrophicus* cell-free extracts and re-purified by Ni-affinity chromatography in order to determine if a more active protein would be found. The 0.5 M imidazole fraction was used to determine substrate specificity, kinetic constants, and subunit molecular weight.

Enzyme assays. All enzyme assays were performed aerobically at 37°C. The buffers were pre-warmed by incubation at 37°C for 10 min. All activities were linear with time and proportional to the amount of protein. Controls for all assays included the deletion of each substrate and the recombinant protein, and the use of heat-treated protein.

Acetate kinase, butyrate kinase, and propionate kinase activities were determined by measuring the formation of the hydroxamate using the modification of Bowmann *et al* (Bowman et al., 1976). The assay mixture contained: 50 mM Tris (pH 8.3), 10 mM magnesium chloride, 500 mM hydroxylamine (pH 7), 10 mM nucleotide triphosphate (adenosine-5'-triphosphate (ATP), guanosine-5'-triphosphate (GTP), or cytidine-5'-triphosphate (CTP)), and 20 mM of the substrate (either potassium acetate, sodium butyrate, or sodium propionate). The reaction was stopped after 20 minutes of incubation at 37°C by the addition of ferric reagent (10% iron (III) chloride, 3% trichloroacetic acid, in 0.7 N hydrochloric acid) and set at room temperature for 15 minutes. The reaction mixture was centrifuged for 5 min at 13,000 x g and the absorbance was measured at 535 nm. The molar extinction coefficient for acetyl hydroxamate under the assay conditions was 594 M^{-1} cm^{-1}.

The ability of the recombinant protein to make ATP from acetyl-phosphate and butyryl-phosphate was determined by coupling ATP formation to the reduction of $NADP^+$ at 340 nm using hexokinase and glucose-6-phosphate dehydrogenase (Szasz et al., 1976). The reaction mixture contained: 11.3 mM triethanolamine (TEA) (pH 7.8), 2.8 mM magnesium chloride, 1.1 mM

nicotinamide adenine dinucleotide phosphate ($NADP^+$), 5.6 mM glucose, and 9 μg of glucose-6-phosphate dehydrogenase/hexokinase (Roche, Indianapolis, IN), and varying concentrations of ADP (0.04-5 mM), and acetyl-phosphate (0.2-10 mM). The reaction was started with the addition of acetyl-phospate, butyryl-phosphate, or the recombinant enzyme. The extinction coefficient for NADPH is 6220 M^{-1} cm^{-1} (McComb et al., 1976). This assay was also used to determine the K_m and V_{max} of the purified recombinant protein.

Lastly, to avoid assay conditions with high hydroxylamine concentrations, the production of ADP from ATP with acetate or butyrate as the substrate was coupled to the oxidation of NADH using pyruvate kinase and lactate dehydrogenase (Schuhle et al., 2003). The assay mixture contained 50 mM Tris buffer (pH 8.5), 10 mM magnesium chloride, 5 mM ATP, 1 mM phosphoenolpyruvate (PEP), 375 μM NADH, 2.2 U pyruvate kinase, and 2.2 U lactate dehydrogenase (Sigma, St. Louis, MO), and 480 μM coenzyme A (CoA). The reaction was started with the addition of butyrate or acetate.

Homology searches. BLASTn and BLASTp were used to identify homologous nucleotide and amino acid sequences, respectively, to SYN_03090 in the NCBI database. Homology amino acid sequence searches were also performed using the UniProtKB/Swiss-Prot (swissprot) database and enhanced domain database. Phylogenetic tree alignments were done using NCBI COBALT: Constraint-based Multiple Protein Alignment Tool (http://www.ncbi.nlm.nih.gov/tools/cobalt/).

Results

Cell-free extracts of *S. aciditrophicus* grown in pure culture contained acetate kinase and butyrate kinase activities (Table 3.1). Acetate kinase and butyrate kinase activities as measured with the hydroxamate method were 0.25 ± 0.05 and 0.19 ± 0.03 μmol min^{-1} mg^{-1} of protein, respectively. The acetate kinase activity in cell-free extracts of pure-culture grown *S. aciditrophicus* was similar to that found in cell-free extracts of the syntrophic butyrate-degrader, *Syntrophomonas wolfei*, an organism known to use acetate kinase for substrate-level phosphorylation (Wofford et al., 1986), but . Much lower specific activities were detected in cell-free extracts of *S. aciditrophicus-M. hungatei* coculture cells grown on crotonate and benzoate (Table 3.1). Neither activity was detected when cyclohexane-1-carboxylate was the substrate. Cell-free extracts of *M. hungatei* grown in pure culture on hydrogen plus carbon dioxide had very low acetate kinase activity and no detected activity for butyrate kinase (Table 3.1), suggesting that the activities detected in coculture cells were from *S. aciditrophicus*.

Table 3.1: Acetate kinase and butyrate kinase activities in cell-free extracts of *S. aciditrophicus*, *M. hungatei*, and *S. wolfei.*

Culture	Growth Substrate	Acetate Kinase (μmol $min^{-1}mg^{-1}$)	Butyrate Kinase (μmol min^{-1} mg^{-1})
S. aciditrophicus	Crotonate	0.25 ± 0.05[a]	0.19 ± 0.03
S. aciditrophicus/ M. hungatei	Crotonate	0.067	0.087
S. aciditrophicus/ M. hungatei	Benzoate	0.073	0.038
S. aciditrophicus/ M. hungatei	Cyclohexane-1-carboxylate	BDL[b]	BDL
M. hungatei	H_2 and CO_2	0.004 ± 0.002	BDL
Syntrophomonas wolfei	Crotonate	0.37	0.06

[a] mean ± standard deviation of three determinations.
[b] BDL, below detection limit.

The *S. aciditrophicus* genome has two candidate genes that could encode acetate kinase activities, SYN_03090 and SYN_01210, which share 99% identity at the nucleotide level, and both annotate as butyrate kinases. The identity of either SYN_01210 or SYN_03090 could not be distinguished as the primers would anneal to both genes. To test the function of SYN_03090, it was PCR amplified from *S. aciditrophicus* and heterologously expressed in *Escherichia coli* Bl21. The recombinant protein was purified by Ni-affinity chromatography. The subunit mass was determined by denaturing gels and was approximately 40 kDa which is consistent with the expected product size of about 39 kDa. The SYN_03090 gene product had acetate kinase activity (0.22 μmol $min^{-1}mg^{-1}$ of protein); no activity was detected with propionate or butyrate as the substrate by the hydroxymate method. ATP was the preferred nucleotide triphosphate with acetate as the substrate (0.11 μmol $min^{-1}mg^{-1}$ of protein). GTP (0.09 μmol $min^{-1}mg^{-1}$ of protein) and CTP (0.02 μmol $min^{-1}mg^{-1}$ of protein) also served as substrates. No butyrate kinase activity was observed with any of the above nucleotide triphosphates. A concern was that the assay conditions such as high hydroxymate concentration may have inhibited the activity of the enzyme. To test this, the activity was measured with a coupled enzyme assay where ADP formation was coupled to NADH oxidation with pyruvate kinase and lactate dehydrogenase. However, the specific activities of the purified recombinant protein with acetate and butyrate were still low, 0.07 ± 0.02 and 0.02 ± 0.004 μmol $min^{-1}mg^{-1}$ of protein, respectively. The removal of imidazole by passage of the purified recombinant protein through a desalting column did not enhance

acetate kinase activity; the specific acetate kinase activities with and without 0.5 M imidazole were 0.12 ± 0.02 and 0.14 ± 0.01 μmol min^{-1} mg^{-1} of protein, respectively. Incubation of the purified recombinant protein with or without 0.5 M imidazole in *S. aciditrophicus* cell-free extracts did not impact the activity. Rather, the specific acetate kinase activities for both preparations decreased, 0.04 ± 0.004 and 0.03 ± 0.005 for the purified recombinant protein with and without imidazole, respectively. These experiments showed that imidazole did not affect enzyme activity and that incubation in *S. aciditrophicus* cell-free extracts to allow post-translational modification did not enhance activity.

To demonstrate that the purified recombinant protein could function to make ATP, its activity was measured in the direction of acetate and ATP formation using hexokinase and glucose-6-phosphate dehydrogenase as coupling enzymes and acyl-phosphates and ADP as substrates. The specific activity was 0.82 ± 0.21 μmol of $min^{-1}mg^{-1}$ of protein with acetyl-phosphate. Only barely detectable activity (0.002 ± 0.001 μmol of $min^{-1}mg^{-1}$ of protein) was observed with butyryl-phosphate, supporting the conclusion that the SYN_03090 gene product is an acetate kinase and not a butyrate kinase (Table 3.2).

The recombinant protein had a V_{max} of 0.91 and 1.03 μmol $min^{-1}mg^{-1}$ of protein and a K_m value of 0.22 ± 0.04 and 0.52 ± 0.09 mM for acetyl-phosphate and ADP, respectively when assayed by coupling ATP formation from acetyl-phosphate and ADP to the reduction of $NADP^+$ with hexokinase and glucose-6-phosphate dehydrogenase (Table 3.2).

Table 3.2: Kinetic characterization of the purified recombinant SYN_03090 gene product.

Enzyme	Substrate	K_m (mM)[a]	V_{max} (µmol min^{-1} mg^{-1})[a]	Highest activity detected (µmol min^{-1} mg^{-1})[b]
Acetate Kinase SYN_03090 gene product	Acetyl-phosphate→ Acetate			
	Acetyl-phosphate	0.22 ± 0.04	0.91 ± 0.04	0.87 ± 0.03[b]
	ADP	0.52 ± 0.09	1.03 ± 0.06	
	Acetate→Acetyl-Phosphate			0.22 ± 0.003

[a] Standard error of the non linear regression plot.
[b] mean ± standard deviation of three determinations.

The BLAST-P program was used to search the NCBI and UniProtKB/Swiss-Prot databases for proteins homologous to SYN_03090 amino acid sequence. Phylogenetic analyses showed a clear distinction between the butyrate kinases and acetate kinases amino acid sequences with SYN_03090/SYN_01210 amino acid sequences grouping with those of the butyrate kinases (Figure 3.1). The SYN_03090 deduced amino acid sequence clustered with 39 other butyrate kinases, sharing greater than 40% identity over 96% of the amino acid sequence. The closest homologous sequence was to a butyrate kinase from *Thermoanaerobacter tengcongensis* MB4 (locus ID: BUK1_THETN), a member of the Clostridia, with 53% identity over 96% of the amino acid sequence. The SYN_03090 deduced amino acid sequence shared 45% identity to over 96% of the amino acid sequence for BUK1_CLOAB and 48% identity to over 97% of the amino acid sequence to BUK2_CLOAB, two butyrate kinases from *Clostridium acetobutylicum* whose activities have been confirmed biochemically (Huang, Huang, Rudolph, & Bennett, 2000). The closest acetate kinase sequences were from *Campylobacter concisus* 13826 (Locus ID: ACKA_HELPJ) and *Campylobacter curvus* 525.92 (Locus ID: ACKA_CAMFF), both members of the Epsilonproteobacteria. The SYN_03090 amino acid sequence shared 39% identity over 43% of the amino acid sequence to both of the above acetate kinases. The region in SYN_03090 amino acid sequence with 35% identity to acetate kinases included the regions between amino acid residues between 140-300, which are predicted to be the active domain for the acetokinase family (pfam00871) that includes acetate kinases, butyrate kinases,

and 2-methylpropanoate kinases (Ward, Ross, van der Weijden, Snoep, & Claiborne, 1999). DELTA-BLAST analyses of the Swissprot database showed the SYN_03090 nucleotide sequence had 20% identity over 96% of the nucleotide sequence to the acetate kinases ACKA_HELPJ and ACKA_CAMFF. The region with closer homology was consistent with the active sites of the proteins and suggests the activity of SYN_03090 could function as an acetate kinase.

Figure 3.1: Neighbor joining phylogentic tree for SYN_03090 (annotated as butyrate kinase) compared to the closest representatives from BLAST-p search. BLAST searches were performed on 01-16-2014.

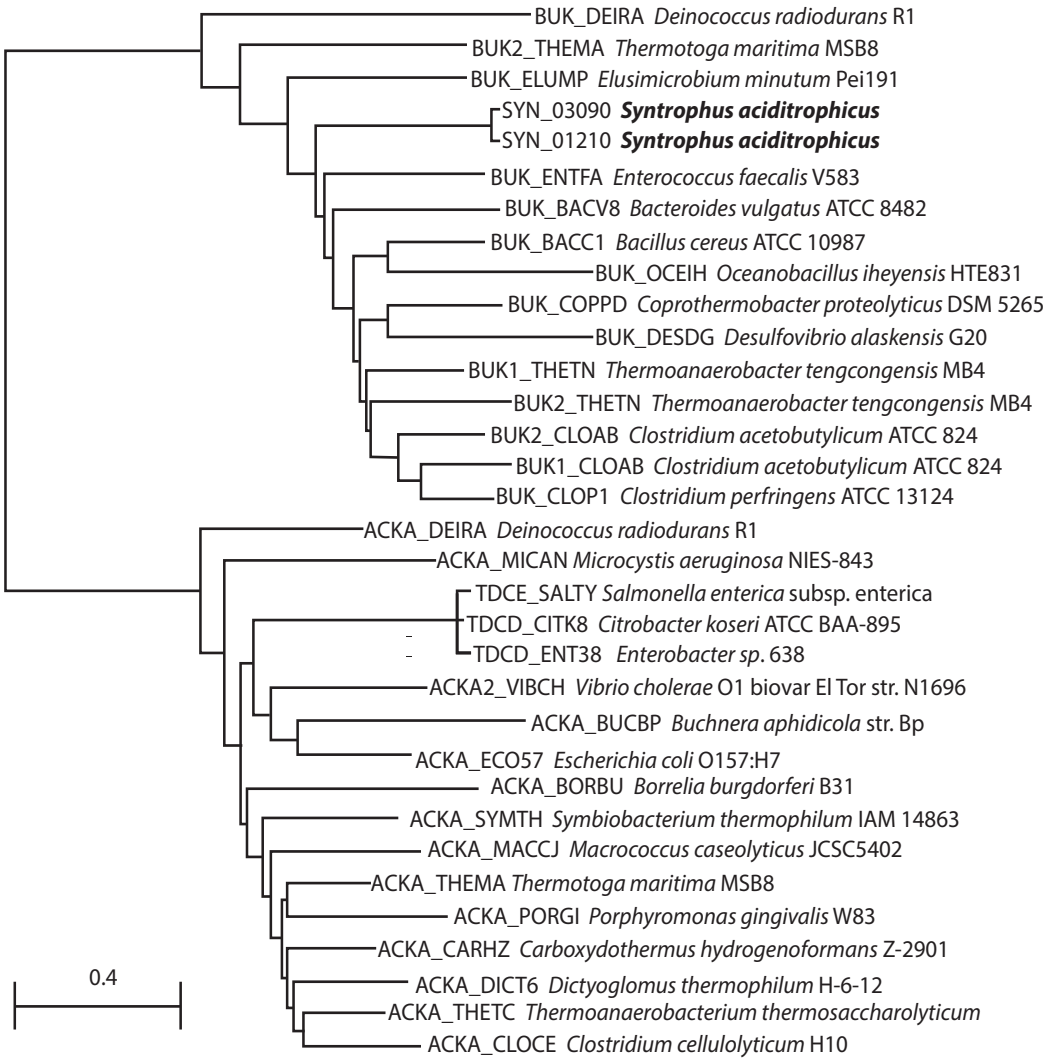

Discussion

Genomic analysis did not detect a gene for acetate kinase in *S. aciditrophicus* (McInerney 2007) even though low levels of acetate kinase have been detected in cell-free extract of *S. aciditrophicus*. The *S. aciditrophicus* genome has two gene clusters, each with butyrate kinase and phosphate acetyl/butyryl transferase genes; the butyrate kinase genes could function as acetate kinases. Heterologous expression of gene product SYN_03090, annotated as a butyrate kinase, showed the expressed protein had acetate kinase activity and no butyrate kinase activity. The recombinant protein preferred ATP, but activity was detected with GTP. Regardless of whether the activity of the purified recombinant protein was measured in the direction of ATP formation (butyryl-phosphate as the substrate) or in the direction of ADP formation (butyrate as the substrate) using coupling enzymes or the hydroxymate method, butyrate kinase activity was either not detected or just above the detection limit. These data support the conclusion that SYN_03090 gene product is an acetate kinase.

The physiological role of SYN_03090 gene product is unclear. The V_{max} for the purified recombinant protein were 0.91 and 1.03 μmol $min^{-1}mg^{-1}$ of protein for acetyl-phosphate and ADP, respectively, which are low compared to known acetate kinases (Table 3.2). The activities for some well-characterized acetate kinases range from 42 μmol $min^{-1}mg^{-1}$ to 1180 μmol $min^{-1}mg^{-1}$ (Chittori, Savithri, & Murthy, 2012; Ren et al., 2007). The low acetate kinase activity of the expressed protein from SYN_03090 could be due to expression problems in

E. coli or that the assay conditions do not reflect *in vivo* conditions. However, it is possible that the SYN_03090 gene product can account for the acetate kinase rates observed in cell-free extracts, as these activities are low (Table 3.1). In support of a role for SYN_03090 in energy conservation in *S. aciditrophicus*, transcripts of SYN_03090 were detected in pure cultures grown on crotonate and crotonate plus benzoate and in cocultures grown on crotonate, benzoate, and cyclohexane-1-carboxylate (see Chapter 2 of this dissertation). In addition, two-dimension, denaturing gel electrophoresis detected polypeptides of SYN_03090 in pure culture grown cells of *S. aciditrophicus* (Chapter 2). While SYN_03090 may be responsible for the observed acetate kinase activities, butyrate kinase activity was not detected with the purified recombinant protein so the protein responsible for this activity remains unknown.

Acetate kinases are found in all domains of life (Ingram-Smith et al., 2006). The phylogenetic analyses show a clear distinction between the butyrate kinases and acetate kinases with SYN_03090 grouping with the butyrate kinases (Figure 3.1). Butyrate kinase anotations in the Swissprot database are assigned based on functional domain alignments to the characterized butyrate kinase from *C. acetobutylicum* (Figure 3.1). Of the butyrate kinases sequenced, only two have confirmed butyrate kinase activities, CLOAB_BUK1 and CLOAB_BUK2 both from *Clostridium acetobutylicum*. Activities from the cloned and expressed CLOAB_BUK2 had a V_{max} of 165 μmol $min^{-1}mg^{-1}$ and K_m of 0.62 mM for butyrate (Huang et al., 2000). No further characterization of other butyrate kinases is known. The data in this study does not support the butyrate kinase annotation

for SYN_03090, Rather, enzyme analyses suggest that the SYN_03090 gene product is an acetate kinase. Both acetate kinases and butyrate kinases are within the acetokinase family of enzymes, and the butyrate kinase group is poorly understood. The lack of butyrate kinase activity could also be attributed to random mutation in the sequence, mismatch amino acids due to rare codon usage, or improper folding of the induced proteins in *E. coli*. Our data suggests that further characterization of the butyrate kinases from representative organisms is necessary to distinguish butyrate kinases from acetate kinases when assigning annotations based on sequence information alone.

Chapter 4: Identification and characterization of a cyclohexane-1-carboxylate:CoA ligase, and of two benzoate:CoA ligase-crotonate:CoA ligases from *S. aciditrophicus*

Abstract

Syntrophus aciditrophicus syntrophically degrades benzoate, alicyclic compounds (such as cyclohexane-1-carboxylate), and some fatty acids when grown in coculture with hydrogen- and/or formate-using microorganisms. It can also ferment crotonate in pure culture. Previous studies indicated that *S. aciditrophicus* uses AMP-forming acyl-CoA synthetases (substrate:CoA ligase) rather than CoA transferases for substrate activation. Here, two crotonate/benzoate:CoA ligases were purified and characterized from cell-free extracts of *S. aciditrophicus*. Peptide analysis showed that these proteins were gene products of SYN_02896 and SYN_02898. The gene SYN_03128, annotated as a long-chain fatty acid-CoA ligase, was cloned and heterologously expressed in *Escherichia coli*. The purified SYN_03128 gene product had high activity and affinity for cyclohexane-1-carboxylate (V_{max} and K_m of 15 ± 0.5 μmol $min^{-1}mg^{-1}$ and 0.04 ± 0.007 mM, respectively), showing that it is a cyclohexane-1-carboxylate:CoA ligase. *S. aciditrophicus* uses benzoate:CoA ligase for activation of both benzoate and crotonate, and a separate ligase for the activation of cyclohexane-1-carboxylate.

Introduction

In methanogenic environments, complex organic matter is degraded to methane and carbon dioxide by a diverse microbial community (McInerney et al., 2009). Fatty acids and aromatic acids are key intermediates in methanogenic decomposition. Their degradation is catalyzed by kinetically coupled associations of two metabolically different microbial species, a hydrogen- and formate-producing bacterium and a hydrogen- and formate-using methanogenic archaeon, in a process known as syntrophy (McInerney et al., 2009). The syntrophic degradation of fatty acids, aromatic compounds, and alcohols is thermodynamically favorable only when the hydrogen and/or formate concentrations are kept at very low levels by the methanogen (McInerney et al., 2009). In methanogenic environments, members of the genus *Syntrophus* catalyze the syntrophic degradation of benzoate and other aromatic compounds (McInerney et al., 2007). *Syntrophus aciditrophicus* serves as the model organism to study syntrophic benzoate metabolism. *S. aciditrophicus* syntrophically degrades benzoate, alicyclic compounds (such as cyclohexane-1-carboxylate), and some fatty acids when grown in coculture with hydrogen- and/or formate-using microorganisms; *S. aciditrophicus* can also ferment crotonate in pure culture (Elshahed et al., 2001; Hopkins et al., 1995; Jackson et al., 1999; Mouttaki et al., 2008).

The metabolism of fatty or aromatic acids involves uptake by the cell and then conversion to acyl-CoA thioesters (Weimar, DiRusso, Delio, & Black, 2002). The activation of fatty acids and aromatic acids to their respective acyl-CoA

thioester is catalyzed by AMP-forming, acyl-CoA ligase or by CoA transferase (Oberender, Kung, Seifert, von Bergen, & Boll, 2012). For example, the activation of benzoate to benzoate-CoA via a benzoate:CoA ligase, involves the hydrolysis of ATP to AMP and pyrophosphate (PP_i) (Equation 1). Ligases are also referred to as AMP-forming, acyl-CoA ligases. Alternatively, the activation of benzoate to benzoyl-CoA via a CoA transferase does not involve ATP hydrolysis. Rather, the CoA moiety is transferred to the acid from an acyl-CoA intermediate, such as acetyl-CoA or succinyl-CoA (Equation 2).

Equation 1: benzoate + CoA + ATP → benzoate-CoA + AMP + PP_i

Equation 2: benzoate + acetyl-CoA → benzoate-CoA + acetate

The photosynthetic benzoate degrader, *Rhodopseudomonas palustris,* uses a benzoate:CoA ligase to activate benzoate (Egland et al., 1995). The use of a ligase reaction ultimately involves the loss of two "high-energy" bonds as pyrophosphate is rapidly hydrolyzed to two phosphates. *Syntrophomonas wolfei,* which syntrophically degrades fatty acids (McInerney et al., 1981), and *Sporotomaculum hydroxybenzoicum*, which syntrophically degrades 3-hydroxybenzoate (Muller & Schink, 2000), both use a CoA transferase to activate their substrates to the respective CoA intermediate (Muller & Schink, 2000; Wofford et al., 1986). In addition, *Geobacter metalireducens* uses a succinyl-CoA:benzoate CoA transferase to activate benzoate to benzoate-CoA (Oberender et al., 2012). The activation of the substrate by CoA transferase is

less energy intensive than activation by an acyl-CoA ligase because only the equivalent of one "high-energy" bond, the CoA thioester bond, is used for substrate activation by the CoA transferase reaction (Equation 2). Given the limited amount of free energy available during the syntrophic catabolism of fatty and aromatic acids (Jackson & McInerney, 2002), one would expect that syntrophic fatty acid and aromatic acid degraders would use a CoA transferase rather than a ligase for substrate activation.

However, enzymatic analyses implicated the use of AMP-forming, benzoate:CoA ligase activity and not a CoA transferase activity for the activation of benzoate in all three *Syntrophus* species, S*. aciditrophicus, S. buswellii* and *S. gentianae* (Elshahed et al., 2001; L. Schocke & Schink, 1999). Neither acetyl-CoA:benzoate CoA transferase nor acetyl-CoA:crotonate CoA transferase activity were detected in cell-free extracts of *S. aciditrophicus* (Elshahed et al., 2001; Mouttaki et al., 2007). The use of AMP-forming acyl-CoA ligases for substrate activation demands less energy than previously assumed, because pyrophosphate can be used to synthesize ATP from AMP by the acetyl-CoA synthetase discussed in Chapter 2 of this dissertation. There are several remaining questions regarding substrate activation in *S. aciditrophicus*. Are the same ligases used for activation of different substrates? What gene products are involved in substrate activation? Genomic analysis detected multiple ligase genes that could be involved in the activation of fatty and aromatic acids in *S. aciditrophicus* (McInerney et al., 2007). The *S. aciditrophicus* genome has two genes annotated as 4-hydroxybenzoate:CoA ligase (SYN_02896 and

SYN_02898), one gene annotated as a 2-aminobenzoate:CoA ligase (SYN_02417), three genes annotated as long-chain fatty acid-CoA ligases (SYN_02640, SYN_02643, and SYN_03128), one gene annotated as a fatty acid-CoA ligase (SYN_01145), one gene annotated as a 2,3-dihydroxybenzoate-AMP ligase (SYN_01638), and one gene annotated as a O-succinylbenzoic acid-CoA ligase (SYN_02620) (McInerney et al., 2007).

Here, I used protein purification and recombinant DNA approaches to identify the gene products involved in the activation of crotonate, benzoate and cyclohexane-1-carboxylate in *S. aciditrophicus*. Two gene products that have both crotonate:CoA ligase and benzoate:CoA ligase activities were purified and characterized from cell-free extracts of *S. aciditrophicus*. In addition, heterologous expression of the SYN_03128 showed that its gene product is likely involved in the activation of cyclohexane-1-carboxylate.

Material and Methods

Media and conditions of cultivation. Anaerobic media and solutions were prepared using a modified Balch technique (Balch & Wolfe, 1976; McInerney et al., 1981). Pure cultures and cocultures of *Syntrophus aciditrophicus* strain SB (DSM 26646) were grown anaerobically in minimal medium without rumen fluid (McInerney and Bryant, 1979). The Wolin's metal solution was modified to include $Na_2MoO_4{\cdot}2H_2O$ (0.01g/L) Na_2SeO_4 (0.01g/L) and $Na_2WO_4{\cdot}2H_2O$ (0.01g/L) (Sieber et al., 2014). The headspace was pressurized to 27.5 kPa with 80% N_2: 20% CO_2 (vol/vol) gas phase. All media and solutions were sterilized by autoclaving (121^{o}C; 15 min; 103 kPa) (Balch et al., 1979; McInerney & Bryant, 1981; Sieber et al., 2014; Tanner, Wolfe, & Ljungdahl, 1978). *S. aciditrophicus* was grown in the above medium in pure culture on 20 mM crotonate and in coculture with *Methanospirillum hungatei* strain JF-1 (ATCC 27890) on 20 mM crotonate, 10 mM benzoate, and 10 mM cyclohexane-1-carboxylate. All cultures were checked for contamination using thioglycollate medium, which does not support the growth of *S. aciditrophicus* and microscopic analysis.

To obtain sufficient biomass for enzyme activity determination and purification of the benzoate:CoA ligase and crotonate:CoA ligase activities, the pure culture of *S. aciditrophicus* was grown in 1.5 L volumes in 2 L Schott bottles on the 20 mM crotonate medium described above. Cells were harvested at mid-log phase by centrifugation (14,300 x g, 20 min, 4°C). The cells were resuspended in 50 mM anoxic phosphate buffer (pH 8.5) and centrifuged as

above. The final pellet was resuspended in 50 mM anoxic phosphate buffer (pH 8.5) and stored at -80°C until used. Cell-free extracts were prepared by breaking cells with a French pressure cells (82.7 MPa) and the lysate was centrifuged (120,000 x g for 60 minutes at 4°C). The soluble portion was designated as the cell-free extract.

To determine the effect of crotonate concentration on the growth, *S. aciditrophicus* was grown in pure culture in the above medium with 2.5, 5, 10, 15 and 20 mM sodium crotonate. The medium was dispensed in 10 ml amounts into Balch tubes and triplicate tubes were used for each concentration.

Enzyme assays. All enzyme assays were performed anaerobically and aerobically to determine the affects of oxygen on activity. All activities were linear with time and proportional to the protein concentration. Controls for all assays included the deletion of each substrate and the cell-free extract, and the use of heat-treated extracts.

AMP-forming, CoA ligase activities were measured by coupling AMP formation to the oxidation of reduced nicotinamide adenine dinucleotide (NADH) spectrophotometrically at 340 with myokinase, pyruvate kinase and lactate dehydrogenase (Schuhle et al., 2003). The assay mixture contained 50 mM Tris-HCl buffer (pH 8.5), 10 mM magnesium chloride, 5 mM ATP, 1 mM phosphoenolpyruvate, 375 μM NADH, 2.8 U myokinase, 2.2 U pyruvate kinase, 2.2 U lactate dehydrogenase, 480 μM coenzyme A (CoA) and either crotonate, benzoate, or cyclohexane-1-carboxylate in varying concentrations as substrate, each as 100 mM stock solutions. The reaction was started with the addition of

the fatty acid. The absorption coefficient for NADH was 6220 M^{-1} cm^{-1} at 340 nm (McComb et al., 1976). The K_m and V_{max} were determined by non-linear regression analysis of data fit to the Michaelis-Menten equation on Kaleidagraph (Synergy Software, Reading, PA). To determine enzyme substrate specificity, each purified product was assayed for activity with the following fatty acids stock solutions: 100 mM sodium benzoate, 100 to 500 mM crotonic acid, 100 mM cyclohexane-1-carboxylic acid, 100 mM cyclohexene-1-carboxylic acid, 100 mM benzoate, 100 to 500 mM crotonate, 100 mM acetate, 100 mM 2-hydroxybenzoate, 100 mM 3-hydroxybenzoate, 100 mM butyrate, and 100 mM succinate.

Purification of crotonate:CoA ligase activity. For purification of the dominant crotonate:CoA ligase activity, approximately 2 grams of crotonate-grown, pure culture cells of *S. aciditrophicus* were broken by French press (82.7 MPa). The cell lysate was ultracentrifuged (120,000 x g for 60 minutes at 4 °C) and two milliliters of soluble portion were loaded onto a diethylaminoethyl (DEAE) sepharose column (Fast Flow, volume 10mL, diameter 0.5 cm, Biorad) at a flow rate of 3 ml min^{-1}. The DEAE column was equilibrated and washed with DEAE binding buffer, which contained 20 mM triethanolamine (TEA) and 5 mM magnesium chloride, pH 7.8. DEAE binding buffer with 500 mM sodium chloride was used to create a linear gradient from 0 to 200 mM sodium chloride to elute the crotonate:CoA ligase activity; 1.5-ml volume fractions were collected. The active crotonate:CoA ligase fractions were pooled (~ 13 ml) and concentrated (~ 5ml) using an Amicon filtration device with a 30-kDA

molecular weight cut off filter. The pooled, crotonate:CoA ligase fraction was desalted on a G20 column equilibrated with DEAE binding buffer. The crotonate:CoA ligase activity was eluted from the G20 column with 3 ml of DEAE binding buffer. Two and a half milliliters of the concentrated active desalted fraction was applied to a 2.5-ml reactive green 19 affinity column (Affinity Media Pre packed reactive green 19 agarose, 2.5 ml, 2-5 mg dye per ml, SIGMA), which was equilibrated with DEAE binding buffer. After loading, the reactive green 19 column was washed with 5 ml of TEA binding buffer (20 mM TEA, 5 mM magnesium chloride, and 5 mM potassium phosphate buffer, pH 7.8). Proteins were eluted by adding 5 ml of TEA buffer with each of the following concentrations of sodium chloride: 62, 125, 250, 500 mM. Five-milliliter fractions were collected and assayed for crotonate:CoA ligase activity. The crotonate:CoA ligase activity eluted at 125 mM sodium chloride (5.5 ml active fraction). The reactive green 19 purified crotonate:CoA ligase activity showed a single band on denaturing gel electrophoresis and was used for kinetic analysis, substrate specificity, and subunit molecular weight analysis. The band was excised and sent to Laboratory for Molecular Biology and Cytometry Research (Oklahoma City, USA) for in gel trypsin digestion and sequencing by high performance liquid chromatography and tandem mass spectrometry (HPLC/MS/MS) (University of Oklahoma Health Sciences Center Proteomics Core Facility, Oklahoma City, OK 73104 (OUHSC)). Kinetic constants for crotonyl-CoA and benzoate:CoA ligase activities were determined with

crotonate (0.4 to 35 mM), CoA (0.01 to 2.5 mM), and sodium benzoate (0.01 to 6 mM) with the co-substrates kept at saturation.

Purification of benzoate:CoA ligase. For purification of the dominant benzoate:CoA ligase activity, approximately 1.5 grams of crotonate-grown, pure culture cells of *S. aciditrophicus* were broken by French press at 82.7 MPa. Three milliliters of the cell-free extract was treated with 45% ammonium sulfate and centrifuged (21,000 x g for 10 minutes at 4°C). The soluble portion contained benzoate:CoA ligase activity and was desalted on a G20 column and equilibrated with DEAE binding buffer. Three milliliters of the desalted ammonium sulfate fraction were applied to a DEAE-Sepharose column and equilibrated with DEAE binding buffer at a flow rate of 3 ml min^{-1}. Proteins were eluted with a linear gradient of 0 to 200 mM sodium chloride in DEAE binding buffer; 1.5-ml fractions were collected. Fractions with benzoate:CoA ligase activity were pooled, concentrated, and desalted using an Amicon filtration device with a 30-kDA molecular weight cut off filter. The concentrated activity was then loaded onto a hydroxyapatite column (MacroPrep, ceramic hydroxyapatite 40 μm, 2.5 ml, 0.5 ml diameter; Biorad, Hercules, CA), equilibrated with hydroxyapatite buffer (20 mM TEA, 5 mM magnesium chloride, and 5 mM potassium phosphate, pH 7.8) at a flow rate of 2 ml per minute. The activity was eluted with hydroxyapatite buffer with 200 mM potassium phosphate by a linear gradient of 5 to 200 mM potassium phosphate. The benzoate:CoA ligase fractions eluted at 40 mM potassium phosphate. The hydroxyapatite-purified fraction was used for further analysis. The hydroxyapatite-purified fraction had

two bands present on denaturing gel. Each band was excised and sent to OUHSC Laboratory for peptide analysis as described above. Kinetic paramenters for benzoate:CoA ligase activity was determined with the following range of substrates benzoate (0.02 to 10 mM) and CoA (0.01 to 1 mM CoA) with the respective co-substrates kept at saturation.

Purification of cyclohexane-1-carboxylate:CoA ligase. Gene SYN_03128, annotated as long-chain-fatty-acid-CoA ligase, was amplified from *S. aciditrophicus* DNA using primers SYN_03128F-$^{5'}$CACCTTGTTATTCTTAAAAAAGGAGGA$^{3'}$and SYN_03128R-$^{5'}$ATCCAAGTCGGGGAAAATCTTTCT$^{3'}$. Gene SYN_03128 was amplified using DNA polymerase Phusion DNA polymerase (Fermentas) with following PCR parameters: initial denaturation of five minutes at 95°C; 30 cycles of one minute denaturation at 95°C, one minute of annealing at 60 °C, and one minute of elongation at 72°C; followed by a final extension of five minutes at 72°C. The PCR product was ligated into Invitrogen PET_101 vector and transformed into *E. coli* Top 10 cells. After transformation, colonies were selected and screened by colony PCR using T7 forward and SYN_03128R primers. Plasmids with the correct PCR fragment size were extracted and sequenced by Oklahoma Memorial Research Foundation DNA Sequencing Facility (OUHSC) to insure the correct gene sequence. Plasmid 3128b had the complete and correct nucleotide sequence and was selected to transform into *E. coli* BL21 for expression. Protein expression was induced when the culture reached an optical density between 0.4-0.6 by the addition of 1 mM IPTG (isopropyl-β-d-

thiogalactopyranoside) followed by overnight incubation at 18°C. The recombinant protein was purified by Ni-affinity chromatography on a 5 ml Ni-chelating Sepharose affinity column (HisTrap HP, GE Healthcare, Piscataway, NJ) and equilibrated with his-tag buffer (20 mM potassium phosphate, 200 mM sodium chloride, 20 mM imidazole, pH 7.5). The recombinant protein was washed with 50 mM imidazole, and eluted with 250 mM imidazole at a flow rate of 2 ml per minute. The active fraction was desalted using a PD-10 column (GE Healthcare, Piscataway, NJ) and transferred into assay buffer. The desalted assay fraction was used to determine substrate specificity, kinetics, and molecular mass. The kinetic parameters of the SYN_03128 gene product were determined with the cyclohexane-1-carboxylate (0.5 μM to 2 mM), CoA (0.03 mM to 1 mM), and 1-cyclohex-1-ene-1-carboxylate (0.5 μM to 5 mM) with the respective co-substrates kept at saturation.

Protein concentration was determined using Bradford assay using Coomassie Plus Protein Assay Reagent (Thermo Scientific, Waltham, MA) and standard was 2 mg/ml bovine serum albumin.

Results

The crotonate:CoA ligase specific activity in extracts was 1.03 ± 0.04 μmol min^{-1} mg^{-1} of protein. Crotonate: CoA ligase activity was purified from the cell-free extracts of *S. aciditrophicus* grown in pure culture on crotonate to determine the identity of the protein used for crotonate activation. The purification of the AMP-forming, crotonate:CoA ligase was carried out in three purification steps involving ultracentrifugation, chromatography by DEAE-sepharose, and reactive green 19 agarose affinity chromatography (Table 4.1). The purification resulted in a homogenous protein that migrated as a single band with an apparent mass of 60 kDA on denaturing gel electrophoresis (Figure 4.1). HPLC/MS/MS analysis identified 52 unique polypeptides to one protein encoded by SYN_02896 (Table 4.2). The purified crotonate:CoA ligase activity accounted for 8% of the initial activity recovered and had a 22-fold higher activity than that detected in cell-free extracts (Table 4.1).

Figure 4.1: Denaturing gel electrophoresis of fractions from the purification of the crotonate:CoA ligase activity (SYN_02896 gene product). Lane 1, protein standards; Lane 2, *S. aciditrophicus* cell-free extract; Lane 3, pooled DEAE fraction; Lane 4, concentrated DEAE pooled fraction; Lane 5, skipped well; Lane 6, desalted concentrated DEAE pooled fraction; Lane7, skipped well; Lane 8, Affinity reactive green fraction; Lane 9, skipped well; Lanes 10-11-12, hydroxyapatite pooled fraction. Bands in lanes 11 & 12 were sent for sequencing.

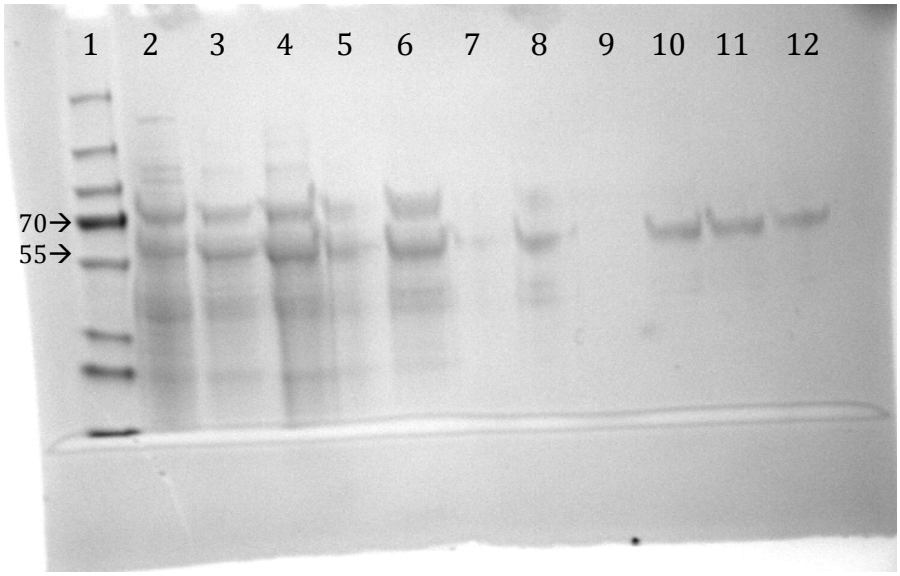

Table 4.1: Purification of crotonate:CoA ligase activity (SYN_02896 gene product) from *S. aciditrophicus* cell-free extracts.

Purification Step	Volume (ml)	Total Protein (mg ml)	Specific Activity (µmol min^{-1} mg^{-1})	Total Activity (µmol min^{-1} ml)	Fold Purifi-cation	% Yield
Cell-free extracts	3	67	0.21	14.1	1	100
DEAE Chromotography	10	12	0.77	9.6	3.6	68
DEAE concentrated desalted	3.5	7	0.61	4.2	2.9	30
Reactive Green	1.5	0.3	4.69	1.2	22	8

Table 4.2: Peptide analysis of the purified crotonate:CoA/benzoate:CoA ligase activity (SYN_02896 gene product) and the partially purified benzoate:CoA/ crotonate:CoA ligase activity (SYN_02896 and SYN_02898 gene products).

Activity	Gene Product	Database Accession	Number of Unique Peptides	Average Intensity	Mascot score
Crotonate & Benzoate:CoA ligase activity	SYN_02896	gi|85858649	52	6.742 E+4	2105
Benzoate:CoA Ligase activity	SYN_02898	gi|85858651	11	2572	1026
	SYN_02896	gi|85858649	25	7.356 E+4	1381

Enzyme specificity and kinetic constants were determined for the purified crotonate:CoA ligase activity (SYN_02896 gene product) to determine its physiological function. The purified SYN_02896 gene product had high crotonate:CoA ligase activity (14.5 μmol $min^{-1}mg^{-1}$) and benzoate:CoA ligase activity (46.2 μmol $min^{-1}mg^{-1}$) (Table 4.3). In addition, the enzyme had lower activity for cyclohexane-1-carboxylate (0.08 μmol $min^{-1}mg^{-1}$) and 1-cyclohex-1-ene-1-carboxylate (0.07 μmol $min^{-1}mg^{-1}$) (Table 4.3). No activity was detected with acetate, butyrate and succinate as substrates (Table 4.4). Kinetic constants were determined for the SYN_02896 gene product for both crotonate and benzoate:CoA ligase activities. The V_{max} for the crotonate:CoA ligase activity was 14 ± 2 μmol $min^{-1}mg^{-1}$ and the K_m values for crotonate and CoA were 4.7 ± 2 mM and 0.5 ± 0.2 mM, respectively (Table 4.3). The V_{max} for the benzoate:CoA ligase activity was 54 ± 2 μmol $min^{-1}mg^{-1}$ and the K_m value for benzoate was 0.3 ± 0.05 mM (Table 4.3).

Table 4.3: Kinetic constants of the purified crotonate:CoA/benzoate:CoA ligase activity (SYN_02896 gene product), the partially purified crotonate:CoA/ benzoate:CoA ligase activity (SYN_02896 and SYN_02898 gene products), and purified recombinant SYN_03128 gene product.

Enzyme	Substrate	K_m (mM)[a]	V_{max} (µmol $min^{-1}mg^{-1}$)[a]	Maximum activity detected (µmol $min^{-1}mg^{-1}$)[b]
Crotonate & Benzoate: CoA ligase activity (SYN_02896 gene product)	Crotonate	4.7 ± 2	14 ± 2	14.5
	CoA (Crotonate)	0.5 ± 0.2	17 ± 4	16.1
	Benzoate	0.3 ± 0.05	54 ± 2	46.2
Benzoate:CoA Ligase activity (SYN_02896 & SYN_02898 gene products present)	Benzoate	0.3 ± 0.2	35 ± 0.6	34.4
	CoA	0.3 ± 0. 1		
SYN_03128 purified recom-binant protein	Cyclohexane-1-carboxylate	0.04 ± 0.007	15 ± 0.5	14.5
	CoA	0.32 ± 0.05		
	Cyclohex-1-ene-1-carboxylate	0.006 ± 0.002	0.64 ± 0.04	0.51
	Crotonate	38 ± 6	0.7 ± 0.04	

[a] Standard error as a function of non linear regression.
[b] mean ± standard deviation of three determinations.

Table 4.4: Substrate specificity of the purified crotonate:CoA/benzoate:CoA ligase activity (SYN_02896 gene product), the partially purified benzoate:CoA/crotonate:CoA ligase activity (SYN_02896 and SYN_02898 gene products), and the purified recombinant SYN_03128 gene product.

	Crotonate & Benzoate:CoA ligase activity (SYN_02896 gene product)	Benzoate:CoA Ligase activity (SYN_02896 & SYN_02898 gene products present)	SYN_03128 purified recombinant protein
	(μmol $min^{-1}mg^{-1}$)	(μmol $min^{-1}mg^{-1}$)	(μmol $min^{-1}mg^{-1}$)
Benzoate	11.9	23	0.18
Crotonate	3.4	0.75	0.03
Cyclohexane-1-carboxylate	0.08	0.56	14.5
Cyclohex-1-ene-1-carboxylate	0.07	BDL	0.59
Acetate	BD[a]	0.13	0.06
2-hydroxybenzoate	ND[b]	BDL	BDL
3-hydroxybenzoate	ND	0.01	BDL
4-hydroxybenzoate	ND	0.02	BDL
Butyrate	BDL	BDL	BDL
Succinate	BDL	BDL	0.13

[a] BDL, below detection limit.
[b] ND, not determined.

The benzoate:CoA ligase specific activity in cell-free extracts was determined to be 7.14 ± 0.4 μmol min^{-1} mg^{-1} of protein. The purification of the AMP-forming benzoate:CoA ligase activity involved ultracentrifugation, ammonium sulfate precipitation, chromatography on DEAE-sepharose, and hydroxyapatite from cells of *S. aciditrophicus* grown on crotonate (Table 4.5). The DEAE column fractions were assayed for both benzoate:CoA ligase and crotonate-CoA ligase activities, which revealed that these two activities migrated as separate peaks (Figure 4.2). The final reactive green 19 agarose fraction contained two protein bands with masses of approximately 60 kDa on denaturing gels (Figure 4.3). HPLC/MS/MS analysis revealed that polypeptides from two different proteins were present. Eleven unique polypeptides were assigned to the SYN_02898 gene product, which has a mass of 58951 daltons; and 8 unique polypeptides were assigned to the SYN_2896 gene product, which has a mass of 59049 daltons (Table 4.2). Both of these proteins are annotated as 4-hydroxybenzoate:CoA ligase/benzoate:CoA ligases. The partially purified benzoate:CoA ligase actitivity accounted for 36% of the initial activity recovered and had a 360-fold higher activity that that detected in cell-free extracts (Table 4.5). The benzoate:CoA ligase activity detected this fraction could be from either or both of the SYN_02896 of SYN_02898 gene products. The reactive green 19 agarose purified protein had maximum detected activity of 34.4 μmol $min^{-1}mg^{-1}$. The V_{max} of the partially purified benzoate:CoA ligase was 35 ± 0.6 μmol $min^{-1}mg^{-1}$ and the apparent K_m values of 0.3 ± 0.2 mM for benzoate and 0.3 ± 0.1 mM for CoA (Table 4.3). The partially purified enzyme

had low activity for crotonate (0.75 μmol $min^{-1}mg^{-1}$), cyclohexane-1-carboxylate (0.56 μmol $min^{-1}mg^{-1}$), acetate (0.13 μmol $min^{-1}mg^{-1}$), 3-hydroxybenzoate (0.01 μmol $min^{-1}mg^{-1}$), and 4-hydroxybenzoate (0.02 μmol $min^{-1}mg^{-1}$) (Table 4.4).

Figure 4.2: Elution of the benzoate:CoA ligase and crotonyl-CoA ligase activities during ion exchange chromatography.

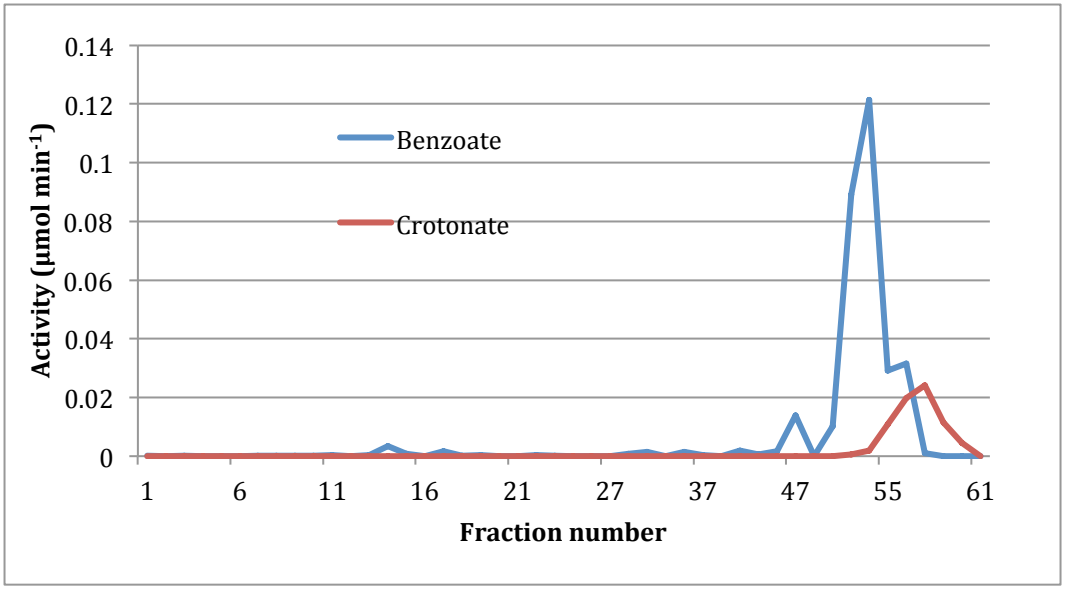

Figure 4.3: Denaturing gel electrophoresis of various fractions during the purification of the benzoate:CoA ligase activity (SYN_02896 and SYN_02898 gene products) from *S. aciditrophicus* cell-free extracts. Lane 1, *S. aciditrophicus* cell-free extract; Lane 2, soluble ammonium sulfate precipitation; Lane 3, DEAE-sepharose; Lane 4, hydroxyapatite; Lane 5, reactive green-sepharose (affinity); Lane 6, protein standards. Analysis of labeled protein bands: A SYN_02898, B SYN_02896.

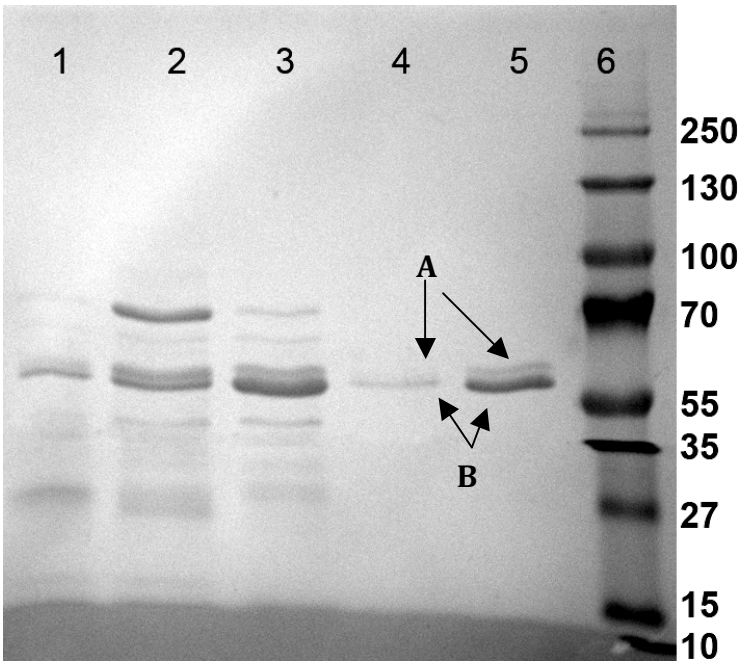

Table 4.5: Purification of benzoate:CoA ligase activity (SYN_02896 and SYN_02898 gene products) from *S. aciditrophicus* cell-free extracts.

	Volume	Total Protein (mg ml)	Activity (µmol $min^{-1}mg^{-1}$)	Total Activity (µmol min^{-1} ml)	Fold Purifi-cation	% Yield
Cell-free extract	3	29	0.15	4.4	1	100
Desalted 45% ammonium sulfate soluble	3.5	18	0.26	4.7	1.7	106
DEAE Concentrated	3	0.09	27	2.4	180	54
Pooled Hydroxyapatite	3	0.03	54	1.6	360	36

Cyclohexane-1-carboxylate:CoA ligase activity in cell-free extracts was 0.45 ± 0.02 μmol min^{-1} mg^{-1} of protein. High-throughput proteomic analysis revealed that peptides from SYN_03128, annotated as a long chain fatty acid CoA ligase, were differentially abundant when *S. aciditrophicus* was grown on the cyclohexane-1-carboxylate and crotonate (Kung, et al., unpublished data). To determine the activity of SYN_03128 gene product, it was over expressed in *E. coli* Bl21. The recombinant protein had the highest specific activity with cyclohexane-1-carboxylate (14.5 μmol $min^{-1}mg^{-1}$) (Table 4.3). The recombinant protein also had activity with cyclohex-1-ene-1-carboxylate (0.59 μmol min^{-1} mg^{-1}), crotonate (0.51 μmol $min^{-1}mg^{-1}$), benzoate (0.18 μmol $min^{-1}mg^{-1}$), butyrate (0.002 μmol min^{-1} mg^{-1}), pimelate (0.07 μmol min^{-1} mg^{-1}), acetate (0.06 μmol $min^{-1}mg^{-1}$), and succinate (0.13 μmol min^{-1} mg^{-1}) (Table 4.3). The kinetic constants for the recombinant protein were determined for cyclohexane-1-carboxylate. The V_{max} was 14.8 ± 0.5 μmol min^{-1} mg^{-1}, and the K_m values for cyclohexane-1-carboxylate and CoA were 0.04 ± 0.01 mM and 0.32 ± 0.05 mM, respectively (Table 4.3). Kinetic constants were also calculated for the recombinant protein with cyclohex-1-ene-1-carboxylate and crotonate as substrates. With cyclohex-1-ene-1-carboxylate as substrate, the V_{max} was 0.6 ± 0.04 μmol min^{-1} mg^{-1} and the K_m was 0.006 mM cyclohex-1-ene-1-carboxylate. With crotonate as substrate, the V_{max} was 0.7 ± 0.04 μmol min^{-1} mg^{-1} and K_m was 38 ± 6 mM crotonate (Table 4.3). These activities indicated that the SYN_03128 gene product most likely functions as a cyclohexane-1-carboxyl-CoA ligase and possibly as an 1-cyclohexene-1-carboxyl-CoA ligase. It is unlikely that this

protein is used by *S. aciditrophicus* to activate crotonate because the K_m for crotonate was 38 mM (Table 4.3), considerably higher than the concentration of crotonate that supports optimal growth (10 mM) (Figure 4.4). Gene product SYN_02896 is a more likely candidate for the crotonate activation to crotonyl-CoA as its K_m for crotonate of 4.7 ± 2 mM is more reflective of the crotonate concentrations that support growth of *S. aciditrophicus* (Figure 4.4).

Figure 4.4: Growth curves of *S. aciditrophicus* in pure culture with 20, 15, 10, 5, and 2.5 mM crotonate concentrations.

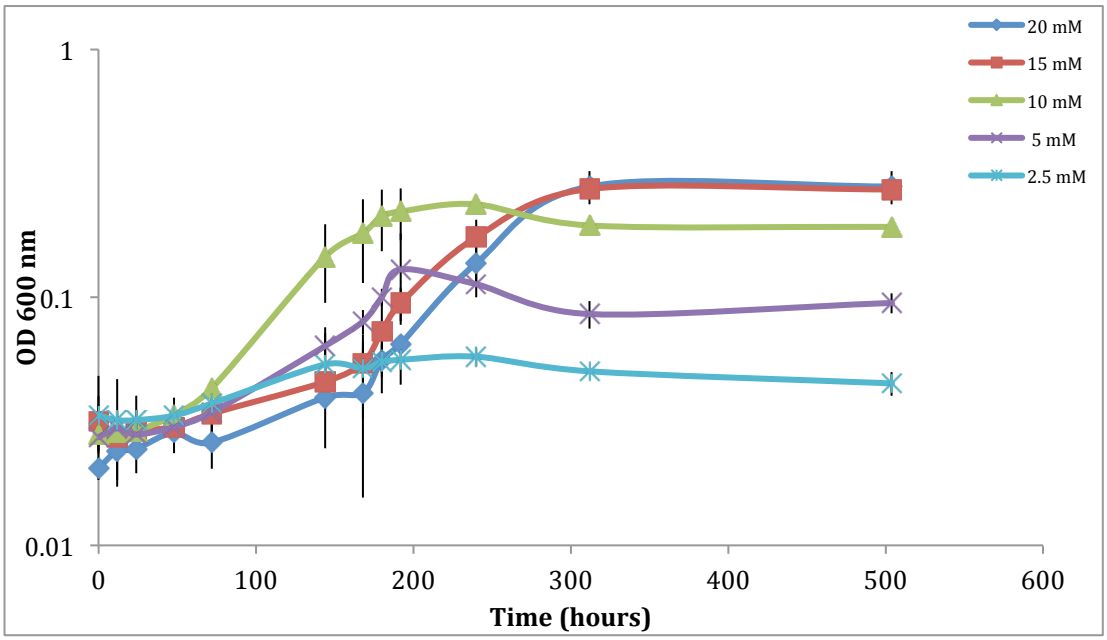

High-throughput proteomic analysis has shown SYN_02896 gene product in high abundance under all growth conditions tested, representing greater than 3%, 6% and 4% of all the peptides detected when crotonate, benzoate, and cyclohexane-1-carboxylate, respectively, were substrates (Figure 4.5). Peptides from SYN_02898 gene product represented 0.8 to 0.9% of the total peptides detected under growth conditions tested. SYN_03128 gene product was abundant when cyclohexane-1-carboxylate and crotonate were substrates (Figure 4.5), consistent with its role in activating cyclohexane-1-carboxylate when it is a substrate and making cyclohexane-1-carboxylate when crotonate is the substrate.

Figure 4.5: Total peptide abundance from high-throughput proteome analysis of acyl-CoA ligases from *S. aciditrophicus* grown on crotonate, benzoate, and cyclohexane-1-carboxylate.

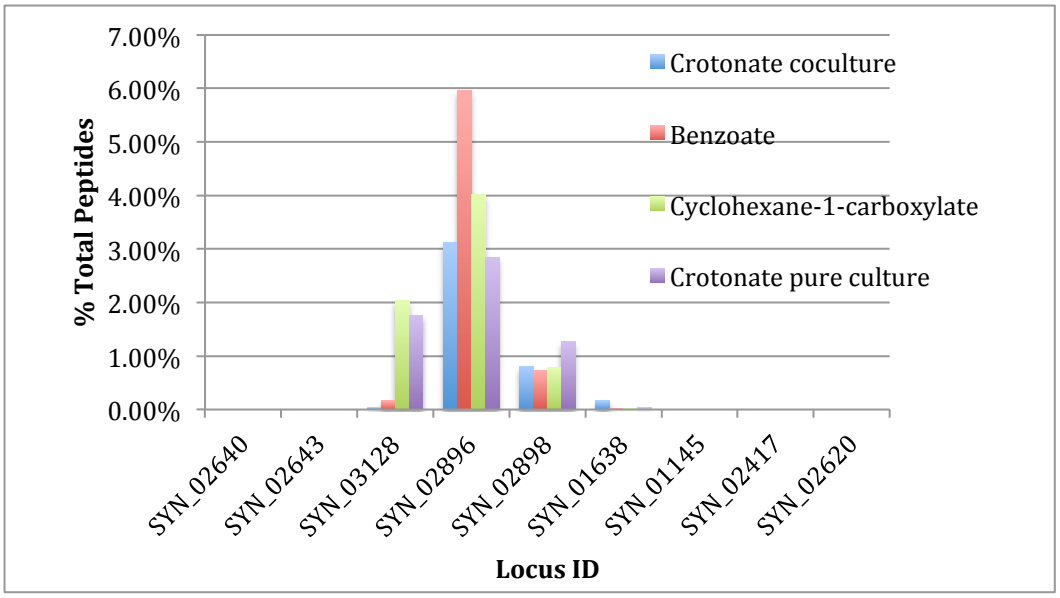

Discussion

The activating enzyme for both benzoate and crotonate metabolism in *S. aciditrophicus* is most likely the gene product SYN_02896. The crotonate:CoA ligase activity purified from cell-free extracts was found to be the SYN_02696 gene product (Table 4.1). The purified SYN_02896 gene product also had high activity with benzoate, but much lower activity with cyclohexane-1- carboxylate and cyclohex-1-ene-1-carboxylate (Table 4.4). To ensure that crotonate:CoA ligase and benzoate:CoA ligase activities were catalyzed by the SYN_02896 gene product, SYN_02896 was heterologously expressed in *E. coli* Bl21 and the activity of the expressed protein was determined (Dr. Johannes Kung, personal communication). The V_{max} and K_m of the recombinant protein for benzoate were 43 μmol min^{-1} mg^{-1} and 0.16 mM, respectively, while the V_{max} and K_m of the recombinant protein for crotonate were 23 μmol min^{-1} mg^{-1} and 4.2 mM. These values are similar to respective V_{max}'s and K_m's of the protein purified from cell-free extracts of *S. aciditrophicus* (Table 4.3). Thus, the SYN_02896 gene product has high affinity for benzoate and low affinity for crotonate. However, the optimum crotonate concentration for growth of *S. aciditrophicus* was about 10 mM and very little growth was observed when 2.5 mM crotonate was used (Figure 4.4). The specific growth rate of *S. aciditrophicus* with 5 mM crotonate was 0.007 per hour, about 47% of the optimal rate at 10 mM crotonate, which is consistent a K_m value of ~ 4 mM for crotonate for the SYN_02896 gene product (Table 4.3). The above kinetic data suggest that the SYN_029896 gene products functions as a crotonate:CoA ligase or benzoate:CoA ligase depending on

whether *S. aciditrophicus* grows with crotonate or benzoate as substrates. High-throughput proteomic analysis showed that the SYN_02896 gene product was abundant under all growth conditions tested (Figure 4.5), suggesting that SYN_02896 may be constitutively expressed.

The purification of the benzoate:CoA ligase activity from cell-free extracts of *S. aciditrophicus* resulted in the most pure fraction containing polypeptides from two gene products, SYN_02896 and SYN_02898, both annotated as 4-hydroxybenzoate:CoA ligases (Figure 4.3). The nearly pure fraction with SYN_02896 and SYN_02898 gene products had high benzoate:CoA ligase activity, but much less activity when crotonate or cyclohexane-1-carboxylate were used as substrates (Table 4.4). To confirm the substrate specificities, SYN_02898 was heterologously expressed in *E. coli* Bl21 (Dr. Johannes Kung, personal communitation). The recombinant protein had a V_{max} of 77 μmol min^{-1} mg^{-1} and K_m value of 0.113 mM for benzoate and a V_{max} of 2.3 μmol min^{-1} mg^{-1} and K_m value of 2.3 mM for crotonate, both of which are in agreement with the values obtained for the nearly pure preparation (Table 4.3). The recombinant SYN_02898 gene product had cyclohexane-1-carboxyl-CoA ligase activity, but cyclohexane-1-carboxylate activation is unlikely to be its physiological role as the K_m value for cyclohexane-1-carboxylate was 12 mM. The SYN_02898 gene product, like the SYN_02896 gene product, most likely functions as a crotonate:CoA ligase or a benzoate:CoA ligase, depending on the growth substrate. Proteome data revealed polypeptides from SYN_02898 represented 0.8 to 0.9% of the total proteomes under all growth conditions

tested, suggesting that SYN_02898 like SYN_02896 is constitutively expressed (Figure 4.5).

SYN_03128 was cloned and expressed in *E. coli* Bl21. The SYN_03128 gene product has high activity and high affinity for cyclohexane-1-carboxylate (Table 4.3). The SYN_03128 also had much lower activity with cyclohex-1-ene-1-carboxylate, benzoate, and several fatty acids (Table 4.4). High-throughput proteomic analysis showed the gene product for SYN_03128 was abundant when *S. aciditrophicus* was grown on cyclohexane-1-carboxylate and crotonate (Figure 4.5). *S. aciditrophicus* makes acetate, cyclohexane-1-carboxylate and traces of benzoate and cyclohex-1-ene-1-carboxylate when grown on crotonate (Elshahed et al., 2001; Mouttaki et al., 2007). Thus, SYN_03128 likely functions to activate cyclohexane-1-carboxylate when cyclohexane-1-carboxylate is the substrate and to produce cyclohexane-1-carboxylate from cyclohexane-1-carboxyl-CoA when crotonate is the substrate.

Conclusion

S. aciditrophicus degrades benzoate and alycyclic acids, cyclohexan-1-carboxylate and cyclohex-1-ene-1-carboxylate to acetate, hydrogen and carbon dioxide. *S. aciditrophicus* also is capable of fermenting crotonate to acetate. The analyses lead to the conclusion that *S. aciditrophicus* uses AMP-forming, acetyl-CoA synthetase to synthesize ATP from acetyl-CoA. In addition, I heterologously expressed the gene product for SYN_03090 and measured its activity to determine if it could explain the presence of low levels of acetate kinase activity detected in cell-free extracts of *S. aciditrophicus*. Lastly, I used protein purification and recombinant DNA approaches to identify the gene products involved in the activation of crotonate, benzoate, and cyclohexane-1-carboxylate in *S. aciditrophicus*. Two crotonate/benzoate:CoA ligases were purified and characterized from cell-free extracts of *S. aciditrophicus*. In addition, heterologous expression of SYN_03128 showed that its gene product is likely involved in the activation of cyclohexane-1-carboxylate.

Figure 4.6: Metabolism of benzoate, cyclohexane-1-carboxylate, and crotonate in *S. aciditrophicus*.

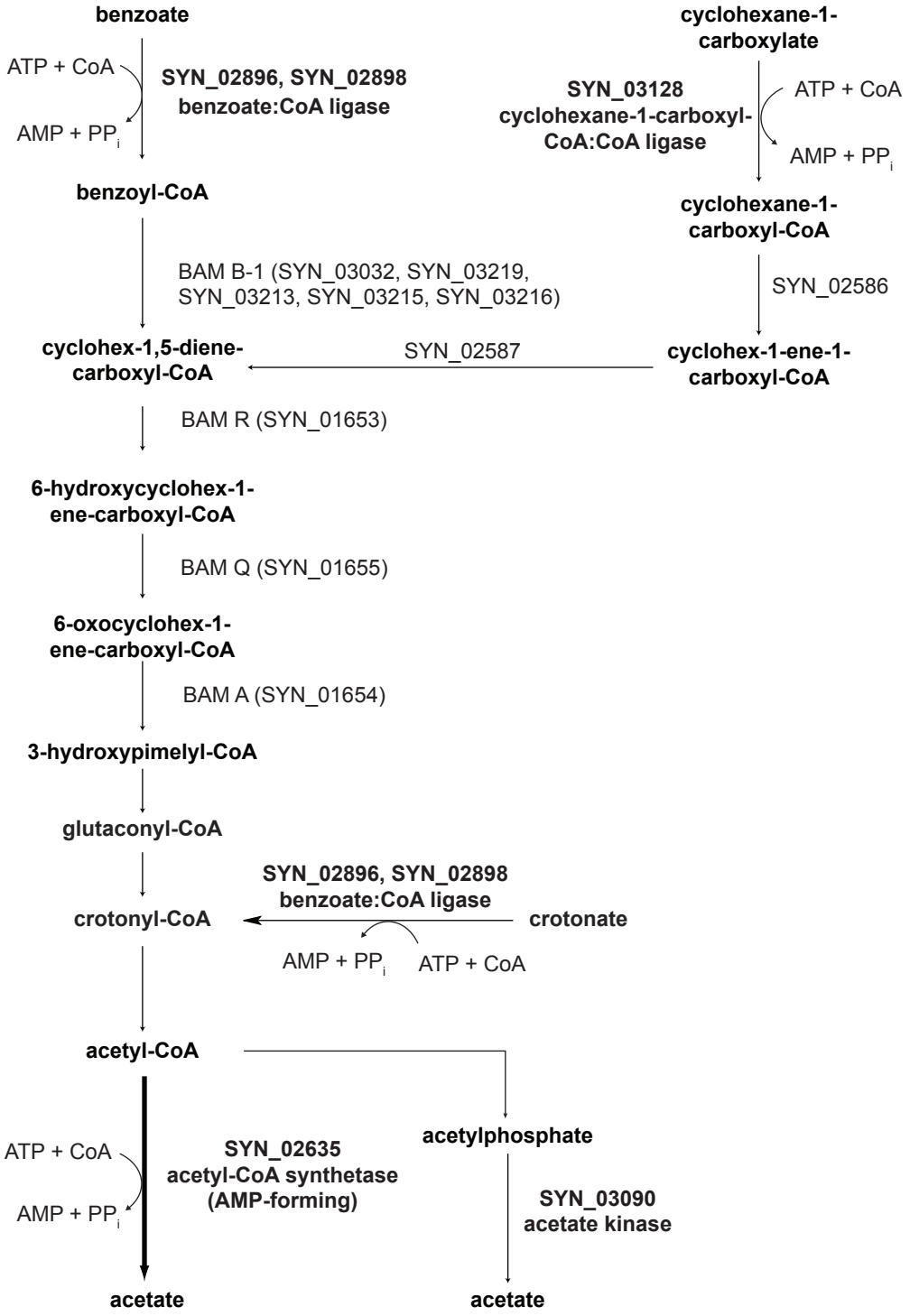

Appendix 1: High-throughput proteome methods

Enhanced filter aided sample preparation (eFASP) of *S. aciditrophicus* cells from cocultures. To increase proteome coverage and reduce peptide loss, phosphate buffered saline (PBS) washed pellets were processed by eFASP (Erde, Loo, & Loo, 2014; Manza, Stamer, Ham, Codreanu, & Liebler, 2005; Sibole & Erdemir, 2012; Wisniewski, Zielinska, & Mann, 2011; Wisniewski, Zougman, Nagaraj, & Mann, 2009). Pellets were suspended in solublization buffer (0.1 % deoxycholic acid, 0.1 % n-octylglucoside, 100 mM Tris-HCl, pH 8.0) containing 4 % ammonium dodecyl sulfate and 50 mM TCEP and boiled for 10 min at 90°C. The samples were sonicated three times for 10 seconds with a Sonic Dismembrator Model 100 (Fisher Scientific) and centrifuged twice (16,000 rcf, 10 min). Glycogen phosphorylase B (rabbit) was added to each sample at a 1:50 ratio for an internal standard. The supernatant and any residual pellet were sonicated and cooled to 37°C. Protein samples were alkylated by addition of 35 mM 4-vinylpyridine (4-VP), incubated, and shaken at 37°C for one hour. Dithiothreitol (DTT) was added to a final concentration of 50 mM. Each sample was aliquotted into 250 µl volumes. Eight volumes of solublization buffer containing 8 M urea were added to the previous aliquotted samples, and concentrated by centrifugation (14,000 rcf, 10 min) with a 30 kDa cutoff Microcon Filter Units from Millipore (Billerica, MA). Bound protein samples were washed twice with 200 µL solubilization buffer containing 8 M urea, followed by three washes with digestion buffer (0.2 % deoxycholic acid in 50 mM ammonium bicarbonate). The Microcon Unit was

incubated (37°C, 12 h) with 100 µl digestion buffer and five µg of trypsin. Samples were eluted into a collection tube by centrifugation and the column was washed twice with 100 µl of 50 mM ammonium bicarbonate and added to the total volume eluate. Eluates were acidified with deoxycholic acid. The acidified sample was washed three times with ethyl acetate (Masuda, Sugiyama, Tomita, & Ishihama, 2011; Masuda, Tomita, & Ishihama, 2008; Yeung, Nieves, Angeletti, & Stanley, 2008). The organic layer was discarded. Peptide samples were dried in a SpeedVac and washed three times with 50% methanol. Peptides were suspended in modified Mobile Phase A (96.5 % H_2O / 3 % CAN / 0.5 % formic acid). Digests were analyzed by shotgun LC-MS^E analysis or fractionated by hydrophilic interaction chromatography (HILIC) prior to LC-MS^E analysis.

Peptide fractionation by HILIC. Peptide samples (70 µg) were resuspended in 150 mM ammonium formate (pH 3). Conditioning buffer (15 mM ammonium formate, pH 3, 90% ACN) was added to TopTips (TT200HIL, polyhydroxyethyl A, PolyLC Inc., Columbia, MD), and incubated in 15 mM ammonium formate buffer (pH 3, 90% acetonitrile). Each peptide solution was added to the TopTip. Acetonitrile was added to bring the solution to a 90% organic phase. The TopTip was centrifuged at 500 rcf. The TopTip washed with binding buffer. Peptides were eluted into separate fractions with release buffers of decreasing organic composition (80, 78, 74, 40, and 10% ACN in 15 mM ammonium formate, pH 3). All fractions were dried in a SpeedVac. Peptides were re-suspended in modified Mobile Phase A (96.5% H_2O/3% ACN/0.5% formic acid), for LC-MS^E analysis.

Analysis by nanoLC-MS^E. Nano scale ultra-performance liquid chromatography tandem mass spectrometry (nanoUPLC) of peptides was performed on an Waters nanoACQUITY UPLC system equipped with a nanoACQUITY UPLC Symmetry C18 180 µm x 20 mm trap column (Waters, 186003514), and a nanoACQUITY UPLC BEH C18 75 µm x 250 mm reversed phase analytical column (Waters, 186003545). Five microliters of the sample was loaded onto the trap with and washed with 99% mobile phase A (0.1% formic acid in water) for 5 minutes, and then injected onto the column in 3% mobile Phase B (0.1% formic acid in acetonitrile). Peptides were eluted from the column with a gradient of 3-40% mobile phase B at a flow rate 300 nl/min, followed by a 5 minute rinse with 95% mobile phase B. The column was re-equilibrated to 3% mobile phase B for 20 minutes. The lock mass compound, [Glu^1]fibrinopeptide (0.5 pmol/µl, 25% ACN, 0.1% formic acid), and the analyte were delivered at 300 nl/min to the NanoLockSpray dual electrospray ion source (Waters, UK) which was equipped with a microcapillary for the lockmass compound, and a PicoTip Emitter (New Objective) for the analyte.

The ion source was interfaced with a Waters Synapt qTof HDMS for mass spectrometric analysis. Acquisition was performed in positive nanoESI mode and the instrument was operated in V-mode with an average resolution of 9500. Accurate mass data for precursor and fragment ions were collected over the 100-2000 m/z range, with the mode of acquisition alternating between low and elevated energy at 1-second intervals, for the duration of analysis. The lock mass channel was sampled every 30 seconds for calibration of MS and MS^E data.

Data processing and protein identification. Raw data files were processed in ProteinLynx Global Server 2.5.2 (PLGS, Waters) to provide an inventory of precursor ions along with their respective fragment ions, to search against a combined database composed of the Uniprot HAMAP complete proteome for *Syntrophus aciditrophicus* (strain SB, August 2011) and the Uniprot HAMAP complete proteome for *Methanospirillum hungatei* (strain JF-1 / DSM 864, August 2011), for peptide and protein identifications (Li et al., 2009). Database search settings employed two missed cleavages, a 4% false positive rate, fixed S-pyridylethyl modification of cysteine residues, and variable oxidation modification of methionine residues. The Waters Expression Informatics component of the PLGS software was utilized to quantify data using glycogen phosphorylase B (Uniprot accession P00489) as the quantification reference (Silva, Denny, et al., 2006; Silva et al., 2005; Silva, Gorenstein, Li, Vissers, & Geromanos, 2006). Tools in Data Extraction and Correction (DECO), a custom MS^E data-analysis software suite, were utilized for peptide-level quantitative and physiochemical comparative analyses (Erde et al., 2014).

Appendix 2: Synthesis of CoA-thioesters

To determine specificity and to measure the reverse reaction rates of the acyl-CoA ligases purified in Chapter 2 and Chapter 4, acetyl-CoA, crotonyl-CoA, benzoyl-CoA, butyryl-CoA, cyclohexane-1-carboxyl-CoA, and cyclohex-1-ene-1-carboxyl-CoA were synthesized using the annhydride or the succinimide of the corresponding fatty acid. All glassware in direct contact with the synthesis reactions were rinsed in acid bath prior to use.

Formation of CoA-thioesters using the anhydride. Acetyl-CoA and crotonyl-CoA were synthesized from the corresponding anhydrides were adapted from (Zhang, 2010). To synthesize the CoA-ester, 50 mg free CoASH (60.9 µmol) was dissolved in 2 ml of 1 M sodium bicarbonate (pH 8). The CoA solution was added via syringe to a sealed serum bottle with 7 ml of degased water under nitrogen headspace. Eleven microliters of corresponding anhydride was added directly to 1.5 ml of acetonitrile, and the solution was added to the CoASH/sodium bicarbonate solution via syringe. The solution was mixed gently with stir bar at room temperature for 15 minutes. After incubation, the reaction was stopped by acidification using 1 M hydrochloric acid to a pH of 1.5-2. The solution was added to a C18 sep-Pak TM column (waters, USA), previously washed with 100% methanol, rinsed with 20 ml of water, and equilibrated with 40 ml of 0.1% triflouroacetic acid. The solution was washed with 20 ml of 0.1% trifluoroacetic acid. The CoA-ester was eluted off the column with a 50:50 solution of 0.1% trifluoroacetic acid and

acetonitrile. The solution was collected in 10 ml falcon tubes and frozen at -80°C. The frozen product was lyophilized and checked for purity of CoA-ester.

Formation of CoA-thioesters using the succinimide. Crotonyl-CoA, cyclohexane-1-carboxyl-CoA, and cyclohex-1-ene-1-carboxyl-CoA were synthesized via the corresponding succinimide intermediates from the free acids as described earlier (Thiele et al., 2008). In the first step, dicyclohexylcarbodiimid (DCC) and N-hydroxysuccinimide are used to activate the carboxylic group to form the corresponding ester. Five millimoles of the free acid and N-hydroxysuccinimide are dissolved in 25 ml of dioxane. A solution of 7.5 mmol DCC in 5 ml of dioxane is added dropwise over 30 minutes. The reaction mixture is stirred at room temperature overnight. The insoluble portion was filtered out using a 20µm nitrocellulose filter. After filtration the solvent was removed by lyophilization.

To form the thioester, all subsequent steps were performed in the anaerobic chamber or anaerobically in a sealed serum bottle. In a 160 ml serum bottle with stir bar, 20 ml of 100 mM sodium bicarbonate (pH 8) is prepared and brought into the chamber. 50 µmol of free CoA and 100 µmol of succinimidylester are dissolved in the anoxic sodium bicarbonate buffer. The serum bottle is then sealed and brought out of the chamber. The reaction is monitored for free CoA using 5,5'-dithio-bis-(2-nitrobenzoic acid) (DTNB). When the reaction is complete (no more CoA can be detected by DTNB) the pH is adjusted to 4.5 with one milliliter of 1 M acetic acid. To remove most of the byproducts, the reaction mixture washed by ether-extraction three times with

30 ml of diethyl ether in a Pyrex pear shaped 200 ml separatory funnel. The resulting liquid was then lyophilized.

CoA-thioester determination. After lyophilization, the mass of the synthesized CoA-thioester was confirmed by LC MS/MS. The product formation was determined by enzymatic analysis of CoA thioesters (Henry E. Valentin, 1994). Acetyl-CoA was detected by a spectrometric method according to Decker (Decker, 1985a). A 20 µl sample was mixed with 100 µl of 5,5'-dithio-bis-2-nitrobenzoic acid (DTNB) in 1 M TRIS/HCl pH 8.0, 790 µl water and 20 µl citrate synthase (220 U/mg). The reaction was started by adding 40 µl of 10 mM oxalacetic acid, and the release of CoASH which reacted with DTNB, was monitored spectrometrically at 412nm (e=13.6 mM -1cm-1).

HPLC analysis was carried out using a Dionex 3000 and UV detection. Samples were anaylzed on a reverse-phase C18 column. Prior to injection of 10 µl of sample, the sample was filtered with (0.45 µm) spin filter or centrifuged for 5 minutes at 14,000 g. A flow rate of 0.75 ml min^{-1} isocratic flow and a step gradient of buffer A (20 mM potassium phosphate buffer pH X) and buffer B (100% acetonitrile) was applied (97% A, 95% A, 85% B, 70% B, 70% B, 97% B, 97% B).

Table A2.1: Retention times for CoA-thioesters used to measure ligase activity in Chapter 2 and Chapter 4.

Compound	Retention Time
Acetyl-CoA	10.2
Benzoate-CoA	21.2
Butyryl-CoA	13.2
Succinyl-CoA	9.2
Benzoate	11.2
CoA	9.1

References

Auburger, G., & Winter, J. (1996). Activation and degradation of benzoate, 3-phenylpropionate and crotonate by *Syntrophus buswellii* strain GA. Evidence for electron-transport phosphorylation during crotonate respiration. *Appl Microbiol Biotechnol, 44*(6), 807-815.

Balch, W. E., Fox, G. E., Magrum, L. J., Woese, C. R., & Wolfe, R. S. (1979). Methanogens: reevaluation of a unique biological group. *Microbiol Rev, 43*(2), 260-296.

Balch, W. E., & Wolfe, R. S. (1976). New approach to the cultivation of methanogenic bacteria: 2-mercaptoethanesulfonic acid (HS-CoM)-dependent growth of *Methanobacterium ruminantium* in a pressureized atmosphere. *Appl Environ Microbiol, 32*(6), 781-791.

Bastiaansen, J. A., Cheng, T., Mishkovsky, M., Duarte, J. M., Comment, A., & Gruetter, R. (2013). In vivo enzymatic activity of acetylCoA synthetase in skeletal muscle revealed by (13)C turnover from hyperpolarized [1-(13)C]acetate to [1-(13)C]acetylcarnitine. *Biochim Biophys Acta, 1830*(8), 4171-4178.

Beaty, P. S., Wofford, N. Q., & McInerney, M. J. (1987). Separation of *Syntrophomonas wolfei* from *Methanospirillum hungatii* in syntrophic cocultures by using percoll gradients. *Appl Environ Microbiol, 53*(5), 1183-1185.

Berger, S., Welte, C., & Deppenmeier, U. (2012). Acetate activation in *Methanosaeta thermophila*: characterization of the key enzymes pyrophosphatase and acetyl-CoA synthetase. *Archaea, 2012*, 315153.

Bergmeyer, H. U., Holz, G., Klotzsch, H., & Lang, G. (1963). [Phosphotransacetylase from *Clostridium Kluyveri*. Culture of the bacterium, isolation, crystallization and properties of the enzyme]. *Biochem Z, 338*, 114-121.

Bowman, C. M., Valdez, R. O., & Nishimura, J. S. (1976). Acetate kinase from *Veillonella alcalescens*. Regulation of enzyme activity by succinate and substrates. *J Biol Chem, 251*(10), 3117-3121.

Bradford, M. M. (1976). A rapid and sensitive method for the quantitation of microgram quantities of protein utilizing the principle of protein-dye binding. *Anal Biochem, 72*, 248-254.

Breas, O., Guillou, C., Reniero, F., & Wada, E. (2001). The global methane cycle: isotopes and mixing ratios, sources and sinks. *Isotopes Environ Health Stud, 37*(4), 257-379.

Brown, T. D., Jones-Mortimer, M. C., & Kornberg, H. L. (1977). The enzymic interconversion of acetate and acetyl-coenzyme A in *Escherichia coli*. *J Gen Microbiol, 102*(2), 327-336.

Bustin, S. A., Benes, V., Garson, J. A., Hellemans, J., Huggett, J., Kubista, M., et al. (2009). The MIQE guidelines: minimum information for publication of quantitative real-time PCR experiments. *Clin Chem, 55*(4), 611-622.

Chittori, S., Savithri, H. S., & Murthy, M. R. (2012). Structural and mechanistic investigations on *Salmonella typhimurium* acetate kinase (AckA): identification of a putative ligand binding pocket at the dimeric interface. *BMC Struct Biol, 12*, 24.

Connerton, I. F., Fincham, J. R., Sandeman, R. A., & Hynes, M. J. (1990). Comparison and cross-species expression of the acetyl-CoA synthetase genes of the *Ascomycete fungi*, *Aspergillus nidulans* and *Neurospora crassa*. *Mol Microbiol, 4*(3), 451-460.

Crable, B. (2013). *Enzyme systems involved in interspecies hydrogen and formate transfer between syntrophic fatty and aromatic acid degraders and Methanospirillum hungatei.* University of Oklahoma, Norman.

David, H., Ozcelik, I. S., Hofmann, G., & Nielsen, J. (2008). Analysis of *Aspergillus nidulans* metabolism at the genome-scale. *BMC Genomics, 9*, 163.

Decker, K. (1985a). Acetyl coenzyme A. . In B.-m. J. Bergmeyer HU, Grassl M (Ed.), *Methods of Enzymatic Analysis* (3rd ed., Vol. 7, pp. 186-193). VCH, Weinheim.

Drake, H. L., & Daniel, S. L. (2004). Physiology of the thermophilic acetogen *Moorella thermoacetica*. *Res Microbiol, 155*(6), 422-436.

Dutton, P. L., & Evans, W. C. (1969). The metabolism of aromatic compounds by *Rhodopseudomonas palustris*. A new, reductive, method of aromatic ring metabolism. *Biochem J, 113*(3), 525-536.

Egland, P. G., Gibson, J., & Harwood, C. S. (1995). Benzoate-coenzyme A ligase, encoded by badA, is one of three ligases able to catalyze benzoyl-

coenzyme A formation during anaerobic growth of *Rhodopseudomonas palustris* on benzoate. *J Bacteriol, 177*(22), 6545-6551.

Elshahed, M. S., Bhupathiraju, V. K., Wofford, N. Q., Nanny, M. A., & McInerney, M. J. (2001). Metabolism of benzoate, cyclohex-1-ene carboxylate, and cyclohexane carboxylate by , *Syntrophus aciditrophicus*, strain SB in syntrophic association with hydrogen-using microorganisms. *Applied and Environmental Microbiology, 67*(4), 1728-1738.

Elshahed, M. S., & McInerney, M. J. (2001). Benzoate fermentation by the anaerobic bacterium *Syntrophus aciditrophicus* in the absence of hydrogen-using microorganisms. *Applied and Environmental Microbiology, 67*(12), 5520-5525.

Erde, J., Loo, R. R., & Loo, J. A. (2014). Enhanced FASP (eFASP) to increase proteome coverage and sample recovery for quantitative proteomic experiments. *J Proteome Res, 13*(4), 1885-1895.

Forster, P. e. a. (2007). *Climate change 2007: the physical science basis. contribution of working group I to the fourth assessment report of the intergovernmental panel on climate change*: Cambridge University Press.

Fuchs, G. (2008). Anaerobic metabolism of aromatic compounds. *Ann N Y Acad Sci, 1125*, 82-99.

Glasemacher, J., Bock, A. K., Schmid, R., & Schonheit, P. (1997). Purification and properties of acetyl-CoA synthetase (ADP-forming), an archaeal enzyme of acetate formation and ATP synthesis, from the hyperthermophile *Pyrococcus furiosus*. *Eur J Biochem, 244*(2), 561-567.

Harwood, C. S., Burchhardt, G., Herrmann, H., & Fuchs, G. (1999). Anaerobic metabolism of aromatic compounds via the benzoyl-CoA pathway.

Harwood, C. S., & Gibson, J. (1988). Anaerobic and aerobic metabolism of diverse aromatic compounds by the photosynthetic bacterium *Rhodopseudomonas palustris*. *Appl Environ Microbiol, 54*(3), 712-717.

Henry E. Valentin, A. S. (1994). Application of enzymatically synthesized short-chain-length hydroxy fatty acid coenzyme A thioesters for assay of polyhydroxyalkanoic acid synthases. *Applied Microbiology and Biotechnology, 40*(5), 699-709.

Hopkins, B. T., McInerney, M. J., & Warikoo, V. (1995). Evidence for anaerobic syntrophic benzoate degradation threshold and isolation of the syntrophic benzoate degrader. *Appl Environ Microbiol, 61*(2), 526-530.

Huang, K. X., Huang, S., Rudolph, F. B., & Bennett, G. N. (2000). Identification and characterization of a second butyrate kinase from *Clostridium acetobutylicum* ATCC 824. *J Mol Microbiol Biotechnol, 2*(1), 33-38.

Huber, R., Rossnagel, P., Woese, C. R., Rachel, R., Langworthy, T. A., & Stetter, K. O. (1996). Formation of ammonium from nitrate during chemolithoautotrophic growth of the extremely thermophilic bacterium *Ammonifex degensii* gen. nov. sp. nov. *Syst Appl Microbiol, 19*(1), 40-49.

Ingram-Smith, C., Martin, S. R., & Smith, K. S. (2006). Acetate kinase: not just a bacterial enzyme. *Trends Microbiol, 14*(6), 249-253.

Jackson, B. E., Bhupathiraju, V. K., Tanner, R. S., Woese, C. R., & McInerney, M. J. (1999). *Syntrophus aciditrophicus* sp. nov., a new anaerobic bacterium

that degrades fatty acids and benzoate in syntrophic association with hydrogen-using microorganisms. *Arch Microbiol, 171*(2), 107-114.

Jackson, B. E., & McInerney, M. J. (2002). Anaerobic microbial metabolism can proceed close to thermodynamic limits. *Nature, 415*(6870), 454-456.

Kirschke, S., Bousquet, P., Ciais, P., Saunois, M., Canadell, J.G., Dlugokencky, E. J., Bergamaschi, P., Bergmann, D., Blake, D.R., Bruhwilier, L., Cameron-Smith, P., Castaldi, S., Chevallier, F., Feng, L., Fraser, A., Heimann, M., Hodson, E.L., Houweling, S., Josse, B., Fraser, P.J., Krummel, P.B., Lamarque, F., Langenfelds, R.L., Quere, C.L., Naik, V. (2013). Three decades of global methane sources and sinks. [Review]. *Nature Geoscience, 6*(October 2013), 813-823.

Kung, J. W., Seifert, J., von Bergen, M., & Boll, M. (2013). Cyclohexanecarboxyl-coenzyme A (CoA) and cyclohex-1-ene-1-carboxyl-CoA dehydrogenases, two enzymes involved in the fermentation of benzoate and crotonate in *Syntrophus aciditrophicus*. *J Bacteriol, 195*(14), 3193-3200.

Kuntze, K., Shinoda, Y., Moutakki, H., McInerney, M. J., Vogt, C., Richnow, H., et al. (2008). 6-Oxocyclohex-1-ene-1-carbonyl-coenzyme A hydrolases from obligately anaerobic bacteria: characterization and identification of its gene as a functional marker for aromatic compounds degrading anaerobes. *Environ Microbiol*.

Kurebayashi, N., Kodama, T., & Ogawa, Y. (1980). P1,P5-Di(adenosine-5')pentaphosphate(Ap5A) as an inhibitor of adenylate kinase in studies

of fragmented sarcoplasmic reticulum from bullfrog skeletal muscle. *J Biochem, 88*(3), 871-876.

Kuver, J., Xu, Y., & Gibson, J. (1995). Metabolism of cyclohexane carboxylic acid by the photosynthetic bacterium *Rhodopseudomonas palustris*. *Arch Microbiol, 164*(5), 337-345.

Lee, S., Son, H., Lee, J., Min, K., Choi, G. J., Kim, J. C., et al. (2011). Functional analyses of two acetyl coenzyme A synthetases in the ascomycete Gibberella zeae. *Eukaryot Cell, 10*(8), 1043-1052.

Li, G. Z., Vissers, J. P., Silva, J. C., Golick, D., Gorenstein, M. V., & Geromanos, S. J. (2009). Database searching and accounting of multiplexed precursor and product ion spectra from the data independent analysis of simple and complex peptide mixtures. *Proteomics, 9*(6), 1696-1719.

Lin, M., & Oliver, D. J. (2008). The role of acetyl-coenzyme a synthetase in *Arabidopsis*. *Plant Physiol, 147*(4), 1822-1829.

Lowe, S. E., Jain, M. K., & Zeikus, J. G. (1993). Biology, ecology, and biotechnological applications of anaerobic bacteria adapted to environmental stresses in temperature, pH, salinity, or substrates. *Microbiol Rev, 57*(2), 451-509.

Manza, L. L., Stamer, S. L., Ham, A. J., Codreanu, S. G., & Liebler, D. C. (2005). Sample preparation and digestion for proteomic analyses using spin filters. *Proteomics, 5*(7), 1742-1745.

Masuda, T., Sugiyama, N., Tomita, M., & Ishihama, Y. (2011). Microscale phosphoproteome analysis of 10,000 cells from human cancer cell lines. *Anal Chem, 83*(20), 7698-7703.

Masuda, T., Tomita, M., & Ishihama, Y. (2008). Phase transfer surfactant-aided trypsin digestion for membrane proteome analysis. *J Proteome Res, 7*(2), 731-740.

Matsunaga, T., Nemoto, M., Arakaki, A., & Tanaka, M. (2009). Proteomic analysis of irregular, bullet-shaped magnetosomes in the sulphate-reducing magnetotactic bacterium *Desulfovibrio magneticus* RS-1. *Proteomics, 9*(12), 3341-3352.

Mayer, F., Kuper, U., Meyer, C., Daxer, S., Muller, V., Rachel, R., et al. (2012). AMP-forming acetyl coenzyme A synthetase in the outermost membrane of the hyperthermophilic crenarchaeon *Ignicoccus hospitalis*. *J Bacteriol, 194*(6), 1572-1581.

McComb, R. B., Bond, L. W., Burnett, R. W., Keech, R. C., & Bowers, G. N., Jr. (1976). Determination of the molar absorptivity of NADH. *Clin Chem, 22*(2), 141-150.

McInerney, M. J., & Bryant, M. P. (1981). Anaerobic degradation of lactate by syntrophic associations of *Methanosarcina barkeri* and *Desulfovibrio species* and effect of hydrogen on acetate degradation. *Appl Environ Microbiol, 41*(2), 346-354.

McInerney, M. J., Bryant, M. P., Hespell, R. B., & Costerton, J. W. (1981). *Syntrophomonas wolfei* gen. nov. sp. nov., an anaerobic, syntrophic, fatty acid-oxidizing bacterium. *Appl Environ Microbiol, 41*(4), 1029-1039.

McInerney, M. J., Rohlin, L., Mouttaki, H., Kim, U., Krupp, R. S., Rios-Hernandez, L., et al. (2007). The genome of *Syntrophus aciditrophicus*: Life at the thermodynamic limit of microbial growth. *Proc Natl Acad Sci U S A*.

McInerney, M. J., Sieber, J. R., & Gunsalus, R. P. (2009). Syntrophy in anaerobic global carbon cycles. *Curr Opin Biotechnol*.

McInerney, M. J., Struchtemeyer, C. G., Sieber, J., Mouttaki, H., Stams, A. J. M., Schink, B., et al. (2008). Physiology, ecology, phylogeny, and genomics of microorganisms capable of syntrophic metabolism. *Ann N Y Acad Sci, 1125*, 58-72.

Miroshnichenko, M. L., Rainey, F. A., Rhode, M., & Bonch-Osmolovskaya, E. A. (1999). *Hippea maritima* gen. nov., sp. nov., a new genus of thermophilic, sulfur-reducing bacterium from submarine hot vents. *Int J Syst Bacteriol, 49 Pt 3*, 1033-1038.

Mountfort, D. O., Brulla, W. J., Krumholz, L. R., & Bryant, M. P. (1984). *Syntrophus buswelli* gen. nov., sp. nov.: a benzoate catabolizer from methanogenic ecosystems. *International Journal of Synstematic and Evolutionary Microbiology, 34*(2), 216-217.

Mouttaki, H. (2007). *Novel aspects of benzoate and crotonate metabolism by the strictly anaerobic bacterium Syntrophus aciditrophicus.* Unpublished Dissertation, Oklahoma University, Norman.

Mouttaki, H., Nanny, M. A., & McInerney, M. J. (2007). Cyclohexane carboxylate and benzoate formation from crotonate in *Syntrophus aciditrophicus*. *Applied and Environmental Microbiology, 73*(3), 930-938.

Mouttaki, H., Nanny, M. A., & McInerney, M. J. (2008). Use of benzoate as an electron acceptor by *Syntrophus aciditrophicus* grown in pure culture with crotonate. *Environ Microbiol, 10*(12), 3265-3274.

Muller, J. A., & Schink, B. (2000). Initial steps in the fermentation of 3-hydroxybenzoate by *Sporotomaculum hydroxybenzoicum*. *Arch Microbiol, 173*(4), 288-295.

Nageswara Rao, B. D., & Cohn, M. (1977). Asymmetric binding of the inhibitor di(adenosine-5') pentaphosphate (Ap5A) to adenylate kinase. *Proc Natl Acad Sci U S A, 74*(12), 5355-5357.

Oberender, J., Kung, J. W., Seifert, J., von Bergen, M., & Boll, M. (2012). Identification and characterization of a succinyl-coenzyme A (CoA):benzoate CoA transferase in *Geobacter metallireducens*. *J Bacteriol, 194*(10), 2501-2508.

Perrotta, J. A., & Harwood, C. S. (1994). Anaerobic metabolism of cyclohex-1-ene-1-carboxylate, a proposed intermediate of benzoate degradation, by *Rhodopseudomonas palustris*. *Appl Environ Microbiol, 60*(6), 1775-1782.

Peters, F., Shinoda, Y., McInerney, M. J., & Boll, M. (2007). Cyclohexa-1,5-diene-1-carbonyl-coenzyme A (CoA) hydratases of *Geobacter metallireducens* and *Syntrophus aciditrophicus*: evidence for a common benzoyl-CoA

degradation pathway in facultative and strict anaerobes. *Journal of Bacteriology, 189*(3), 1055-1060.

Peters, F., Shinoda, Y., McInerney, M. J., & Boll, M. (2007). Cyclohexa-1,5-diene-1-carbonyl-coenzyme A (CoA) hydratases of *Geobacter metallireducens* and *Syntrophus aciditrophicus*: Evidence for a common benzoyl-CoA degradation pathway in facultative and strict anaerobes. *J Bacteriol, 189*(3), 1055-1060.

Pfaffl, M. W. (2001). A new mathematical model for relative quantification in real-time RT-PCR. *Nucleic Acids Res, 29*(9), e45.

Qiu, Y. L., Hanada, S., Ohashi, A., Harada, H., Kamagata, Y., & Sekiguchi, Y. (2008). *Syntrophorhabdus aromaticivorans* gen. nov., sp. nov., the first cultured anaerobe capable of degrading phenol to acetate in obligate syntrophic associations with a hydrogenotrophic methanogen. *Appl Environ Microbiol, 74*(7), 2051-2058.

Qiu, Y. L., Sekiguchi, Y., Hanada, S., Imachi, H., Tseng, I. C., Cheng, S. S., et al. (2006). *Pelotomaculum terephthalicum* sp. nov. and *Pelotomaculum isophthalicum* sp. nov.: two anaerobic bacteria that degrade phthalate isomers in syntrophic association with hydrogenotrophic methanogens. *Arch Microbiol, 185*(3), 172-182.

Qiu, Y. L., Sekiguchi, Y., Imachi, H., Kamagata, Y., Tseng, I. C., Cheng, S. S., et al. (2003). *Sporotomaculum syntrophicum* sp. nov., a novel anaerobic, syntrophic benzoate-degrading bacterium isolated from methanogenic

sludge treating wastewater from terephthalate manufacturing. *Arch Microbiol, 179*(4), 242-249.

Ren, N. Q., Lin, H. L., Zhang, K., Zheng, G. X., Duan, Z. J., & Lin, M. (2007). Cloning, expression, and characterization of an acetate kinase from a high rate of biohydrogen bacterial strain *Ethanoligenens sp*. hit B49. *Curr Microbiol, 55*(2), 167-172.

Sattley, W. M., Madigan, M. T., Swingley, W. D., Cheung, P. C., Clocksin, K. M., Conrad, A. L., et al. (2008). The genome of *Heliobacterium modesticaldum*, a phototrophic representative of the Firmicutes containing the simplest photosynthetic apparatus. *J Bacteriol, 190*(13), 4687-4696.

Schocke, L., & Schink, B. (1997). Energetics of methanogenic benzoate degradation by *Syntrophus gentianae* in syntrophic coculture. *Microbiology, 143*(7), 2345-2351.

Schocke, L., & Schink, B. (1998). Membrane-bound proton-translocating pyrophosphatase of *Syntrophus gentianae*, a syntrophically benzoate-degrading fermenting bacterium. *Eur J Biochem, 256*(3), 589-594.

Schocke, L., & Schink, B. (1999). Energetics and biochemistry of fermentative benzoate degradation by *Syntrophus gentianae*. *Arch Microbiology, 171*, 331-337.

Schuhle, K., Gescher, J., Feil, U., Paul, M., Jahn, M., Schagger, H., et al. (2003). Benzoate-coenzyme A ligase from *Thauera aromatica*: an enzyme acting in anaerobic and aerobic pathways. *J Bacteriol, 185*(16), 4920-4929.

Sibole, S. C., & Erdemir, A. (2012). Chondrocyte deformations as a function of tibiofemoral joint loading predicted by a generalized high-throughput pipeline of multi-scale simulations. *PLoS One, 7*(5), e37538.

Sieber, J. (2011). *Investigations of interspecies electron transfer mechanisms important to syntrophic metabolism.* University of Oklahoma, Norman.

Sieber, J. R., Le, H. M., & McInerney, M. J. (2014). The importance of hydrogen and formate transfer for syntrophic fatty, aromatic and alicyclic metabolism. *Environ Microbiol, 16*(1), 177-188.

Sieber, J. R., McInerney, M. J., & Gunsalus, R. P. (2012). Genomic insights into syntrophy: the paradigm for anaerobic metabolic cooperation. *Annu Rev Microbiol, 66*, 429-452.

Sieber, J. R., Sims, D. R., Han, C., Kim, E., Lykidis, A., Lapidus, A. L., et al. (2010). The genome of *Syntrophomonas wolfei:* new insights into syntrophic metabolism and biohydrogen production. *Environ Microbiol*.

Silva, J. C., Denny, R., Dorschel, C., Gorenstein, M. V., Li, G. Z., Richardson, K., et al. (2006). Simultaneous qualitative and quantitative analysis of the *Escherichia coli* proteome: a sweet tale. *Mol Cell Proteomics, 5*(4), 589-607.

Silva, J. C., Denny, R., Dorschel, C. A., Gorenstein, M., Kass, I. J., Li, G. Z., et al. (2005). Quantitative proteomic analysis by accurate mass retention time pairs. *Anal Chem, 77*(7), 2187-2200.

Silva, J. C., Gorenstein, M. V., Li, G. Z., Vissers, J. P., & Geromanos, S. J. (2006). Absolute quantification of proteins by LCMSE: a virtue of parallel MS acquisition. *Mol Cell Proteomics, 5*(1), 144-156.

Stadtman, E. R. (1952). The purification and properties of phosphotransacetylase. *J Biol Chem, 196*(2), 527-534.

Starai, V. J., & Escalante-Semerena, J. C. (2004). Acetyl-coenzyme A synthetase (AMP forming). *Cell Mol Life Sci, 61*(16), 2020-2030.

Stouthamer, A. H. (1973). A theoretical study on the amount of ATP required for synthesis of microbial cell material. *Antonie Van Leeuwenhoek, 39*(3), 545-565.

Struchtemeyer, C. G., Elshahed, M. S., Duncan, K. E., & McInerney, M. J. (2005). Evidence for aceticlastic methanogenesis in the presence of sulfate in a gas condensate-contaminated aquifer. *Appl Environ Microbiol, 71*(9), 5348-5353.

Szasz, G., Gruber, W., & Bernt, E. (1976). Creatine kinase in serum: 1. Determination of optimum reaction conditions. *Clin Chem, 22*(5), 650-656.

Takasaki, K., Shoun, H., Yamaguchi, M., Takeo, K., Nakamura, A., Hoshino, T., et al. (2004). Fungal ammonia fermentation, a novel metabolic mechanism that couples the dissimilatory and assimilatory pathways of both nitrate and ethanol. *Journal of Biological Chemistry, 279*(13), 12414-12420.

Tanner, R. S., Wolfe, R. S., & Ljungdahl, L. G. (1978). Tetrahydrofolate enzyme levels in *Acetobacterium woodii* and their implication in the synthesis of acetate from CO2. *Journal of Bacteriology, 134*(2), 668-670.

Wanner, B. L., & Wilmes-Riesenberg, M. R. (1992). Involvement of phosphotransacetylase, acetate kinase, and acetyl phosphate synthesis in control of the phosphate regulon in *Escherichia coli*. *J Bacteriol, 174*(7), 2124-2130.

Ward, D. E., Ross, R. P., van der Weijden, C. C., Snoep, J. L., & Claiborne, A. (1999). Catabolism of branched-chain alpha-keto acids in *Enterococcus faecalis*: the bkd gene cluster, enzymes, and metabolic route. *J Bacteriol, 181*(17), 5433-5442.

Weimar, J. D., DiRusso, C. C., Delio, R., & Black, P. N. (2002). Functional role of fatty acyl-coenzyme A synthetase in the transmembrane movement and activation of exogenous long-chain fatty acids. Amino acid residues within the ATP/AMP signature motif of *Escherichia coli* FadD are required for enzyme activity and fatty acid transport. *J Biol Chem, 277*(33), 29369-29376.

Wisniewski, J. R., Zielinska, D. F., & Mann, M. (2011). Comparison of ultrafiltration units for proteomic and N-glycoproteomic analysis by the filter-aided sample preparation method. *Anal Biochem, 410*(2), 307-309.

Wisniewski, J. R., Zougman, A., Nagaraj, N., & Mann, M. (2009). Universal sample preparation method for proteome analysis. *Nat Methods, 6*(5), 359-362.

Wofford, N. Q., Beaty, P. S., & McInerney, M. J. (1986). Preparation of cell-free extracts and the enzymes involved in fatty acid metabolism in *Syntrophomonas wolfei*. *J Bacteriol, 167*(1), 179-185.

Wohlbrand, L., Jacob, J. H., Kube, M., Mussmann, M., Jarling, R., Beck, A., et al. (2013). Complete genome, catabolic sub-proteomes and key-metabolites of *Desulfobacula toluolica* Tol2, a marine, aromatic compound-degrading, sulfate-reducing bacterium. *Environ Microbiol, 15*(5), 1334-1355.

Yeung, Y. G., Nieves, E., Angeletti, R. H., & Stanley, E. R. (2008). Removal of detergents from protein digests for mass spectrometry analysis. *Anal Biochem, 382*(2), 135-137.

Yvon-Durocher, G., Allen, A. P., Bastviken, D., Conrad, R., Gudasz, C., St- Pierre, A., Thanh-Duc, N., Giogio, P. A. (2014). Methane fluxes show consistent temperature dependence across microbial to ecosystem scales. [Letter]. *Nature, 507*(13164), 488-491.

Zhang, J. (2010). *On the Enzymatic Mechanism of 4-hydroxybutyryl-CoA Dehydratase and 4-hydroxybutyrate CoA-transferase from Clostridium Aminobutyricum.* Unpublished Desseration, Philipps University of Marburg, Lahn, Germany.